

Synthesis and characterization of cationically and anionically modified poly(vinyl alcohol) microfibrils

*Thesis submitted in partial fulfillment of the requirements for the degree of
Master of Science (Polymer Science)*

by

Helen Chirowodza



at the

University of Stellenbosch

Supervisor: Prof. R.D Sanderson

March 2009

Declaration

I, the undersigned, hereby declare that the work contained in this thesis is my own work and that I have not previously in its entirety or in part submitted it at any university for a degree.

Helen Chirowodza

March 2009

*To my parents, siblings, nephews, nieces, colleagues and my beloved fiancé
Rueben.*

Abstract

In papermaking, the addition of filler can be detrimental to the properties of the resulting paper hence the use of additives that enhance paper properties are of paramount importance.

Syndiotacticity rich poly(vinyl alcohol) (PVA) microfibrils were prepared for use as filler retention aids. They were prepared via *in situ* fibrillation during the saponification of high molecular weight poly(vinyl pivalate). The resulting fibers had high thermal stability and crystalline melting temperature. They were not fully soluble in water even at 100 °C. In order to make them less water resistant the syndiotacticity of the PVA microfibrils was varied by copolymerizing vinyl pivalate with vinyl acetate and saponifying the resultant copolymer. It was observed that changes in syndiotacticity had a significant effect on the crystallinity, morphology and thermal properties of the resultant PVA.

The surfaces of the fibers were modified by first crosslinking using glyoxal (a dialdehyde), and then attaching cationic and anionic groups by grafting and by carboxymethylation. Crosslinking prior to modification was beneficial in minimizing the solubility of the fibers in the aqueous media in which they were modified. Heterogeneous modification techniques were employed so that fiber properties could be preserved. Carboxymethylation was carried out using the two step Williamson's ether synthesis. The first step involves the formation of a highly reactive alkoxide by the reaction of PVA with a strong base and the second its etherification using a functional alkyl halide. Poly(methacryloyloxy ethyl trimethyl ammonium chloride) and poly(acrylic acid) were grafted from the PVA microfibrils using the KPS/ $\text{Na}_2\text{S}_2\text{O}_3$ redox initiation system. Grafting was confirmed by FTIR and NMR spectroscopy.

Differential scanning calorimetry (DSC) and thermogravimetric analysis (TGA) were carried out on both modified and unmodified PVA microfibrils. The results showed that crosslinking resulted in an enhancement of the thermal properties of the microfibrils. A decline in the onset temperature for thermal degradation and crystalline melting temperature were observed, and were attributed to the modification of the PVA microfibrils.

Opsomming

In papierproduksie kan die byvoeging van vulstowwe 'n nadelige effek hê op papier eienskappe en dit maak die aanwending van bymiddels wat hierdie eienskappe verbeter van kardinale belang.

Sindiotaktiese ryk poliviniel alkohol (PVA) mikrovesels wat gebruik kan word as vulstof retensiemiddel is berei deur gebruik te maak van in situ fibrillasie tydens die saponifikasie van hoë molekulêre massa poly(viniel pivalaat). Die gevormde vesels beskik oor hoë termiese stabiliteit en kristallyne smelt temperatuur en is nie ten volle oplosbaar in water nie, selfs by 100°C. Om die vesels meer waterbestand te maak is die sindiotaksisiteit van die PVA mikrovesels gevarieer deur die kopolimerisasie van vinielpivalaat met vinielasetaat en die gevormde kopolimeer gesaponifiseer. Dit is bevind dat die verandering in sindiotaksisiteit 'n betekenisvolle effek op die kristalliniteit, morfologie en termiese eienskappe van die gevormde PVA het.

Die oppervlakte van die vesels is eerstens gekruisbind deur gebruik te maak van etaan-1,2-dioon ('n dialdehyd) en daarna gewysig deur kationiese of anioniese groepe aan te heg deur gebruik te maak van enting en karboksiemetielasie. Kruisbinding voor wysiging het die oplosbaarheid van die vesels in 'n waterige medium, waarin dit gewysig is, verminder. Heterogene wysigingstegnieke is gebruik om veseleienskappe te behou. Karboksiemetielasie is uitgevoer deur gebruik te maak van die twee stap Williamson's etersintese. Die eerste stap behels die bereiding van 'n hoogs reaktiewe alkoksied deur die reaksie van PVA met 'n sterk basis en die tweede stap die eterifikasie deur gebruik te maak van 'n funksionele alkielhalied. Poli(metakrieloioeloksie etiel trimetiel ammonium chloried) en poliakrielsuur is geënt aan die PVA mikrovesels deur gebruik te maak van 'n KPS/Na₂S₂O₃ redoks sisteem. Enting is bevestig deur FTIR en KMR spektroskopie.

Differensiële skandeer kaloriemeting (DSK) en termogravimetriese analise (TGA) is uitgevoer op beide die gewysigde en ongewysigde PVA mikrovesels. Die resultate het getoon dat kruisbinding 'n verbetering in die termiese eienskappe van die mikrovesels tot gevolg gehad het. 'n Vermindering in die begintemperatuur van termiese degradasie en kristallyne smelt temperatuur is opgemerk, en dit word toegeskryf aan die wysiging van die PVA mikrovesels.

Acknowledgements

Firstly I want to thank God Almighty for his guidance throughout this study, for without him I would not have come this far.

My immense gratitude goes to my supervisor Professor R.D Sanderson for his guidance, financial and academic support.

I would also like to thank the following people and organizations for their contributions to this project:

All the staff at the Department of Chemistry and Polymer Science, Dr Margie Hurndall, Mrs Erinda Cooper, Mrs Aneli Fourie, Mr Deon Koen, Mr Jim Motshweni and Mr Calvin Maart

The analysts Dr Jean McKenzie and Elsa Malherbe for NMR analysis, Illana Bergh for PAS-FTIR, Madeline Frazenburg for SEM, Gareth for SEC and Dr Jan Gertenbach for DSC, TGA and XRD

All Free Radical Lab members and Mondi Uncoated Fine Paper group members : Dr M. Zou, Christo, Howard, Ingrid, Donna, Carin, Ashwell and Marehette

Friends and family for their encouragement and motivation

Mondi Uncoated Fine Paper and NRF for funding

Rueben, my love and pillar of strength, for standing by my side throughout my studies.

May God bless you all.

Table of Contents

Declaration.....	ii
Abstract	iv
Opsomming.....	v
Acknowledgements	vi
Table of Contents.....	vii
Table of Figures.....	xii
Table of Schemes	xiv
List of Symbols	xv
List of Abbreviations.....	xvi
Chapter 1	1
Introduction and objectives	1
1.1 Introduction	1
1.2 Objectives.....	1
1.3 Layout of thesis	2
References.....	4
CHAPTER 2	5
Historical and theoretical background	5
2.1 History of poly(vinyl alcohol)	5
2.2 General properties and applications	5
2.3 Synthesis of PVA.....	6
2.3.1 Free radical polymerization	7
2.3.1.1 Initiation.....	7
2.3.1.2 Propagation	9
2.3.1.3 Termination.....	9
2.3.2 General polymerization kinetics	10
2.3.3 Converting poly(vinyl ester) to poly(vinyl alcohol)	11
2.4 Structure–property relationships.....	12
2.4.1 Stereoregularity.....	13
2.4.1.1 Factors affecting stereoregularity in PVA.....	15
2.5 Modification of PVA.....	16
2.5.1 Why the need for modified PVA?	16

2.5.2 Types of modification	17
2.5.3 Copolymerization.....	17
2.5.3.1 Determination of copolymer composition.....	18
2.5.4 Anionic and cationic modification of PVA by copolymerization	19
2.5.4.1 Copolymerization with anionic monomers.....	20
2.5.4.2 Copolymerization with cationic monomers.....	21
2.5.5 Post polymerization modification of PVA	22
2.5.5.1 Graft copolymerization.....	22
2.5.5.2 Grafting from PVA with anionic monomers	23
2.5.5.3 Grafting from PVA with cationic monomers	23
2.5.6 Reactions of the hydroxyl group.....	23
2.5.6.1 Etherification.....	24
2.5.6.2 Esterification	24
2.5.7 Crosslinking PVA	25
2.6 Poly(vinyl alcohol) fiber.....	26
2.6.1 Synthesis of PVA fibers	26
2.6.2 <i>In situ</i> fibrillation of PVA	27
2.6.2.1 Mechanism of <i>in situ</i> fibrillation of PVA fiber.....	27
2.6.3 Modification of PVA fiber	28
References.....	29
CHAPTER 3	34
Synthesis of poly(vinyl alcohol) precursor.....	34
3.1: Introduction	34
3.2 Polymerization of VPi and VAc	35
3.2.1 Materials.....	35
3.2.1.1 Purification of reagents.....	35
3.2.2 Synthesis of poly(vinyl pivalate) by thermal initiated polymerization.....	36
3.2.3 Synthesis of poly(vinyl pivalate) by photoinitiated polymerization.....	36
3.3 Analyses.....	37
3.3.1 Size exclusion chromatography (SEC)	37
3.3.2 Proton nuclear magnetic resonance spectroscopy (¹ H NMR)	37
3.3.3 Conversions by gravimetry.....	38
3.4 Results and discussion	38
3.4.1 Conversions	38

3.4.2 Molecular weight and molecular weight distributions.....	39
3.4.3 PVPI/PVAc copolymer compositions.....	40
3.5 Conclusions	43
References.....	44
CHAPTER 4	45
Synthesis of syndiotacticity rich poly(vinyl alcohol) microfibrils.....	45
4.1 Introduction	45
4.2 <i>In situ</i> fibrillation of PVA	46
4.2.1. Materials.....	46
4.2.1.1 Purification of reagents.....	46
4.2.2 Saponification of PVPI.....	46
4.2.3 Saponification of PVPI-co-VAc	47
4.3 Analyses.....	47
4.3.1 ¹ H and ¹³ C NMR.....	47
4.3.2 Scanning electron microscopy (SEM)	47
4.3.3 Thermal analysis	47
4.3.4 X-ray diffraction (XRD).....	47
4.4 Results and discussion	48
4.4.1. Degree of polymerization of PVA	48
4.4.2 Microstructural analysis	48
4.4.2.1 Degree of saponification.....	49
4.4.2.2 Stereoregularity.....	50
4.4.3 Number average lengths.....	55
4.4.4 Crystallinity of PVA	56
4.4.5 Effect of syndiotacticity on the morphology of PVA microfibrils.....	57
4.4.6 Effect of syndiotacticity on thermal properties	60
4.5 Conclusions	63
References.....	64
CHAPTER 5	66
Heterogeneous modification of PVA microfibrils	66
5.1 Introduction	66
5.1.1 Crosslinking of PVA fibers	66
5.1.2 Heterogeneous cationic and anionic modification of PVA fibers.	67
5.2 Crosslinking PVA microfibrils with glyoxal	68

5.2.1 Materials	68
5.2.2 Procedure	68
5.2.3 Analyses	69
5.2.3.1 NMR	69
5.2.3.2 Thermal analysis	69
5.2.4 Results and discussion.....	69
5.2.4.1 Evidence of crosslinking	69
5.2.4.2 Factors affecting the degree of crosslinking	70
5.2.5 Thermal properties	71
5.3 Cationic and anionic modification.....	73
5.3.1 Materials	73
5.3.2 Anionic modification	74
5.3.2.1 Carboxymethylation of PVA microfibrils	74
5.3.2.2 Grafting PAA from PVA microfibrils.....	74
5.3.3 Cationic modification.....	75
5.3.3.1 Grafting PDMC from PVA microfibrils.....	75
5.3.4 Analyses	76
5.3.4.1 Grafting parameters.....	76
5.3.4.2 PAS-FTIR spectroscopy	76
5.4 Results and discussion	76
5.4.1 Carboxymethylation of PVA microfibrils.....	76
5.4.1.1 Evidence of carboxymethylation.....	76
5.4.1.2 Thermal analysis	77
5.4.1.3 SEM analysis	79
5.4.2 Grafting PAA from PVA microfibrils.....	79
5.4.2.1 Evidence of grafting	79
5.4.2.2 Grafting parameters.....	82
5.4.2.3 Thermal analysis	82
5.4.2.4 SEM analysis	84
5.4.3 Grafting PDMC from PVA microfibrils	84
5.4.3.1 Evidence of grafting	84
5.4.3.2 Grafting parameters.....	86
5.4.3.3 Thermal analysis	86
5.4.3.4 SEM analysis	88

5.5 Conclusions	89
References.....	90
Chapter 6	92
Summary, conclusions and suggestions for future work	92
6.1 Summary	92
6.2 Conclusions	93
6.3 Recommendation for future research	94
References.....	95
Appendix 1.....	96
¹³ C NMR analysis of syndiotactic PVA.....	96
Appendix 2.....	98
XRD analysis of PVA samples of varying syndiotacticities.....	98
Appendix 3.....	99
SEM image of PVA with an s-diad content of 60.3%	99
Appendix 4.....	100
Infrared spectrum of unmodified PVA microfibrils	100
Appendix 5.....	101
¹ H NMR spectrum of CMPVA	101
Appendix 6.....	102
DSC analysis of CMPVA	102
Appendix 7.....	103
SEM image of carboxymethylated PVA fibres.....	103
Appendix 8.....	104
¹ H NMR analysis of PAA homopolymer extracts.....	104
Appendix 9.....	105
SEM image of PVA-g-PAA microfibrils.....	105
Appendix 10.....	106
¹ H NMR analysis of PDMC homopolymer extracts	106
Appendix 11.....	107
SEM image of PVA-g-PDMC microfibrils	107

Table of Figures

Fig. 2.1 Monomer placements in PVA.....	13
Fig. 2.2. Isotactic, syndiotactic and atactic sequences of fully hydrolyzed PVA.....	13
Fig. 2.3 PVA diad sequences.....	14
Fig. 2.4 PVA triad sequences for fully hydrolyzed PVA.....	14
Fig. 2.5 Block, random, alternating and graft copolymers.....	17
Fig. 2.6 Cationic monomers copolymerized with VAc.....	22
Fig. 3.1 Conversion–time plot of UV initiated bulk polymerization of VPi. ($[VPi]/[AIBN] = 1721$).....	39
Fig. 3.2 1H NMR spectra of PVAc (A) and PVPi (B).....	40
Fig. 3.3 1H NMR spectra of VPi/VAc copolymers of varying VPi feed ratios (mol %).	41
Fig. 4.1 Poly(vinyl alcohol): (A) partially hydrolyzed and (B) fully hydrolyzed.....	49
Fig. 4.2 1H NMR spectra of PVA with varying degrees of saponification: (A) 98 % and (B) > 99%.....	50
Fig. 4.3 ^{13}C NMR spectrum of PVA: (A) methine carbon region and (B) methylene carbon region.....	51
Fig. 4.4 Effect of VPi content on syndiotacticity of PVA.....	55
Fig. 4.5 Number average lengths of PVA.....	56
Fig. 4.6 X-ray powder diffraction profile of syndiotactic PVA microfibrils.....	57
(s-diad content = 60.3%).....	57
Fig. 4.7 Unit cell of PVA (monoclinic) (solid lines represent covalent bonds and dotted lines represent hydrogen bonds.....	58
Fig. 4.8 Images of PVAs with different s-diad contents: (A) 61.8% (i) optical micrograph and (ii) SEM image; (B) 58.0% (i) x1000 and (ii) x2500; (C) 57.1% (i) x1660 and (ii) x3000; (D) 55.7% (i) x3470 and (ii) x25000.....	59
Fig. 4.9 TG and DTGA thermograms of PVA microfibrils.....	61
Fig. 5.1 1H NMR spectra of crosslinked and unmodified PVA microfibrils.....	70
Fig. 5.2 TGA (solid line) and DTGA (dotted line) thermograms of uncrosslinked (grey) and crosslinked (black) PVA microfibrils.....	72
Fig. 5.3 PAS-FTIR spectra of PVA and carboxymethylated PVA (CMPVA).....	77
Fig. 5.4 Thermogravimetric analysis of CMPVA.....	78
Fig. 5.5 PAS-FTIR spectra of PVA and PVA-g-AA.....	80
Fig. 5.6 1H NMR spectra of PVA and PVA-g-PAA.....	81

Table of Figures

Fig. 5.7 ^{13}C NMR spectrum of PVA-g-AA.	81
Fig. 5.8 DTGA thermograms of PVA (black) and PVA-g-AA (grey).	83
Fig. 5.9 PAS-FTIR spectra of PVA and PVA-g-PDMC.	85
Fig. 5.10 ^1H NMR spectrum of PVA-g-PDMC.	85
Fig. 5.11 ^{13}C NMR spectrum of PVA-g-PDMC.	86
Fig. 5.12 TGA thermogram (black) and DTGA curve (grey) of PVA-g-PDMC.	87
Fig. A1 ^{13}C NMR spectrum of methine carbon atom of PVA measured in $\text{DMSO-}d_6$	96
Fig. A2 X-ray powder diffraction profiles for PVA samples of varying s-diad contents.	98
Fig. A.3 SEM image of PVA (s-diad content of 60.3 %, VPi content in precursor: 98.8 mol %).	99
Fig. A4 FT-IR spectrum of unmodified poly(vinyl alcohol).	100
Fig. A5 ^1H NMR spectrum of carboxymethylated PVA fibers.	101
Fig. A6 DSC thermograms of carboxymethylated PVA microfibrils (CMPVA).	102
Fig. A7 SEM image of carboxymethylated PVA microfibrils	103
Fig. A8 ^1H NMR spectrum of extracted PAA homopolymer in $\text{DMSO-}d_6$	104
Fig. A9 SEM image of PVA-g-PAA microfibrils.	105
Fig. A10 ^1H NMR spectrum of extracted PDMC homopolymer in D_2O	106
Fig. A11 SEM image of PVA-g-PDMC microfibrils.	107

Table of Schemes

Scheme 2.1: Tautomerization of vinyl alcohol to acetaldehyde	7
Scheme 2.2 Preparation of poly(vinyl alcohol) from poly(vinyl acetate)	12
Scheme 2.3 Copolymerization and hydrolysis of acrylic acid and vinyl acetate.....	20
Scheme 2.4 Copolymerization and alcoholysis of vinyl acetic acid and vinyl acetate	20
Scheme 2.5 Copolymerization and hydrolysis of maleic anhydride and vinyl acetate.....	21
Scheme 2.6 Copolymerization and hydrolysis of itaconic acid and vinyl acetate	21
Scheme 2.7 Williamson's etherification of PVA.....	24
Scheme 2.8 Esterification reaction of PVA with succinic anhydride	25
Scheme 3.1 Polymerization of vinyl pivalate	35
Scheme 3.2: Copolymerization of vinyl pivalate and vinyl acetate.....	35
Scheme 5.1 Crosslinking of PVA with glyoxal	67
Scheme 5.2 Carboxymethylation of crosslinked PVA	67
Scheme 5.3 Hydrogen bonding between carboxylic acid groups of CMPVA	78

List of Symbols

$[M]$	Monomer concentration
f	Initiator efficiency
I_a/I_0	Intensity of light absorbed
k_d	Initiator decomposition rate constant
k_{ij} ($i, j = 1, 2, 3, \dots$)	Rate constant for the addition of monomer j to monomer i
k_p	Propagation rate constant
k_{tc}	Rate constant for termination via combination
k_{td}	Rate constant for termination via disproportionation
M	Monomer species
M_n	Number average molecular weight
P_n/DP	Number average degree of polymerization
r_i	Reactivity ratio of monomer i
ν	Kinetic chain length
Φ	Quantum yield

List of Abbreviations

AA	Acrylic acid
ADMVN	2,2'-Azobis (2,4-dimethylvaleronitrile)
AIBN	2,2'-Azobis (isobutyronitrile)
BPO	Benzoyl peroxide
CMPVA	Carboxymethylated PVA
DMC	2-methacryloyloxy ethyl trimethyl ammonium chloride
DMSO	Dimethylsulfoxide
DSC	Differential scanning calorimetry
DTGA	Differential mass loss (TGA)
FRP	Free radical polymerization
IR	Infrared spectroscopy
KOH	Potassium hydroxide
KPS	Potassium persulfate
MCAA	Monochloroacetic acid
MEK	Methyl ethyl ketone
MeOH	Methanol
MHz	Megahertz
Na ₂ S ₂ O ₃	Sodium thiosulfate
NaOH	Sodium hydroxide
NMR	Nuclear magnetic resonance spectroscopy
PAS-FTIR	Photoacoustic Fourier transform infrared spectroscopy
PDI	Polydispersity index
PVA	Poly(vinyl alcohol)
PVAc	Poly(vinyl acetate)
PVEst	Poly(vinyl ester)
PVPi	Poly(vinyl pivalate)
S-diad	Diad syndiotacticity content (<i>r</i>)
SEC	Size exclusion chromatography
TBA	Tertiary butyl alcohol
TGA	Thermogravimetric analysis

List of Abbreviations

THF	Tetrahydrofuran
T _m	Crystalline melting temperature
T _{onset}	Onset temperature for thermal decomposition
UV	Ultraviolet
VAc	Vinyl acetate
VPi	Vinyl pivalate
XRD	X-ray powder diffraction

Chapter 1

Introduction and objectives

1.1 Introduction

Polymers can be classified into two main groups based on their origin: synthetic and natural. Natural polymers include all naturally occurring macromolecules such as cellulose, starch, DNA, proteins and natural rubber, whilst synthetic polymers are man-made polymers and include most plastics, e.g. polyethylene, polypropylene, polystyrene and poly(vinyl alcohol). Most of these synthetic polymers can be tailor-made to suit desired functions. The greatest obstacles for some applications are biocompatibility and biodegradability.

Poly(vinyl alcohol) (PVA) finds wide use in industries such as the medical,^{1,2} packaging,³ paper^{3,4} and building industries⁵⁻⁹ because of its extraordinary properties, which include excellent mechanical and thermal properties, oxygen barrier properties, solvent and oil resistance, water solubility, biocompatibility and biodegradability.^{10,11} As a result of these desirable properties, PVA is often spun into fibers and used in a range of applications which include paper making.¹²

In order to impart the desired properties for advanced applications PVA can be modified by pre- or post-polymerization techniques. The former involves copolymerization of the vinyl ester monomer i.e. vinyl acetate, with a monomer of required functionality, followed by saponification.¹³⁻¹⁵ The latter involves secondary reactions of the hydroxyl groups,¹⁶ or grafting.^{17,18}

The properties of PVA can be controlled by varying its stereoregularity.³ Stereochemical control is achieved by varying the vinyl ether and ester monomers used for the preparation of the precursor of PVA. Syndiotacticity rich PVA is most desirable as an additive in the paper industry because of its enhanced thermal and mechanical properties, arising from its high crystallinity compared to atactic PVA.^{19,20} Hence the syndiotactic PVA was the main focus in this work.

1.2 Objectives

The main objectives in this work were to:

- i. Prepare syndiotactic PVA microfibrils for use as a polymeric additive in the paper industry. Here the aims were to:
 - investigate and design a simple method of preparing syndiotactic PVA microfibrils
 - synthesize PVA microfibrils of varying syndiotacticities
 - investigate the effects of syndiotacticity on the morphology, thermal stability and crystalline melting temperature of PVA.
- ii. Modify the syndiotactic PVA microfibrils using cationic and anionic monomers in order to enhance fiber–filler and fiber–fiber interactions.
- iii. Investigate the thermal properties of modified PVA microfibrils and study the effects of modification on the thermal properties

1.3 Layout of thesis

A brief introduction to the topic of this study and the objectives of the study are given in Chapter 1.

An overview of the chemistry of PVA, including structure–property relationships and PVA modification is presented in Chapter 2. *In situ* fibrillation is introduced as a relatively simple method for the preparation of syndiotacticity rich PVA microfibrils.

The preparation of poly(vinyl pivalate) by thermoinitiated and photoinitiated free radical polymerization (FRP) is described in Chapter 3. The influences of the method of initiation on the molecular weight and polydispersity index values (PDIs) of the resultant polymer were investigated. PVPi-co-PVAc polymers of varying comonomer composition were also prepared with the aim of varying the syndiotacticity in PVA. The polymers were characterized by nuclear magnetic resonance spectroscopy (NMR) and size exclusion chromatography (SEC).

Chapter 4 focuses on the preparation of syndiotactic PVA microfibrils by saponification of PVPi and PVPi/PVAc copolymers and their characterization by X-ray powder diffraction (XRD), NMR, thermogravimetric analysis (TGA) and differential scanning calorimetry (DSC). A novel method for the preparation of syndiotacticity rich PVA particles that does not involve the conventional suspension or emulsion polymerization techniques is also reported.

A smart method of surface modification of PVA microfibrils is described in Chapter 5. The chapter is divided into two main sections: the first describes the crosslinking of PVA microfibrils and the second describes the modification of the crosslinked microfibrils using cationic and anionic monomers.

The final chapter presents the conclusions, brief mention of the challenges encountered during the study, and suggestions for future research.

References

1. Reisa, E. F. d.; Campmposa, F. S.; Lagea, A. P.; Leitea, R. C.; Heneineb, L. G.; Vasconcelosc, W. L.; Lobatoa, Z. I. P.; Mansurc, H. S. *Mater. Res. Bull.* **2005**, 9, 185–191.
2. Li, W.; Xue, F.; Cheng, R. *Polymer* **2005**, 46, 12026–12031.
3. Finch, C. A., *Poly(vinyl alcohol) : Properties and Applications*. John Wiley and Sons: London, 1973.
4. Finch, C. A., *Poly(vinyl alcohol) : Developments*. John Wiley and Sons: London, 1992.
5. Garrett, P. D.; Grubb, D. T. *Polym. Commun.* **1988**, 29, 60.
6. Su, J.; Wang, Q.; Wang, K.; Zhang, Q.; Fu, Q. *J. Appl. Polym. Sci.* **2008**, 107(6), 4070–4075.
7. Lee, Y. J.; Shin, D. S.; Kwon, O. W.; Park, W. H.; Choi, H. G.; Lee, Y. R.; Han, S. S.; Noh, S. K.; Lyoo, W. S. *J. Appl. Polym. Sci.* **2007**, 106, 1337–1342.
8. Bhat, G. S.; Tock, R. W.; Parameswaran, S.; Ramkumar, S. S. *J. Appl. Polym. Sci.* **2004**, 96, 557–559.
9. Wang, Y.; Hsieh, Y. L. *J. Membr. Sci.* **2008**, 309, 73–81.
10. Nagara, Y.; Nakano, T.; Okamoto, Y.; Gotoh, Y.; Nagura, M. *Polymer* **2001**, 42, 9679–9686.
11. Lyoo, W. S.; Ha, W. S. *Polymer* **1999**, 40, 497–505.
12. Hollander, O. Poly(vinyl alcohol) fibers containing acicular colloidal clay. US4157275, 1977.
13. Moritani, T.; Yamauchi, J. *Polymer* **1998**, 39, 559–572.
14. Moritani, T.; Yamauchi, J. *Polymer* **1998**, 39, 553–557.
15. Moritani, T.; Okaya, T. *Polymer* **1998**, 39(4), 923–931.
16. Mukherjee, G. S.; Shukla, N.; Singh, R. K.; Mathur, G. N. *J. Sci. Ind. Res.* **2004**, 63, 596–602.
17. Zhou, Z.; Xu, W.; He, D.; Fan, J.; Yu, F.; Ren, F. *J. Appl. Polym. Sci.* **2007**, 103, 848–852.
18. Atta, A. M.; Maysour, N. E.; Arndt, K. F. *J. Polym. Res* **2006**, 13, 53–63.
19. Lyoo, W. S.; Blackwell, J. *Macromolecules* **1998**, 31, 4253–4259.
20. Lyoo, W. S.; Han, S. S.; Kim, J. H.; Yoon, W. S.; Lee, C. J.; Kwon, I. C.; Lee, J.; Ji, B. C.; Han, M. H. *Angew. Makromol. Chem.* **1999**, 271, 46–52

CHAPTER 2

Historical and theoretical background

2.1 History of poly(vinyl alcohol)

Poly(vinyl alcohol) (PVA) was first prepared by Herrmann and Haehnel in 1924 via the base catalyzed alcoholysis of poly(vinyl esters).¹ The reactions were not commercially viable as large amounts of heat were evolved, which made the reactions hazardous. In 1925, the duo developed new and safe methods for the large scale production of poly(vinyl acetate),¹ resulting in vinyl acetate (VAc) becoming the most widely used monomer for the preparation of PVA precursor.

The PVA prepared was colloidal in form and was used in textile sizing. In 1931 they then proposed the preparation of PVA fiber. This was a novel idea, which was only put into practice seven years later by Sakurada *et al.* (cited in Finch¹) who prepared acetalized PVA fiber which closely resembled viscose rayon and cotton fibers. At that time PVA fibers were regarded as a possible replacement for cellulose in some applications.¹ However, due to the high costs associated with their production PVA fibers have not yet reached their full potential.

2.2 General properties and applications

Polymer application is indisputably related to polymer structure. Typically PVA is a polyhydroxyl polymer (with a 1, 3 glycol structure) capable of undergoing both intra and intermolecular hydrogen bonding. The small size and the strong hydrogen bond interactions of the hydroxyl groups force the polymer chains into a crystal lattice resulting in PVA being partially crystalline. Consequently PVA has excellent mechanical and thermal properties; excellent oxygen barrier properties; oil, grease and organic solvent resistance; low moisture permeability; high heat resistance and UV and IR radiation stability. In addition to this it is biodegradable and non-toxic. Likewise fibers derived from PVA have similar properties and in addition, they have high tensile and compressive strengths, high tensile modulus and high abrasion resistance.

As a result of these unparalleled properties PVA has found usage as adhesives,¹⁻³ colloids in emulsion polymerization,^{1,4} binders in the paper industry,^{1,2} films,⁵⁻⁷ membranes,^{8,9} as drug

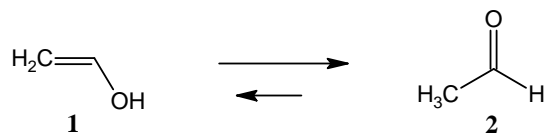
delivery systems in medicines, cancer cell-killing embolic material^{2,10-13} and in textile and paper sizing^{1,2}. PVA fibers have been used in the clothing and building industries. As a result of their similarity to cellulose fibers in structure and properties, PVA fibers are potential replacements of cellulose in numerous applications.²

The major contributory factor towards the wide application of PVA is its water solubility. Water solubility is dependent upon the degree of hydrolysis, molecular weight, crystallinity and temperature.¹ The aqueous solubility of fully hydrolyzed PVA is brought about by its hydroxyl groups which have a high affinity to water resulting in strong hydrogen bonding. Partially hydrolyzed PVA has hydrophobic residual acetate groups which are expected to reduce solubility, but these however weaken intra and intermolecular hydrogen bonding, causing dissymmetry and lowered crystallinity so resulting in an increase in water solubility.²

PVA properties vary with the method of preparation of the precursor (such as PVAc) i.e. in bulk, solution, or emulsion/suspension. Bulk and solution polymerizations often result in colloids upon hydrolysis, while emulsion/suspension results in spherical particles. The type of monomer used also influences the properties. Divinyl compounds,¹ vinyl ethers^{14,15} and esters¹⁶⁻¹⁸ have been used in PVA synthesis. Vinyl esters are preferred as they are inexpensive to obtain and their polymerization is relatively economical compared to divinyl compounds and vinyl ethers. Therefore the focus will be on the preparation of PVA from poly(vinyl esters).

2.3 Synthesis of PVA

PVA cannot be synthesized directly from its vinyl alcohol monomer. This is because vinyl alcohol **1** tautomerizes to the more stable acetaldehyde **2**, as shown in Scheme 2.1. As a result of this tautomerization PVA is often synthesized via a two-step process, with the first step involving synthesis of the appropriate poly(vinyl ester) (PVEst) and the second step being the hydrolysis of the PVEst to PVA. Industrially, PVA is prepared via the hydrolysis of poly(vinyl acetate) (PVAc) synthesized by bulk,¹⁹ solution^{20,21} or suspension²² free radical polymerization.



Scheme 2.1: Tautomerization of vinyl alcohol to acetaldehyde

2.3.1 Free radical polymerization

Free radical polymerization (FRP) is preferred industrially because it can be carried out under undemanding conditions compared to ionic or coordination polymerizations. FRP can tolerate trace amounts of impurities such as oxygen and inhibitor, and is also tolerant to most functional groups. The general steps in FRP are initiation, propagation and termination.

2.3.1.1 Initiation

Initiation involves the production of primary free radicals. Primary radicals can be produced via four basic initiating systems: thermal, redox, photochemical and ionizing radiation.

Thermal initiation: involves the homolytic decomposition of the initiating molecule resulting in the formation of two primary radicals (I) as shown in Table 2.1. Commonly used thermoinitiators are azo and peroxy compounds, such as 2,2' azobisisobutyronitrile (AIBN) and benzoyl peroxide (BPO).

The rate of thermoinitiation (v_i) is determined by initiator decomposition and is given by equation 2.1

$$v_i = 2fk_d[I] \quad (2.1)$$

where [I] is the initiator concentration, k_d is the initiator decomposition rate constant, f is the initiator efficiency defined as the fraction of radicals produced that proceed to initiate polymerization, and 2 is the factor illustrating that radical production is in pairs.

Redox initiation: involves the production of radicals via oxidation–reduction reactions. There are four main types of redox initiator systems: peroxide/reducing agent, inorganic reductant/inorganic oxidant, organic/inorganic redox pairs, and the case where the monomer is part of the redox pair. Examples of these are given in Table 2.1.

Table 2.1 Free radical polymerization initiation systems

Initiating system	Description
Thermal ^{20,23}	$I \xrightarrow[k_d]{\Delta} 2 I^\bullet$ e.g. AIBN, ADMVN
Redox ^{21,24-27}	1) Peroxide with a reducing agent: $H_2O_2 + Fe^{2+} \longrightarrow HO^- + HO^\bullet + Fe^{3+}$ 2) Inorganic reducer and inorganic oxidizer $\bar{O}_3SOOSO_3^- + S_2O_3^{2-} \longrightarrow SO_4^{2-} + \bullet SO_4^- + \bullet S_2O_3^{2-}$ 3) Organic–inorganic redox pair $RCH_2OH + Ce^{4+} \longrightarrow Ce^{3+} + H^+ + \dot{R}CHOH$
Photochemical ²⁸⁻³¹	$M + h\nu \longrightarrow {}^3[M]^* \longrightarrow R^\bullet + R'^\bullet$ e.g. AIBN,ADMVN $M + h\nu \longrightarrow {}^3[M]^* \xrightarrow{R-H} R^\bullet + \bullet M-H$ e.g. benzil or benzophenone and a tertiary amine/ether
Ionizing radiation ³²	$M + \text{radiation} \longrightarrow M^{\bullet+} + e^-$ e.g. γ -radiation

I- thermoinitiator, ADMVN – 2,2'-azobis (2,4-dimethylvaleronitrile), R, R'- initiating radicals, M, M* - photoinitiator/monomer in the ground state and excited triplet state respectively, R-H - co-initiator (tertiary amine)

The rate of redox initiation is dependent upon the decomposition rate constant and is given as shown in equation 2.2.

$$v_i = k_d[\text{red}][\text{ox}] \quad (2.2)$$

where [red] and [ox] are the concentrations of the reducing and oxidizing agents respectively.

Photochemical initiation: this mode of initiation occurs when radicals are produced by ultra-violet radiation or visible light. Primary radicals can be produced via two main processes, both of which involve excitation of the initiating molecule following energy absorption. In the first case the molecule undergoes decomposition into radicals and in the second the excited molecule interacts with a second molecule (co-initiator or monomer), abstracts a hydrogen atom and forms the initiating radicals. These two phenomena are illustrated in Table 2.1.

The rate of photochemical initiation is given by

$$v_i = 2\phi I_a \quad (2.3)$$

where I_a is the intensity of light absorbed in moles and ϕ the quantum yield defined as the number of propagating chains initiated per photon of light absorbed, and 2 a factor indicating the number of radicals produced.

Ionizing radiation: there are a number of radioactive sources and particle accelerators for initiation by ionizing radiation. These include electrons, neutrons, α -particles, γ and X-rays. The equation in Table 2.1 illustrates the generation of a cationic radical. The route taken by the generated species thereafter is dependent on the reaction conditions, implying it can either undergo cationic or free radical polymerization.

2.3.1.2 Propagation

Following primary radical production, monomer adds to the initiating radical in a process termed propagation and the result is a propagating radical. Attachment of the monomer can occur via two possible routes resulting in a 1, 3 placement (head to tail) or 1, 2 placement (head to head). Which arrangement is favored is dependent on both steric hindrance and resonance stability.

In general the equation for propagation is given as:



The rate of propagation v_p is thus given by:

$$v_p = k_p [M^\bullet] [M]^n \quad (2.5)$$

where k_p is the propagation rate constant, $[M]$ and $[M^\bullet]$ are the concentrations of monomer and monomeric radicals respectively.

2.3.1.3 Termination

Termination is a bimolecular process which occurs by either combination or disproportionation, as illustrated in equations 2.6 and 2.7



k_{tc} and k_{td} are the rate constants for termination via combination and disproportionation respectively.

Apart from initiation, propagation and termination, other reactions are known to take place in the reaction media namely:

- fragmentation of primary radicals³³
- primary radical termination by inhibitors^{33,34}
- cage reactions³⁴
- chain transfer reactions³³

Only chain transfer reactions will be referred to later in this work as they predominantly affect vinyl ester polymerizations.³³

2.3.2 General polymerization kinetics

The extent to which propagation takes place before termination occurs is referred to as the kinetic chain length (ν). The kinetic chain length is defined as the total number of monomer units consumed per total number of initiator fragments produced. In a thermoinitiated system ν is given by:

$$\nu = k_p \frac{[M]}{2 (f k_d k_t [I])^{1/2}} \quad (2.8)$$

where f is the initiator efficiency and 2 is a factor arising from the fact that radical production occurs in pairs; k_p , k_t , k_d are the propagation, termination and decomposition rate constants respectively whilst, $[I]$ and $[M]$ are the initiator and monomer concentrations respectively.

In a photoinitiated system ν is given by:

$$v = k_p \frac{[M]}{(I_0 \phi l \epsilon k_t [I])^{1/2}} \quad (2.9)$$

where I_0 is the incident light intensity, ϕ is the quantum efficiency, l is the path length and ϵ is the molar absorptivity (extinction coefficient).

When equations 2.8 and 2.9 are simplified the kinetic chain length is directly related to the degree of polymerization (DP) as follows:

$$DP = 2 v \quad (2.10)$$

$$DP = v \quad (2.11)$$

Equation 2.10 is typical when termination is via combination. The kinetic chain length doubles because one polymer chain is formed from two polymer chains. When termination is via disproportionation one polymer chain is formed for every kinetic chain, and the result is an insignificant change in kinetic chain length as shown in equation 2.11.

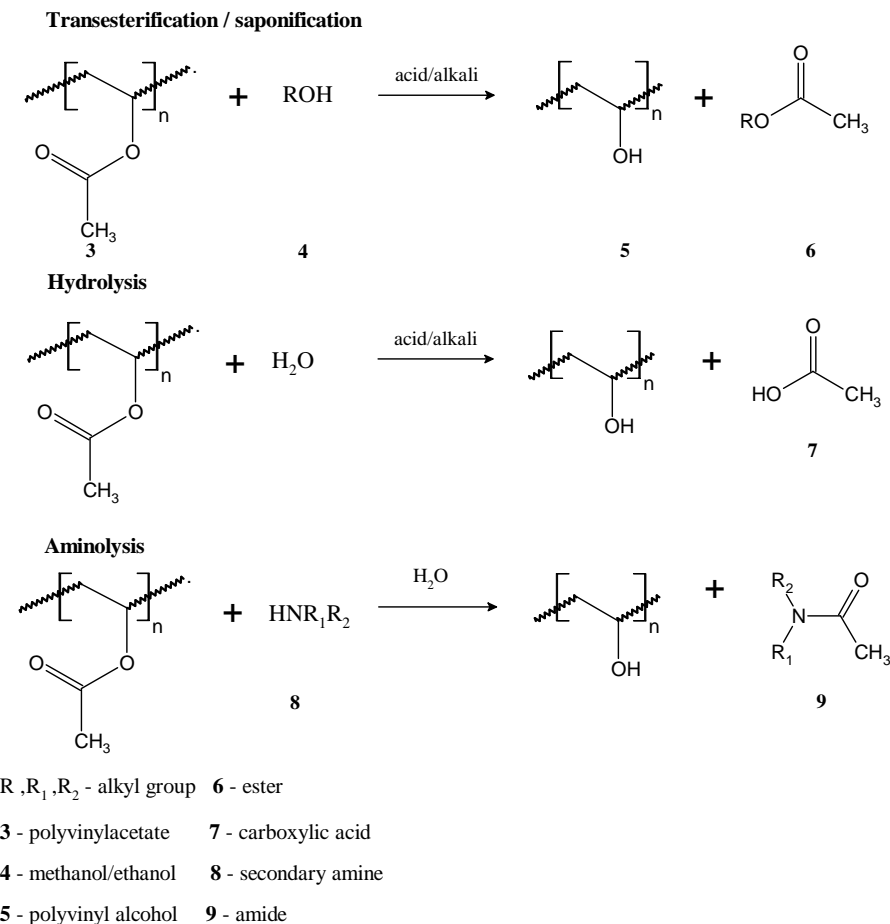
The relationship between the number average molecular weight (M_n) and the degree of polymerization (DP) is given by:

$$M_n = M_0 \times DP \quad (2.12)$$

where M_0 is the molecular weight of monomer.

2.3.3 Converting poly(vinyl ester) to poly(vinyl alcohol)

Poly(vinyl esters) (PVEs) are converted to PVAs by any of the following techniques transesterification/saponification, hydrolysis and aminolysis (as illustrated in Scheme 2.2). Saponification and hydrolysis can either be base or acid catalyzed. Common base catalysts used include sodium or potassium hydroxide and sodium methoxide, while acid catalysts used include hydrochloric and sulphuric acids.



Scheme 2.2 Preparation of poly(vinyl alcohol) from poly(vinyl acetate)

The extent to which a PVEst can be hydrolyzed is dependent upon the quantity of catalyst/hydrolyzing agent and the duration and temperature of hydrolysis. With the manipulation of these conditions PVA of varying degrees of hydrolysis, and therefore varying properties can be obtained.

2.4 Structure–property relationships

PVEsts from which PVA is derived are seldom crystallizable because of the random steric patterns of the ester groups. PVA on the other hand is crystallizable regardless of the stereoregularity due to the presence of the relatively small hydroxyl group. PVA is thus semi-crystalline.

PVA chain microstructure can be described in terms of sequence distribution and tacticity. In sequence distribution the normal head-to-tail additions result in a 1, 3 glycol structure (Fig. 2.1A). Occasionally there can be head-to-head or tail-to-tail insertions, which result in a 1, 2

glycol structure (Fig. 2.1B). These anomalies have adverse effects on the polymer properties such as lowering of the thermal stability and crystallinity of the resultant PVA.



Fig. 2.1 Monomer placements in PVA.

Incomplete hydrolysis of PVEst also affects the physical properties of the resultant polymer. Moreover, the presence of a substantial number of ester groups leads to a polymer with properties completely different from those of the fully hydrolyzed PVA or the unhydrolyzed PVEst.

2.4.1 Stereoregularity

Polymer configuration and conformation describe its geometric structure. Configuration refers to the order that is determined by chemical bonds which can not be altered unless chemical bonds are broken, while conformation refers to the order arising from the rotation of molecules about the single bonds. Configuration of polymer chains is described by the stereoregularity.

Stereoregularity refers to the arrangement of adjacent repeating units in a polymer chain. Three distinct features are often associated with the stereoregularity of monosubstituted vinyl polymers (monomer type $\text{CH}_2=\text{CHX}$): isotactic, syndiotactic and atactic. When a polymer is isotactic (structure **10**, Fig. 2.2) all the substituents are on the same side of the polymer chain. In the case of a syndiotactic polymer **11**, the polymer chain is composed of alternating substituent groups. In an atactic polymer there is random arrangement of the substituents on either side of the polymer chain (structure **12**).

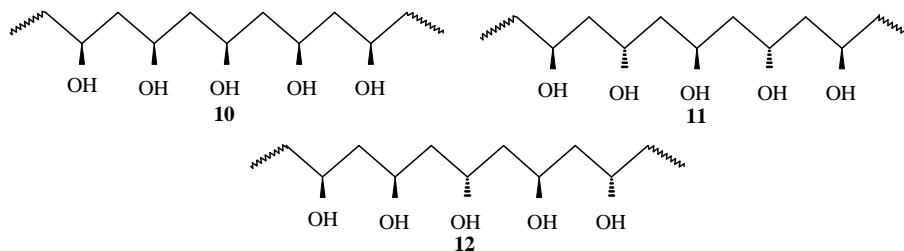


Fig. 2.2. Isotactic, syndiotactic and atactic sequences of fully hydrolyzed PVA.

Depending on the number of repeat units under consideration, tacticity can be further classified in terms of diads, triads, tetrads, pentads e.t.c where by two, three, four and five repeat units are considered. When dealing with diad sequences, the pairs of adjacent repeating units can either be isotactic (meso, structure **13**) or syndiotactic (racemo, structure **14**) to one another as shown in Fig. 2.3



Fig. 2.3 PVA diad sequences.

For triad sequences, three adjacent repeat units are under consideration and they can be described as being isotactic (*mm*, structure **15**), heterotactic (*mr*, structure **16**) or syndiotactic (*rr*, structure **17**) to one another.

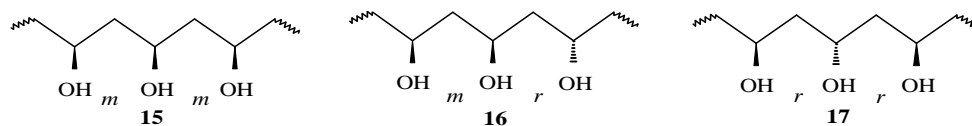


Fig. 2.4 PVA triad sequences for fully hydrolyzed PVA.

Tetrad sequences are given as *mmm*, *mmr*, *rmr*, *mrm*, *rrm* and *rrr*. The same general rules for the assignment of stereosequences are observed for higher tacticities i.e. pentad, heptad, etc.

Generally the FRP propagation mechanism follows Bernoullian statistics.^{34,35} This means that the stereoregularity of the growing chain is not affected by the ultimate or penultimate monomer to be added to the polymer chain. Stereoregularity can be determined by nuclear magnetic resonance (NMR) via integration of the relevant signals³⁶⁻³⁸ or be calculated using the probability parameters P_m and P_r ^{35,38}. P_m is the probability that the polymer chain will add a monomer giving the same sequence, while P_r is the probability that a different sequence will result.

The stereoregularity of polymers has a huge effect on their physical and chemical properties. Industrially, stereochemical control is applied to polyolefins in order to obtain polymers with varying chemical and physical properties.²⁵ Likewise, PVA of different stereoregularities has different properties and stereochemical control is brought about by varying the reaction conditions.

2.4.1.1 Factors affecting stereoregularity in PVA

Stereochemical control in PVA is attained by varying the polymerization conditions and precursor monomer type. Ideally in order to enhance both mechanical and thermal properties of PVA the syndiotacticity should be increased. This is because the higher the syndiotacticity the more regular the distribution of the hydroxyl groups, and consequently the chain packing becomes more compact and dense.

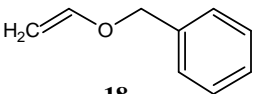
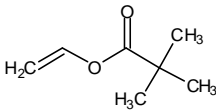
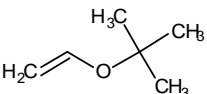
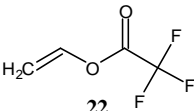
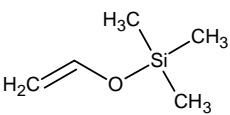
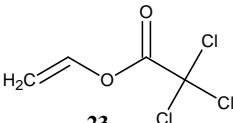
Effect of solvent on stereoregularity of PVA. Initially it was thought that the nature of the solvent had little effect on the stereoregularity of PVA derived from PVAc. Friedlander *et al.*³⁹ polymerized vinyl acetate in the presence of amyl acetate, *n*-butyraldehyde, isobutyraldehyde and methyl ethyl ketone and observed that the tacticity remained the same. However, the intriguing observation made was that there were changes in chemical properties; these were attributed to the differences in molecular weight and chain branching. In 1986 Imai *et al.*⁴⁰ polymerized VAc using a different set of solvents, i.e. DMSO, ethylene carbonate (EC), ethyl acetate (EAc), methanol (MeOH), dilute phenol (17.6% v/v (phenol/water)) and phenol (PhOH). DMSO, EC and EAc resulted in a decrease in syndiotacticity while MeOH, aq-PhOH and PhOH resulted in an increase. This variation in syndiotacticity was attributed to the interactions between the solvents and the monomer.

Nagara *et al.*¹⁷ recently obtained highly syndiotactic PVA from PVAc synthesized in the presence of fluoroalcohols. Hydrogen bonding between the monomer and solvent made the monomer bulkier, consequently favoring syndiotacticity.⁴¹

Effect of monomer on stereoregularity of PVA. The stereoregularity of PVA can be varied by using various vinyl esters or ethers (illustrated in Table 2.2). Vinyl ethers such as benzyl vinyl ether (structure **18**), tert-butyl vinyl ether (structure **19**)^{14,15} and trimethyl silyl vinyl ether (structure **20**)¹⁴ have been used in the preparation of isotactic PVA. Syndiotactic PVA has been prepared from vinyl pivalate **21**,^{17,42-44} vinyl trifluoroacetate **22**^{18,41,45,46} and vinyl trichloroacetate **23**.

The ability of these vinyl ethers and esters to form stereoregular PVA lies in the presence of the bulky groups which favor isotacticity in the former and syndiotacticity in the latter. Yamada *et al.*⁴¹ polymerized various vinyl esters with bulky groups in the presence of fluoroalcohols. They observed that the bulkiness of the monomers was enhanced in the presence of fluoroalcohols due to hydrogen bonding.

Table 2.2 Isotactic and syndiotactic monomers used for PVA synthesis

Isotactic monomers	Syndiotactic monomers
 <p style="text-align: center;">18</p>	 <p style="text-align: center;">21</p>
 <p style="text-align: center;">19</p>	 <p style="text-align: center;">22</p>
 <p style="text-align: center;">20</p>	 <p style="text-align: center;">23</p>

Preparing a polymer with the desired properties is of paramount importance to industry. In addition to changing monomer and solvent so that PVA of the desired stereoregularity and consequently, properties is obtained, PVA can also be modified by pre- and post-polymerization reactions with various compounds, as described in Section 2.5.

2.5 Modification of PVA

2.5.1 Why the need for modified PVA?

PVA is a sought-after polymer because of its excellent properties which include biocompatibility; oil, grease and solvent resistance; low moisture permeation; oxygen barrier properties; and non-toxicity.

In the medical industry, PVA is insolubilized by crosslinking. The hydrogels produced are used in the preparation of contact lenses and materials for drug delivery.⁴⁷⁻⁴⁹ PVA fibers for application in the clothing and construction industries are crosslinked (usually with dialdehydes)⁵⁰ prior to use. Anionic groups are attached onto PVA in order to prepare temperature and pH sensitive hydrogels,⁵¹ soft tissue replacement hydrogels,⁵² water-alcohol separation membranes,^{8,53} and high strength transparent films.^{54,55}

In the paper industry PVA is added as a polymeric additive where it imparts oil, oxygen and moisture resistance properties.² In order to enhance the interactions between PVA and

cellulosic fibers the chemical modification of PVA by attachment of ionic groups is desirable. Attachment of cationic groups enhances the interaction between the anionic cellulosic fibers and the PVA.^{56,57} The ionic bonds formed are stronger than hydrogen bonds, and a combination of the two types of bonds yields better fiber–fiber interactions.

2.5.2 Types of modification

The hydroxyl functionality of PVA undergoes all the reactions typical of secondary alcohols. Modification can thus be brought about by two techniques:

- Copolymerization of the vinyl ester with a second monomer with the required functionality, followed by hydrolysis.^{48,57-59}
- Post polymerization modification, whereby PVA is first prepared and then modified^{24,26,27,52,54,60-72}

2.5.3 Copolymerization

Copolymerization occurs when two or more different types of monomers are incorporated in a polymer chain. Copolymers can be divided into four main groups based on the arrangement of their monomeric units, as illustrated in Fig. 2.5: block **24**, random **25**, alternating **26** and graft **27** polymers.

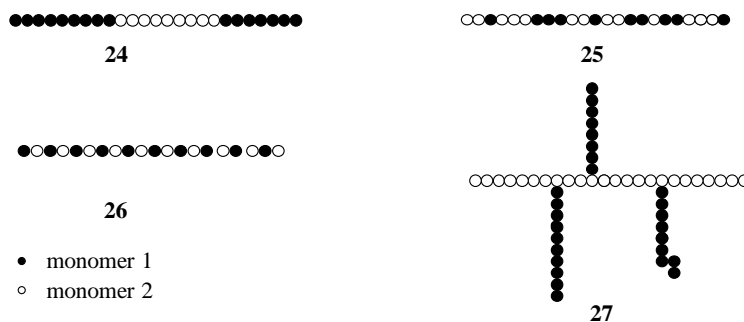


Fig. 2.5 Block, random, alternating and graft copolymers.

Block copolymers comprise two or more homopolymer subunits linked together. The resultant polymer often has properties characteristic of the distinct homopolymer chains. Random copolymers are self explanatory; there is generally no order of monomer arrangement. Alternating copolymers comprise alternating dissimilar monomer units while graft copolymers are branched copolymers, with the main chain being composed of different monomer units to the branches.

For a conventional FRP system the mode of copolymerization, i.e. random, alternate or block copolymerization, is dependent upon the reactivity ratios of the monomers in that system. This is explained further in Section 2.5.3.1. The mechanism of grafting involves the generation of a polymeric radical via the abstraction of a labile atom from a dead polymer.⁷³ Hence the same general rules for determining copolymer composition do not apply. Grafting in this work will thus be considered as a post-polymerization technique.

2.5.3.1 Determination of copolymer composition

In a reaction medium where there are two types of monomers (M_1 and M_2) present monomer addition can occur in one of the four ways illustrated in equations 2.13–2.16.



where k_{11} is the rate constant for the addition of M_1 monomer to a radical ending with the monomer M_1 and k_{12} is the rate constant for the addition of M_2 to a radical ending with the monomer M_1 , etc.

The method of copolymerization that occurs is dependent on the monomer addition rate constants. The propensities are summarized as follows:

- If $k_{11} > k_{12}$ and $k_{22} > k_{21}$ there is a tendency towards block and/or homopolymer formation.
- If $k_{12} > k_{11}$ and $k_{21} > k_{22}$ an alternating copolymer results.
- If $k_{11} = k_{12}$ and $k_{22} = k_{21}$ a random copolymer is formed.^{73,74}

The rate of addition of monomer M_2 to a propagating radical ending with monomer M_1 is equal to the rate of addition of monomer M_1 to the propagating radical ending with monomer M_2 i.e.

$$k_{21} [M_2^\bullet] [M_1] = k_{12} [M_1^\bullet] [M_2] \quad (2.17)$$

The rate for the disappearance of M_1 and M_2 is thus given by:

$$-\frac{d[M_1]}{dt} = k_{11}[M_1][M_1^\bullet] + k_{21}[M_1][M_2^\bullet] \quad (2.18)$$

$$-\frac{d[M_2]}{dt} = k_{22}[M_2][M_2^\bullet] + k_{12}[M_1^\bullet][M_2] \quad (2.19)$$

It can be shown that the composition of copolymer being formed at any given time is given by equation 2.20. By definition:

$$\frac{d[M_1]}{d[M_2]} = \frac{[M_1]}{[M_2]} \frac{r_1[M_1] + [M_2]}{r_2[M_2] + [M_1]} \quad (2.20)$$

where $r_1 = \frac{k_{11}}{k_{12}}$ and $r_2 = \frac{k_{22}}{k_{21}}$

The above is called the **copolymer equation**.

Monomer reactivity ratios (r_1 and r_2) are defined as the ratios for the rate constants for the addition of a monomer to its own propagating radical. If $r_1 > 1$ then the propagating radical M_1 prefers to add monomer M_1 and if $r_1 < 1$ then the propagating radical M_1 prefers to add monomer 2.

A copolymer system is said to be ideal when the two types of propagating radicals show the same preference for adding one or the other of the two monomers i.e. $r_1 r_2 = 1$. In an alternating system the propagating radical prefers to react exclusively with the other monomer, i.e. $r_1 = r_2 = 0$. The result is that monomers alternate regularly along the chain regardless of the composition of monomer feed. In most cases however, the situation lies between ideal and alternating, i.e. $0 < r_1 r_2 < 1$. When $r_1 r_2 > 1$ (i.e. $r_1 > 1$ and $r_2 > 1$) then there is the tendency for the copolymer to form blocks.

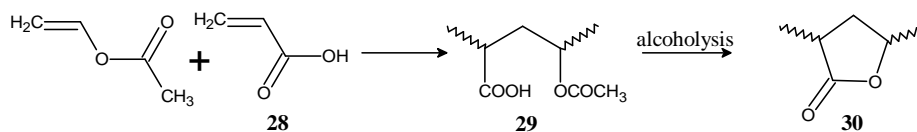
The above rules apply for the modification of polymers in general. In Section 2.5.4 copolymerization will be discussed as a technique used for the modification of PVA and in Section 2.5.5 the post polymerization techniques which include grafting will be considered.

2.5.4 Anionic and cationic modification of PVA by copolymerization

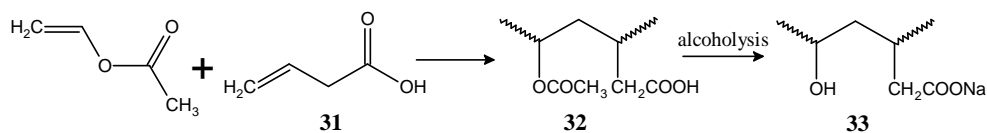
Copolymerizing vinyl esters with vinyl monomers of selected functionality followed by hydrolysis will afford PVA with the required functionality. However, not every cationic or anionic monomer can be used because of side reactions that are known to take place during the hydrolysis.

2.5.4.1 Copolymerization with anionic monomers

Copolymerization of vinyl acetate with a carboxylic acid group containing vinyl monomer followed by alcoholysis appears to be the easiest and most convenient way of obtaining anionic PVA. This is true for certain types of monomers, but for most monocarboxylic acid monomers such as acrylic, crotonic and methyl methacrylic acids alcoholysis results in γ lactone formation (illustrated in Scheme 2.3, structure **30**).^{59,75} When vinyl acetic acid was copolymerized with vinyl acetate and the resultant copolymer hydrolyzed a stable δ hydroxycarboxylate **33** (Scheme 2.4) resulted. The differences in behavior were because the formation of a six membered lactone was relatively slower than the formation of a five membered lactone. Thus the δ hydroxycarboxylate is more stable than the γ hydroxycarboxylate.⁵⁹

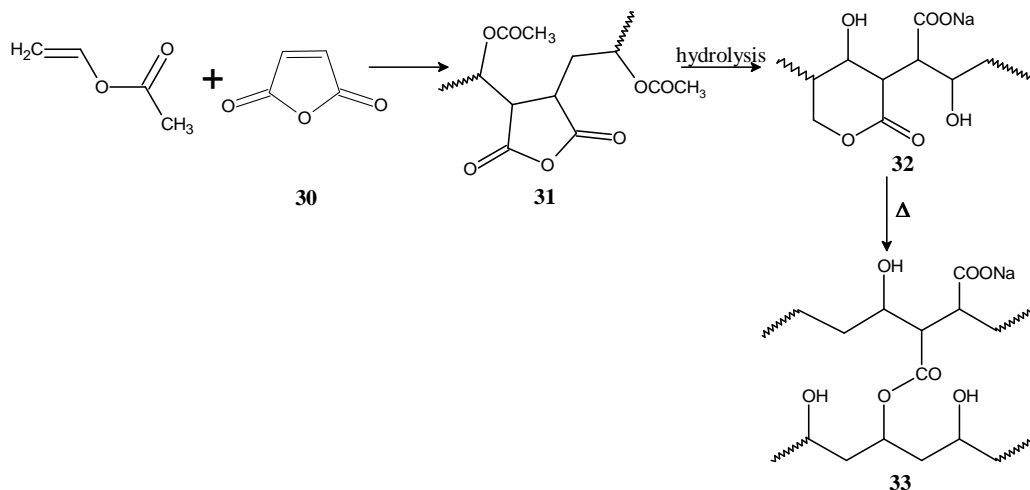


Scheme 2.3 Copolymerization and hydrolysis of acrylic acid and vinyl acetate



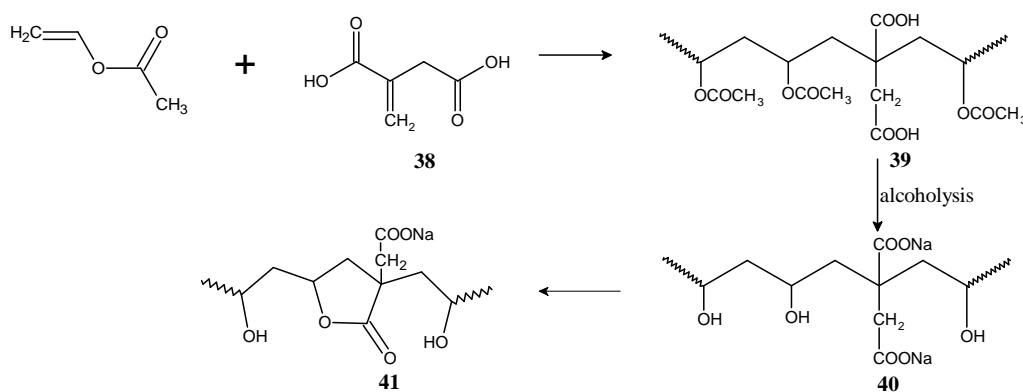
Scheme 2.4 Copolymerization and alcoholysis of vinyl acetic acid and vinyl acetate

Monomers such as maleic anhydride, dimethyl maleate, dimethyl itaconate and monomethyl itaconate yield PVA containing carboxylate groups in the presence of excess NaOH.⁵⁹ When NaOH is not in excess lactone formation takes place and crosslinking results, as illustrated in Scheme 2.5.



Scheme 2.5 Copolymerization and hydrolysis of maleic anhydride and vinyl acetate

Dicarboxylic acids such as itaconic, fumaric and maleic acids can be copolymerized with VAc to afford upon alcoholysis PVA with the carboxylate functionality. When itaconic acid is used the γ - and δ -hydroxycarboxylates (illustrated as structure **40** in Scheme 2.6) are formed. The former is converted to a γ -lactone while the latter remains unchanged (structure **41**).⁵⁹ The major draw back associated with the above monomers is their slight solubility in vinyl acetate. Itaconic acid and maleic acid show a solubility of up to 3 wt % while fumaric acid shows a solubility of up to 1 wt % in a mixture of vinyl acetate and methanol (90/10 wt/wt).



Scheme 2.6 Copolymerization and hydrolysis of itaconic acid and vinyl acetate

2.5.4.2 Copolymerization with cationic monomers

A wide range of cationic monomers have been used to prepare cationic PVA (see Fig. 2.6). 2-acryloyloxy ethyl trimethylammonium chloride **42**, trimethyl-(vinylxyethyl) ammonium chloride **43**, 1-vinyl-2,3-dimethylimidazolium **44**, 3-(methacryloylamino) propyl

trimethylammonium chloride **45** and 3-(methacryloylamino)-3-tetramethylbutane-1-trimethyl ammonium chloride **46** were copolymerized with VAc, followed by alcoholysis using methanol and NaOH.⁵⁷

Copolymerization of VAc with monomer **42** resulted in a 2 mol % incorporation of the monomer in the copolymer. However, upon alcoholysis, the cationic group was removed and a γ -lactone was formed.⁵⁷ Monomers **43** and **44** can be used for the preparation of stable cationic PVA but the only drawback is their low reactivity in copolymerization with VAc. Monomers **45** and **46** are considered to be best for copolymerization because the amide linkage has good resistance towards alkaline hydrolysis. In addition to this the monomers are highly reactive, resulting in then being incorporated.⁵⁷

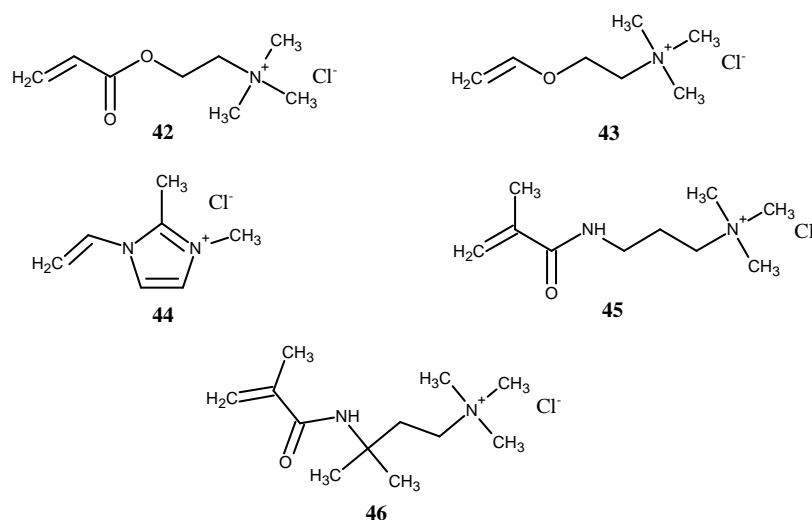


Fig. 2.6 Cationic monomers copolymerized with VAc.

2.5.5 Post polymerization modification of PVA

Post polymerization modification techniques include:

- grafting
- secondary reactions of the hydroxyl group

2.5.5.1 Graft copolymerization

Three methods exist for the synthesis of graft copolymers:

- “Grafting onto”, which involves the reaction of complimentary functional groups of polymers^{25,67}

- b) “Grafting from”, which involves the growing of a polymer chain from a polymeric macroradical (in FRP).^{25,26,61}
- c) “Grafting through”, which involves the copolymerization of a vinyl macromonomer²⁵

Methods (a) and (b) have been reported for the modification of PVA. Generation of polymeric radicals can be brought about by γ radiation,⁵¹ photolysis,⁶¹ electron beam pre-irradiation and redox systems.^{24,27,61} These methods will be discussed briefly in section 2.5.5.2. In this study method (b) was employed.

2.5.5.2 Grafting from PVA with anionic monomers

Grafting from relies on the generation of a radical on the polymer chain and the subsequent addition of the monomer to the polymeric radical. Trimnell and Stout grafted acrylic acid from PVA and starch using photolysis.⁶¹ The graft copolymer obtained had 40–66% graft content and a homopolymer content of between 19–36%. Park et al prepared PVA hydrogels using γ -radiation and subsequently modified them with acrylic and methacrylic acids.⁵¹ They obtained PVA hydrogels with very high degrees of grafting and observed that the degree of grafting increased with an increase in the monomer concentration. Belfakova *et al.*²⁷ used a potassium persulfate/sodium thiosulfate redox initiation system to graft methacrylic acid from PVA and starch. It was observed that using a mixture of such an initiator component system the grafting yield and the grafting percentage increased. Despite its merits of being media insensitive (i.e. can be carried out in homo and heterogeneous media) grafting has its major drawback of homopolymer formation.²⁷

2.5.5.3 Grafting from PVA with cationic monomers

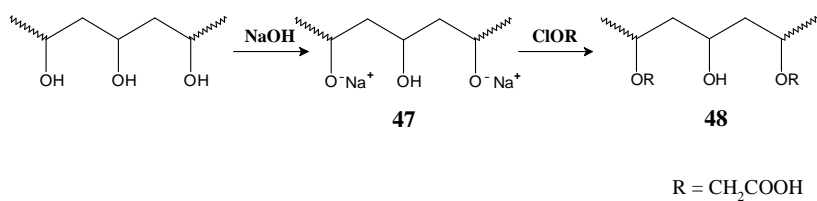
Zheng *et al.*²⁴ grafted water soluble monomers containing the quaternary ammonium group from PVA using ceric ions. They grafted 2-(methacryloyloxy) ethyl trimethylammonium chloride and its derivatives from PVA making use of the ceric ammonium nitrate-nitric acid redox system. In so doing they prepared cationic, water soluble PVA that can be used as a flocculating agent in water treatment or as retention aids in the manufacture of mineral filled paper.²⁴

2.5.6 Reactions of the hydroxyl group

PVA can undergo esterification and etherification reactions with monomers with the appropriate functionality to yield both anionic and cationic PVA.

2.5.6.1 Etherification

Williamson's ether synthesis has been used in the preparation of anionic and cationic PVA, cellulose⁷⁶ and starch.^{77,78} It is a two step process: the first step involves the alkalization of the hydroxyl group with a strong base such as sodium hydroxide and the second step the reaction of that alkoxide with an alkyl halide to yield the ether. PVA has been functionalized by etherification with a functional alkyl halide. Scheme 2.7 summarizes the steps involved in Williamson's etherification of PVA.^{54,79}

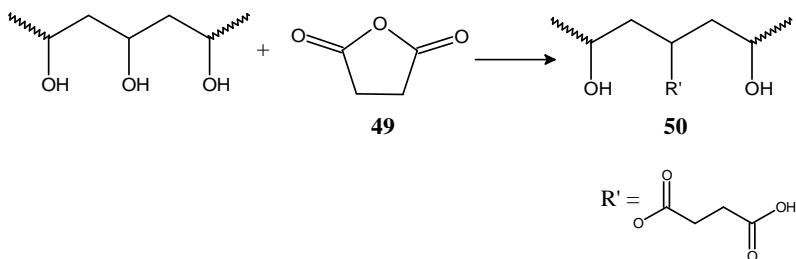


Scheme 2.7 Williamson's etherification of PVA

Anionic or cationic PVA can be synthesized by using anionic or cationic alkyl halides. Haack *et al.*⁷⁸ prepared cationic starch electrolytes via Williamson's ether synthesis using 3-chloro-2-hydroxypropyl trimethyl ammonium chloride and 2,3-epoxypropyltrimethyl ammonium chloride as the etherifying agents.

2.5.6.2 Esterification

PVA can also be modified by esterification with carboxylic acids or anhydrides. Giménez *et al.*⁶³ synthesized anionic PVA by reacting PVA with phthalic anhydride and succinic anhydride. The esterification reaction is illustrated in Scheme 2.8



Scheme 2.8 Esterification reaction of PVA with succinic anhydride

2.5.7 Crosslinking PVA

The above mentioned post polymerization modification techniques are also used in crosslinking PVA. Crosslinking is carried out in order to render PVA insoluble in what would otherwise be its solvent e.g. water. Various techniques can be used to crosslink PVA: irradiation,^{64,80-82} chemical^{47,63,69,72,83-85} and physical methods.⁸⁶

Radiation crosslinking of PVA has been carried out using gamma rays produced by the decomposition of ⁶⁰Co.⁶⁴ Following irradiation the polymer absorbs energy and radicals are produced via the homolytic cleavage of a weak bond e.g. C–H bond alpha to the hydroxyl group. This is then followed by the coupling of two polymeric radicals, resulting in the formation of intermolecular crosslinks. Radiation crosslinking is advantageous because it is a clean method and it yields polymer networks that are not harmful when used in biomedical applications.^{51,61} This is because no catalysts or additives are required to effect the crosslinking. The greatest disadvantage of this technique is that crosslinking is often accompanied by polymer degradation.⁶⁴

The commonly used physical technique in PVA crosslinking is freezing and thawing.⁸⁶ Repetitive freeze–thaw cycles of the PVA solutions result in the formation of crystalline regions that remain intact upon the addition of water, thus rendering PVA insoluble.⁸⁷

Chemical crosslinking of PVA with multifunctional compounds is the most widely used technique for the preparation of PVA networks. The general mechanism involves the reaction of the complimentary functional group of the crosslinking agent with the hydroxyl group of PVA. Examples of crosslinking agents include dialdehydes,^{50,66,84,88,89} dicarboxylic acids,⁶⁹ dianhydrides^{47,63} and diisocyanates.⁸⁵ PVA undergoes esterification with dicarboxylic acids and dianhydrides, acetalization with dialdehydes (in the presence of Lewis or Brønsted acid catalysts) and carbamate (urethane) linkages are formed with diisocyanates.

Moritani and Okaya⁴⁸ prepared self-crosslinkable PVA by copolymerizing vinyl acetate with a range of vinyl monomers with the amide linkage. Following saponification, the PVA was heat-treated in the presence of ammonium chloride to yield crosslinked polymer networks. The concentration of the crosslinking agent present in a polymer is the prime controlling parameter of the degree of crosslinking in the resultant polymer matrix. Characterization of crosslinked polymer networks has been carried out using IR,^{85,90} NMR,^{63,66,83,91} DSC⁹² and swelling studies.^{93,94}

2.6 Poly(vinyl alcohol) fibers

PVA fibers are high performance materials. They have high tensile and impact strengths, high tensile modulus, high abrasion resistance, excellent oxygen barrier properties and good binding properties. The PVA microfibrils prepared in this study have potential application as reinforcing fillers in the paper industry.¹⁶ In order to enhance this application, anionic and cationic modifications of PVA fibers were carried out. The former is to promote the flocculation/dispersion of precipitated calcium carbonate and the latter to enable the microfibrils to adsorb onto fibrous pulp.⁵⁷

2.6.1 Synthesis of PVA fibers

The basic technique involved in fiber formation is extrusion i.e. forcing a thick viscous liquid through the tiny holes of a device called a spinneret. There are generally four methods of spinning fibers⁹⁰ namely:

- Wet spinning: the fiber forming material is dissolved in an appropriate solvent and then the solution extruded onto a precipitating liquid.
- Dry spinning: the fiber forming material is dissolved in a suitable solvent and then the solution is extruded, and dried in a stream of air or inert gas.
- Melt spinning: the fiber forming material is melted and extruded, and it solidifies upon cooling
- Gel spinning: the fiber forming material in gel form is extruded and dried.

After extrusion, the fibers are drawn in order to pull the molecular chains together and thus orient them along the fiber axis.

PVA fibers have been formed via the following methods:

- gel spinning⁸⁸
- zone drawing^{95,96}
- crystal mat drawing⁹⁷
- wet spinning⁹⁸
- electrospinning⁹⁹

Electrospinning is the method most commercially used for the synthesis of PVA fibers. It involves the following basic steps: emulsification of core materials, dissolution of fiber forming polymers, electrospinning of solution and harvesting of composite fiber.

All the fiber forming techniques mentioned thus far involve relatively complex multistep processes. Lyoo *et al.*^{10,12,16,42,54,55,100-103} reported the synthesis of well oriented PVA fibers via the saponification of PVPi under shear (with stirring). This was novel for PVA. Another polymer known to form without spinning in this way poly(*p*-phenylene terephthalamide)¹⁰⁴ which forms a microfibrillar structure during its synthesis. This behavior was attributed to its rigid rod conformation and the proposed mechanism was similar to the one for native cellulose, whereby self ordering and chain packing occurs.

2.6.2 *In situ* fibrillation of PVA

Well oriented PVA fibrillar structures can be prepared from PVPi upon saponification if the microstructures are significantly syndiotactic and linear.^{10,12,42,100,105} PVAs with an *s*-diad content of > 57% result in fiber formation while a lower *s*-diad content of 52–55% result in shapeless globular morphologies.¹⁰⁰

The following factors were investigated and found to affect *in situ* fibrillation of PVA: molecular weight, syndiotacticity, degree of saponification, solvent used for precursor, saponifying agent, water presence, saponification time and temperature, oxygen presence, shear speed and type of stirring device. The parameters required for fibrillation are described in Chapter 4 (Section 4.1)

2.6.2.1 Mechanism of *in situ* fibrillation of PVA fiber

The following mechanism has been suggested for the *in situ* fibrillation of PVA¹²: During saponification, the pivaloyl groups initially convert into blocks of hydroxyl groups (a definite fraction of the hydroxyl groups binds with water). As a result of the weakening intermolecular hydrogen bonding between polymer chains (due to the presence of water), an oriented gel

structure appears. As a result of the shear forces from the continuous stirring, the gel converts into microfibrillar structure. The PVA/water interbridges collapse and the intermolecular distance of PVA remains constant so that chain packing occurs. The intermolecular hydrogen bonding between adjacent hydroxyl groups in PVA is strengthened and the crystal structure of syndiotactic PVA is formed.

2.6.3 Modification of PVA fiber

PVA fibers are insolubilized by crosslinking. In this study crosslinking was carried out in order to hinder dissolution of PVA microfibrils in the aqueous media in which they were modified. Varma and Nedungadi¹⁰⁶ crosslinked PVA fibers using hexamethylene diisocyanate and the resulting fiber had improved elastic properties and crease resistance. Grubb and Kearney⁸⁸ also crosslinked gel drawn PVA fibers with formaldehyde. PVA fibers are reacted with aldehydes and dialdehydes in order to insolubilize them. When PVA fibers are reacted with aldehydes the presence of the hydrophobic groups insolubilizes the fibers in water whereas when reacted with dialdehydes intermolecular crosslinks are formed. Commonly used dialdehydes are glyoxal, glutaraldehyde, isophthalaldehyde and phthalaldehyde. With dialdehydes, in addition to crosslinking, the fiber structure is also preserved.⁵⁰ Acetals or hemiacetals can be formed, hence further modification of the fibers is probable.

The PVA microfibrils synthesized in this work will be modified using the post-polymerization techniques described in Section 2.5.5.

References

1. Finch, C. A., *Poly(vinyl alcohol) : Properties and Applications*. John Wiley and Sons: London, 1973.
2. Finch, C. A., *Poly(vinyl alcohol) : Developments*. John Wiley and Sons: London, 1992.
3. Mohsen-Nia, M.; Modarress, H. *J. Adhesion Sci. Technol.* **2006**, 20(12), 1273–1280.
4. Suzuki, A.; Fujiwara, M.; Nishijima, M. *Colloid Polym Sci* **2008**, 286, 525–534.
5. Liou, F. J.; Wang, Y. J. *J. Appl. Polym. Sci.* **1996**, 59, 1395–1403.
6. Choi, J. H.; Cho, Y. W.; Ha, W. S.; Lyoo, W. S.; Lee, C. J.; Ji, B. C.; Han, S. S.; Yoon, W. S. *Polym. Int.* **1998**, 47, 237–242.
7. Chen, C.; Wang, F.; Mao, C.; Yang, C. *J. Appl. Polym. Sci.* **2007**, 105, 1086–1092.
8. Nam, S. Y.; Chun, H. J.; Lee, Y. M. *J. Appl. Polym. Sci.* **1999**, 72, 241–249.
9. Ajji, Z.; Ali, A. M. *Nucl. Instrum. Methods Phys. Res., Sect. B* **2007**, 265, 362–365.
10. Lyoo, W. S.; Ha, W. S. *Polymer* **1996**, 37(14), 3121–3129.
11. Choi, J. H.; Lyoo, W. S.; Ko, S. W. *Macromol. Chem. Phys.* **1999**, 200, 1421–1427.
12. Lyoo, W. S.; Ha, W. S. *Polymer* **1999**, 40, 497–505.
13. Lyoo, W. S.; Han, S. S.; Yoon, W. S.; Ji, B. C.; Lee, J.; Cho, Y. W.; Choi, J. H.; Ha, W. S. *J. Appl. Polym. Sci.* **2000**, 77, 123–134.
14. Ohgi, H.; Sato, T.; Hu, S.; Horii, F. *Polymer* **2006**, 47, 1324–1332.
15. Ohgi, H.; Sato, T. *Polymer* **2002**, 43, 3829–3836.
16. Lyoo, W. S.; Kim, J. H.; Ghim, H. D. *Polymer* **2001**, 42, 6317–6321.
17. Nagara, Y.; Nakano, T.; Okamoto, Y.; Gotoh, Y.; Nagura, M. *Polymer* **2001**, 42, 9679–9686.
18. Kenney, J. F.; Willcockson, G. W. *J. Polym. Sci., Part A-1* **1966**, 4, 679–698.
19. Baudry, R.; Sherrington, D. C. *Macromolecules* **2006**, 39, 5230–5237.
20. Lyoo, W. S.; Han, S. S.; Choi, J. H.; Ghim, H. D.; Yoo, S. W.; Lee, J.; Hong, S. I.; Ha, W. S. *J. Appl. Polym. Sci.* **2001**, 80, 1003–1012.
21. Matyjaszewski, K.; Davis, T. P., *Handbook of Radical Polymerisation*. John Wiley and Sons: New York, 2002.
22. Lyoo, W. S.; Lee, S. G.; Kim, J. P.; Han, S. S.; Lee, C. J. *Colloid Polym. Sci.* **1998**, 276, 951–959.
23. Lyoo, W. S.; Yeum, J. H.; Kwon, O. W.; Shin, D. S.; Han, S. S.; Kim, B. C.; Jeon, H. Y.; Noh, S. K. *J. Appl. Polym. Sci.* **2006**, 102, 3934–3939.

24. Zheng, S.; Chen, Z.; Lu, D.; Lin, X. *J. Appl. Polym. Sci.* **2005**, *97*, 2186–2191.
25. Odian, G., *Principles of Polymerization*. Fourth ed.; John Wiley and Sons: New Jersey, 2004.
26. Chowdhury, P.; Pal, C. M. *Eur. Polym. J.* **1999**, *35*, 2207–2213.
27. Beláková, M. K.; Aly, A. A.; Abdel-Mohdy, F. A. *Starch/Stärke* **2004**, *56*, 407–412.
28. Tasdelen, M. A.; Kumbaraci, V.; Talinli, N.; Yagci, Y. *Polymer* **2006**, *47*, 7611–7614.
29. Tasdelen, M. A.; Kiskan, B.; Yagci, Y. *Macromol. Rapid Commun.* **2006**, *27*, 1539–1544.
30. Mah, S.; Koo, D.; Jeon, H.; Kwon, S. *J. Appl. Polym. Sci.* **2002**, *84*, 2425–2431.
31. Bhaduri, R.; Aditya, S. *Colloid Polym. Sci.* **1978**, *256*, 659–662.
32. Mesquita, A. C.; Mori, M. N.; Vieira, J. M.; Silvan, L. G. A. *Radiat. Phys. Chem.* **2002**, *63*, 465–468.
33. Moad, G.; Solomon, D. H., *The Chemistry of Radical Polymerisation*. Second ed.; Elsevier: Amsterdam, 2006.
34. Bovey, F. A.; Bowden, M. J.; Kwei, T. W.; Loan, L. D.; Matsuoka, S.; Winslow, F. H., *Macromolecules : An Introduction to Polymer Science*. Academic Press Inc: New Jersey, 1979.
35. Bovey, F. A.; Mirau, P. A., *NMR of Polymers*. Academic Press: New Jersey, 1996.
36. Tonelli, A. E. *Macromolecules* **1985**, *18*, 1086–1090.
37. Wu, T. K.; Sheer, M. L. *Macromolecules* **1977**, *10*(3), 529–531.
38. Moritani, T.; Kuruma, I.; Shibatani, K.; Fujiwara, Y. *Macromolecules* **1972**, *5*(5), 577–580.
39. Friedlander, H. N.; Harris, H. E.; Pritchard, J. G. *J. Polym. Sci., Part A-1* **1966**, *4*, 649–664.
40. Imai, K.; Shiomi, T.; Oda, N. *J. Polym. Sci., Part A: Polym. Chem.* **1986**, *24*, 3225–3231.
41. Yamada, K.; Nakano, T.; Okamoto, Y. *J. Polym. Sci., Part A: Polym. Chem.* **1999**, *37*, 2677–2683.
42. Lyoo, W. S.; Ha, W. S. *J. Polym. Sci., Part A: Polym. Chem.* **1997**, *35*, 55–67.
43. Kim, S. S.; Seo, I. S.; Yeum, J. H.; Ji, B. C.; Kim, J. H.; Kwak, J. W.; Yoon, W. S.; Noh, S. K.; Lyoo, W. S. *J. Appl. Polym. Sci.* **2004**, *92*, 1426–1431.
44. Katsuraya, K.; Hatanaka, K.; Matsuzaki, K.; Amiya, S. *Polymer* **2001**, *42*, 9855–9858.
45. Pritchard, J. G.; Vollmer, R. L.; Lawrence, W. C.; Black, W. B. *J. Polym. Sci., Part A-1* **1966**, *4*, 707–712.

46. Harris, H. E.; Kenney, J. F.; Willcockson, G. W.; R.Chiang; Friedlander, H. N. *J. Polym Sci., Part A-1* **1966**, 4, 665–677.
47. Ruiz, J.; Mantecón, A.; Cádiz, V. *Polymer* **2001**, 42, 6347–6354.
48. Moritani, T.; Okaya, T. *Polymer* **1998**, 39(4), 923–931.
49. Kumeta, K.; Nagashima, I.; Matsui, S.; Mizoguchi, K. *J. Appl. Polym. Sci.* **2003**, 90, 2420–2427.
50. Shtyagina, L. M.; Vainburg, V. M.; Vinogradova, L. E. *Russ. J. Appl. Chem* **2001**, 74(8), 1408–1409.
51. Park, S.; Nho, Y.; Lim, Y.; Kim, H. *J. Appl. Polym. Sci.* **2004**, 91, 636–643.
52. Mishra, S.; Panda, A.; Sing, B. C. *J. Appl. Polym. Sci.* **1999**, 73(5), 677–683.
53. Chiang, W.; Lin, Y. H.; . *J. Appl. Polym. Sci.* **2002**, 86, 2854.
54. Mukherjee, G. S.; Shukla, N.; Singh, R. K.; Mathur, G. N. *J. Sci. Ind. Res.* **2004**, 63, 596–602.
55. Mukherjee, G. S. *J. Mater. Sci* **2005**, 40, 3017–3019.
56. Chen, X.; Huang, R.; Pelton, R. *Ind. Eng. Chem. Res.* **2005**, 44, 2075–2085.
57. Moritani, T.; Yamauchi, J. *Polymer* **1998**, 39, 559–572.
58. Moritani, T.; Yamauchi, J. *Polymer* **1998**, 39, 553–557.
59. Moritani, T.; Kajitani, K. *Polymer* **1997**, 38(12), 2933–2945.
60. Salmawi, K. M. E. *J. Macromol. Sci., Pure Appl. Chem.* **2007**, 44, 541–545.
61. Trimnell, D.; Stout, E. I. *J. Appl. Polym. Sci.* **1980**, 25, 2431–2434.
62. Asman, G.; Sanlı, O.; Tuncel, D. *J. Appl. Polym. Sci.* **2008**, 107, 3005–3012.
63. Giménez, V.; Mantecón, A.; Ronda, J. C.; Cádiz, V. *J. Appl. Polym. Sci.* **1997**, 65, 1643–1651.
64. Mishra, S.; Bajpai, R.; Katare, R.; Bajpai, A. K. *Polymer Letters* **2007**, 1(7), 407–415.
65. Matheson, M.; Auer, E.; Bevilacqua, E.; Hart, E. J. *J. Am. Chem. Soc* **1949**, 71, 497–504.
66. Hansen, E. W. *Polymer* **1997**, 38(19), 4863–4871.
67. Zhou, Z.; Xu, W.; He, D.; Fan, J.; Yu, F.; Ren, F. *J. Appl. Polym. Sci.* **2007**, 103, 848–852.
68. Yin, Y.; Li, J.; Liu, Y.; Li, Z. *J. Appl. Polym. Sci.* **2005**, 96, 1394–1397.
69. Gohil, J. M.; Bhattacharya, A.; Ray, P. *J. Polym. Res* **2004**, 13, 161–169.
70. Bo, J. *J. Appl. Polym. Sci.* **1992**, 46, 783–786.
71. Park, J. S.; Park, J. W.; Ruckenstein, E. *Polymer* **2001**, 42, 4271–4280.
72. Giménez, V.; Mantecón, A.; Reina, J. A.; Cádiz, V. *Acta Polym.* **1999**, 50, 187–195.

73. Miller, M. L., *The Structure of Polymers*. Reinhold Publishing Corporation: Connecticut, 1968.
74. Billmeyer, F. W., *Textbook of Polymer Science*. John Wiley and Sons: New York, 1970.
75. Alfrey, T.; Lewis, C.; Magel, B. *J. Am. Chem. Soc.* **1949**, 71, 3793–3795.
76. Aguir, C.; M'Henni, M. F. *J. Appl. Polym. Sci.* **2006**, 99, 1808–1816.
77. Volkerta, B.; Lotha, F.; Lazikb, W.; Engelhardt, J. *Starch/Stärke* **2004**, 56, 307–314.
78. Haack, V.; Heinze, T.; Oelmeyer, G.; Kulicke, W.-M. *Macromol. Mater. Eng.* **2002**, 287, 495–502.
79. Sinha, A.; Agrawal, A.; Nayar, S.; Das, S. K.; Ramachandrarao, P. *J. Mater. Synth. Proces.* **2002**, 10(3), 149–153.
80. Mühlebach, A.; Müller, B.; Pharisa, C.; Hofmann, M.; Seiferling, B.; Guerry, D. *J. Polym. Sci., Part A: Polym. Chem.* **1997**, 35, 3603–3611.
81. Peppas, N. A.; Merrill, E. W. *J. Appl. Polym. Sci.* **1976**, 20, 1457–1465.
82. Miranda, T. M.; Gonçalves, A. R.; Amorim, M. P. *Polym. Int.* **2001**, 50, 1068–1072.
83. Gauthier, M. A.; Luo, J.; Calvet, D.; Ni, C.; Zhu, X. X.; Garon, M.; Buschmann, M. *D. Polymer* **2004**, 45, 8201–8210.
84. Xu, G. G.; Yang, C. Q.; Deng, Y. *J. Appl. Polym. Sci.* **2004**, 93, 1673–1680.
85. Krumova, M.; López, D.; Benavente, R.; Mijangos, C.; Pereña, J. M. *Polymer* **2000**, 41, 9265–9272.
86. Hickey, A. S.; Peppas, N. A. *Polymer* **1997**, 38(24), 5931–5936.
87. Hassan, C. M.; Peppas, N. A. *J. Appl. Polym. Sci.* **2000**, 76, 2075–2079.
88. Grubb, D. T.; Kearney, F. R. *J. Appl. Polym. Sci.* **1990**, 39, 695–705.
89. Park, J.; Park, J.; Ruckenstein, E. *J. Appl. Polym. Sci.* **2001**, 82, 1816–1823.
90. Shukla, S.; Bajpai, A. K.; Kulkarni, R. A. *J. Appl. Polym. Sci.* **2005**, 95, 1129–1142.
91. Kobayashi, M.; Ando, I.; Ishii, T.; Amiya, S. *J. Mol. Struct.* **1998**, 440, 155–164.
92. Li, W.; Xue, F.; Cheng, R. *Polymer* **2005**, 46, 12026–12031.
93. Atta, A. M.; El-Ghazaway, R. A. M. *Int. J. Polym. Mater* **2003**, 52, 623–636.
94. Atta, A. M.; Maysour, N. E.; Arndt, K. F. *J. Polym. Res* **2006**, 13, 53–63.
95. Kunugi, T.; Kawasumi, T.; Ito, T. *J. Appl. Polym. Sci.* **1990**, 40, 2101.
96. Garrett, P. D.; Grubb, D. T. *Polym. Commun.* **1988**, 29, 60.
97. Kanamoto, T.; Kiyooma, S.; Tovmasyan, Y.; Sano, H.; Narukawa, H. *Polymer* **1990**, 31, 2039–2046.

98. Su, J.; Wang, Q.; Wang, K.; Zhang, Q.; Fu, Q. *J. Appl. Polym. Sci.* **2008**, 107(6), 4070–4075.
99. Thandavamoorthy, S.; Bhat, G. S.; Tock, R. W.; Parameswaran, S.; Ramkumar, S. S. *J. Appl. Polym. Sci.* **2004**, 96, 557-559.
100. Lyoo, W. S.; Blackwell, J. *Macromolecules* **1998**, 31, 4253–4259.
101. Lyoo, W. S.; Chvalun, S.; Ghim, H. D.; Kim, J. P.; Blackwell, J. *Macromolecules* **2001**, 34, 2615–2623.
102. Lyoo, W. S.; Ghim, H. D.; Kim, J. H. *Macromolecules* **2003**, 36, 5428–5431.
103. Lyoo, W. S.; Kim, J. H. *Macromolecules* **2001**, 34, 3982–3987.
104. Wang, W.; Ruland, W.; Cohen, V. *Acta Polym.* **1993**, 44(6), 273–278.
105. Lyoo, W. S.; Han, S. S.; Kim, J. H.; Yoon, W. S.; Lee, C. J.; Kwon, I. C.; Lee, J.; Ji, B. C.; Han, M. H. *Angew. Makromol. Chem.* **1999**, 271, 46–52.
106. Varma, D. S.; Nedungadi, C. *J. Appl. Polym. Sci.* **1976**, 20, 681–688.

CHAPTER 3

Synthesis of poly(vinyl alcohol) precursor

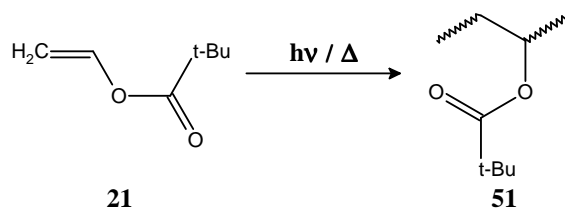
3.1: Introduction

The main objective of this work was to prepare PVA microfibrils by *in situ* fibrillation. A high degree of emphasis was placed on the syndiotacticity and the molecular weight of the precursor. PVA derived from PVAc prepared by FRP in bulk or solution is colloidal, atactic, of low molecular weight, and contains a substantial amount of branching.¹ In order to improve the physical properties of PVA it is important to increase its syndiotacticity and molecular weight.²⁻⁴ According to literature when VPi was used as a monomer high molecular weight, syndiotacticity rich PVA (s-diad content > 55 %)^{2,5} is obtained. The saponification of PVPi polymerized in bulk or solution yields microfibrillar fibers after saponification.^{4,6} Fiber formation is dependent on the syndiotacticity and molecular weight of the precursor,^{2-4,7,8} hence it was important to employ polymerization conditions that enhanced these two features.

High molecular weight PVPi can be prepared by not only decreasing the initiator to monomer ratio but also by reducing the polymerization temperature such that chain transfer reactions are minimized. When chain transfer reactions are minimized, termination is primarily by combination, and the number average molecular weight (M_n) is increased.⁹ To facilitate low temperature thermoinitiated polymerization, azo initiators such as 2,2'-azobis (2,4-dimethylvaleronitrile) (ADMVN) and 2,2'-azobis (isobutyronitrile) (AIBN) have been used.^{4,10-13} Industrially this is not viable as the half-lives ($t_{1/2}$) of AIBN and ADMVN at 50 °C are 72 and 10 hours respectively. This means that long reaction times are required for high conversions to be attained during low temperature polymerization reactions. Radiation induced and photoinitiated polymerizations have been used to polymerize VPi and VAc at low temperatures (down to -10 °C). In photoinitiated polymerization systems UV sensitive initiators such as benzil, benzophenone and AIBN have been used to achieve high conversions within short periods of time.⁷

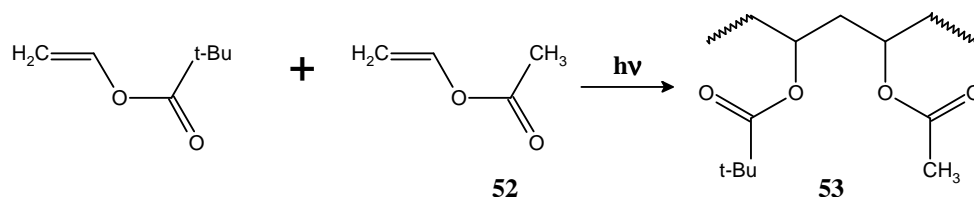
In this study, VPi was polymerized via thermoinitiation (at 45 °C and 50 °C) and photoinitiation (at room temperature) using AIBN as the initiator. The typical VPi polymerization mechanism is illustrated in Scheme 3.1. A comparison was made of the conversion and molecular weight of the PVPi prepared by thermoinitiation and that prepared

by photoinitiation. The syndiotacticities of the resultant PVAs were also compared. Despite thermoinitiation being superior in yielding high molecular weight PVPi for reasons explained later, the use of photoinitiation was preferred for this study as it yielded PVA microfibrils with higher syndiotacticities.



Scheme 3.1 Polymerization of vinyl pivalate

With the intention of varying syndiotacticity and consequently studying the effect that this had on the morphology of the resultant PVA, VPi was copolymerized with VAc as shown in Scheme 3.2. Copolymerization offers an inexpensive way of achieving stereochemical control in PVA.^{2,14}



Scheme 3.2: Copolymerization of vinyl pivalate and vinyl acetate

3.2 Polymerization of VPi and VAc

3.2.1 Materials

Vinyl pivalate (VPi, Sigma-Aldrich); vinyl acetate (VAc, Sigma-Aldrich); 2,2' azobis (isobutyronitrile) (AIBN, Riedel de Haën), tertiary butyl alcohol (TBA, Merck); potassium hydroxide (KOH, Merck), anhydrous magnesium sulphate (MgSO_4 , Saarchem), methanol (MeOH, Merck), inhibitor remover column packing (Sigma-Aldrich).

3.2.1.1 Purification of reagents

Monomers (VPi and VAc) were washed successively with aqueous KOH and water, dried over anhydrous MgSO_4 and then purified by passing through a column packed with inhibitor remover. They were then stored over molecular sieves in the refrigerator ($< 4^\circ\text{C}$). AIBN was

recrystallized from MeOH, vacuum dried and stored at < 4 °C. TBA was purified by drying over anhydrous $MgSO_4$ for 24 h and then distilling under vacuum. The purified TBA was stored over molecular sieves.

3.2.2 Synthesis of poly(vinyl pivalate) by thermal initiated polymerization

The FRP of VPi was conducted at 45 °C and 50 °C using AIBN as the initiator and TBA as the solvent. The conditions used for these thermoinitiated polymerization reactions are tabulated in Table 3.1.

Table 3.1 Parameters used for VPi thermoinitiated solution polymerization

Sample	[AIBN] per mol VPi	[TBA] per mol VPi	Temperature (°C)	Duration (h)
1	5.27×10^{-5}	3.74×10^{-1}	45	72
2	5.58×10^{-5}	3.45×10^{-1}	50	72

Procedure. The following typical procedure was used for the thermoinitiated FRP of VPi, e.g. Sample 1: A dry Schlenk flask was charged with vinyl pivalate (10.08 g, 0.078 moles), AIBN (6.30 mg, 3.80×10^{-5} moles) and TBA (2.16 g, 2.91×10^{-3} moles), and a magnetic stirrer bar was added. The mixture was thoroughly degassed by three successive freeze pump thaw cycles, backfilled with nitrogen, sealed and immersed into an oil bath preheated and thermostated at 45 °C. The reaction was stopped after stirring for 72 h by opening the flask to allow termination of radicals by oxygen. The slightly viscous polymer was then precipitated from a methanol/water mixture (1/3 (v/v)). The polymer was filtered and dried under vacuum at 60 °C. Conversion was determined gravimetrically.

3.2.3 Synthesis of poly(vinyl pivalate) by photoinitiated polymerization

UV initiated polymerizations of VPi and VPi/VAc were carried out at room temperature and in bulk. VPi/VAc monomer feed ratios of 100/0, 90/10, 60/40, 50/50 and 30/70 (mol %/mol %) were used. The conditions used for these polymerizations are tabulated in Table 3.2

Procedure. The following typical procedure was used for the photoinitiated polymerization of VPi e.g. Sample 3: A dry Schlenk flask was charged with vinyl pivalate (10.08 g, 0.078 moles) and AIBN (6.30 mg, 3.80×10^{-5} moles), and a magnetic stirrer bar was added. The mixture was thoroughly degassed by three successive freeze pump thaw cycles, backfilled with nitrogen, sealed and irradiated with a high pressure 400 watt mercury lamp. As the

polymerization proceeded the reaction mixture became very viscous and the reaction stopped when the magnetic follower could no longer effect stirring. The polymer was dissolved in THF and precipitated from a methanol/water mixture (1/3 (v/v)). The polymer was filtered and then dried under vacuum at 60 °C. Conversion was determined gravimetrically (see Table 3.3 later).

Table 3.2 Conditions used for VPi and VPi/VAc photoinitiated bulk polymerization

Sample	[AIBN]/mol VPi ^a	^b Monomer feed ratios		^c Copolymer composition	
		VPi (mol %)	VAc (mol %)	VPi (mol %)	VAc (mol %)
3	5.72×10^{-4}	100	0	100	0
4	5.76×10^{-4}	90.0	10.0	98.8	1.2
5	4.20×10^{-4}	60.0	40.0	76.9	23.1
6	5.20×10^{-4}	50.0	50.0	58.8	41.2
7	5.40×10^{-4}	30.0	70.0	38.5	61.5

^a mols AIBN/mol VPi, ^b Schlenk flask charged with VPi and VAc, ^c VPi/VAc content in copolymer determined by ¹H NMR

3.3 Analyses

3.3.1 Size exclusion chromatography (SEC)

A SEC instrument comprising of a Waters 717plus Autosampler, Waters 600E system controller and a Waters 610 fluid unit was used. The detector used was a Waters 410 differential refractometer (at 35 °C). Two PLgel 5µm Mixed-C columns and a PLgel 5µm guard column were used. The column injection volume was 100 µL and the column oven was kept at a temperature of 30 °C. The eluent was THF (HPLC grade, BHT stabilized) at a flow rate of 1mL/min. Calibration was carried out using narrow polystyrene standards with a molecular weight range of 800–2 x 10⁶ g/mol. All SEC data obtained is reported as polystyrene equivalents.

3.3.2 Proton nuclear magnetic resonance spectroscopy (¹H NMR)

All ¹H NMR spectra were acquired using a Varian VNMRS 300 MHz spectrometer. The chemical shifts are reported in parts per million (ppm) in deuterated chloroform (CDCl₃) with tetramethylsilane (TMS) as a reference.

3.3.3 Conversions by gravimetry

The monomer conversion-time data were obtained gravimetrically. Fig. 3.1 was obtained for the bulk polymerization of VPi in a UV initiated system. The resulting polymer was dried and weighed after 30, 60, 90, 180, 240 and 300 and 350 minutes of reaction time. The yield (mass of purified and dried polymer) was then used to determine the conversion (at time t) as shown in equation 3.1

$$\text{Conversion (at time t) (\%)} = \frac{\text{Yield (g)} - \text{AIBN (g)}}{\text{Monomer (g)}} \times 100 \quad (3.1)$$

3.4 Results and discussion

A comparison was made between the vinyl pivalate homopolymers prepared by thermoinitiation and photoinitiation (samples 1 and 3). The observed discrepancies in conversion, molecular weight and PDI between the products are explained in the following sections (3.4.1–3.4.3).

3.4.1 Conversions

Higher conversions were attained with photoinitiation (sample 3) compared to thermoinitiation (sample 1), as shown in Table 3.3. This was because of the differences in activation energies (E_a) for the two processes. Thermoinitiation is temperature dependent with an E_a of 30 kcal/mol.⁹ Therefore, at low temperatures fewer radicals are produced and consequently lower conversions are obtained. Photoinitiation, on the other hand, has an activation energy of 0 and is thus temperature independent.⁹ Radicals are produced in large concentrations regardless of the temperature and consequently high conversions are obtained. This makes photoinitiated polymerization a better technique for carrying out low temperature polymerizations compared to thermoinitiated polymerization.

Fig. 3.1 shows the evolution of conversion with time for the UV initiated FRP of VPi. A long inhibition period was observed in the first 150 minutes. This was indicated by the very low conversion rate, and can be attributed to the presence of oxygen or other impurities. After the inhibition period the rate of monomer conversion increased to greater than 80% in 300 min.

Table 3.3 Conversions and molecular weight distributions of PVPI and PVPI-co-VAc

Sample	^a Conv (%)	^b M _n (g/mol)	PDI
1	35.16	754 505	1.74
2	48.50	214 258	1.54
3	92.50	460 429	2.03
4	69.60	494 263	1.90
5	77.90	537 899	1.90
6	79.40	322 698	2.60
7	71.20	218 794	3.84

^a Conversions determined gravimetrically using equation 3.1, ^b M_n – number average molecular weight obtained from SEC, ^c M_w/M_n – PDI

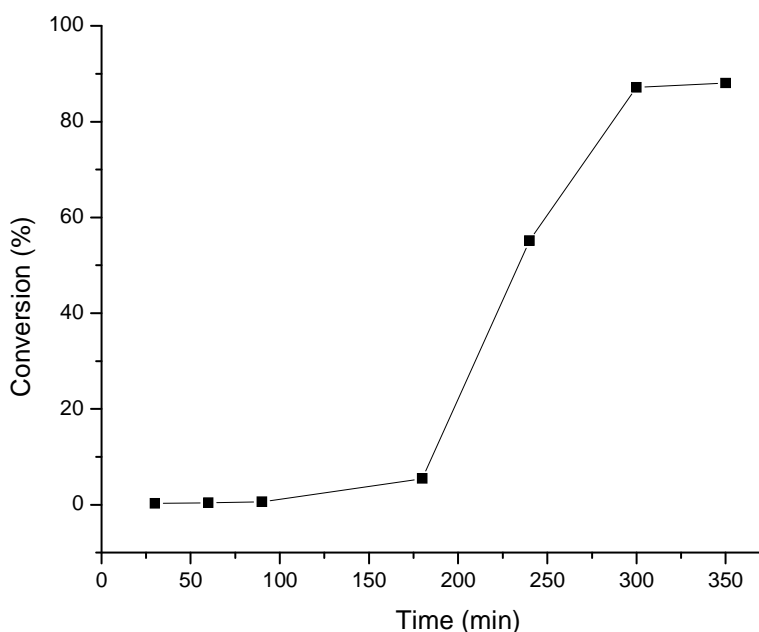


Fig. 3.1 Conversion–time plot of UV initiated bulk polymerization of VPI. ([VPI]/[AIBN] = 1721).

3.4.2 Molecular weight and molecular weight distributions

High polydispersity index (PDI) values (shown in Table 3.3) were obtained which is typical of conventional FRP. It was however observed that the PDI values for the thermoinitiated system (samples 1–2) were narrower than those for the UV initiated systems (samples 3–7). In the case of the latter, high conversions were obtained and the polymerizations stopped after the reaction mixtures had become viscous and the magnetic followers had stopped stirring. Under such conditions (high viscosity), autoacceleration (also known as the Trommsdorf

effect) is prevalent. The Trommsdorf effect is characterized by a decrease in the rate of termination and an increase in the rate of polymerization (this occurs because monomer can still diffuse within the matrix and chain propagation continues). The resulting effect is an increase in the weight average molecular weight (M_w) and the number average molecular weight M_n . These increases in M_n and M_w lead to the broadening of the PDI.

3.4.3 PVPI/PVAc copolymer compositions

The PVPI-co-PVAc copolymer compositions were determined using ^1H NMR spectroscopy. The solvent used for all samples was CDCl_3 . Figs. 3.2A and B are examples of proton spectra of purified and dried PVAc and PVPI respectively. The signals at 4.8 ppm and 1.8 ppm (labeled a and b respectively) are attributed to the methine ($-\text{CH}-$) and methylene ($-\text{CH}_2-$) protons of the homo and copolymers.^{7,8,15,16} The signal at 1.2 ppm (labeled d) in Fig. 3.2B is attributed to the pivaloyl protons while that at 2.2 ppm (labeled c) in Fig. 3.2A is ascribed to the methyl protons of the PVAc. In Fig. 3.2B the signals at 3.75 and 2.10 ppm are likely to be ethanol and acetone solvent contaminants respectively.

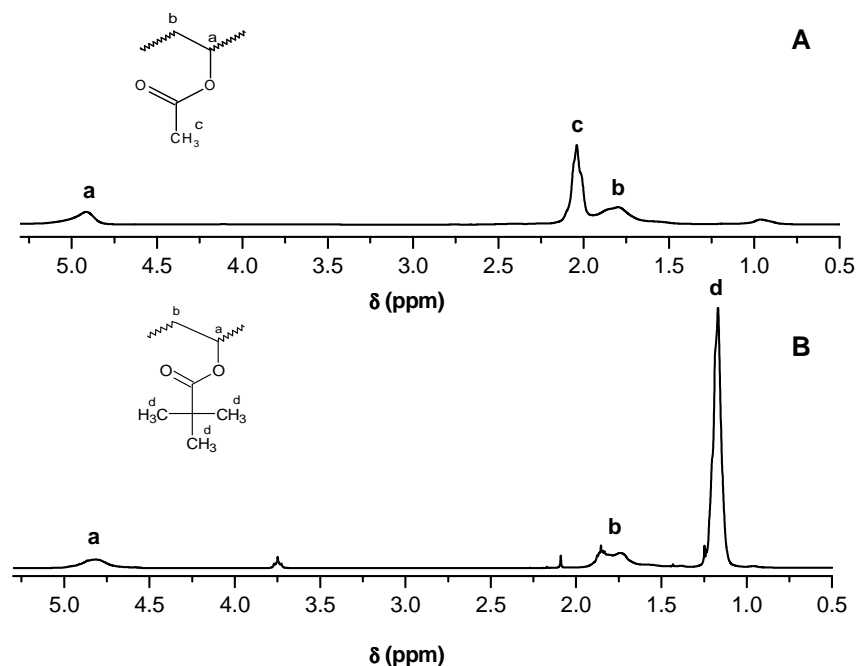


Fig. 3.2 ^1H NMR spectra of PVAc (A) and PVPI (B).

The copolymer compositions were determined using equations 3.2 and 3.3 by comparing the area intensities of the methyl and pivaloyl proton signals labeled c and d respectively

$$\text{VPi (mol \%)} = \frac{\text{Area}_d}{\text{Area}_d + 3 \text{Area}_c} \times 100 \quad (3.2)$$

$$\text{VAc (mol\%)} = \frac{3 \text{Area}_c}{\text{Area}_d + 3 \text{Area}_c} \times 100 \quad (3.3)$$

Area_c and area_d are the area intensities of the methyl and pivaloyl protons respectively. The factor 3 accounts for the presence of 3 sets of methyl protons per pivaloyl group.

Fig. 3.3 shows how the copolymer content varied with the monomer feed ratio. As the amount of VAc increased, the signal due to the methyl protons (labeled c) became more intense and that owing to the pivaloyl protons (labeled d), reduced in intensity. This was in agreement with the variations in the monomer feed ratios given in Table 3.2.

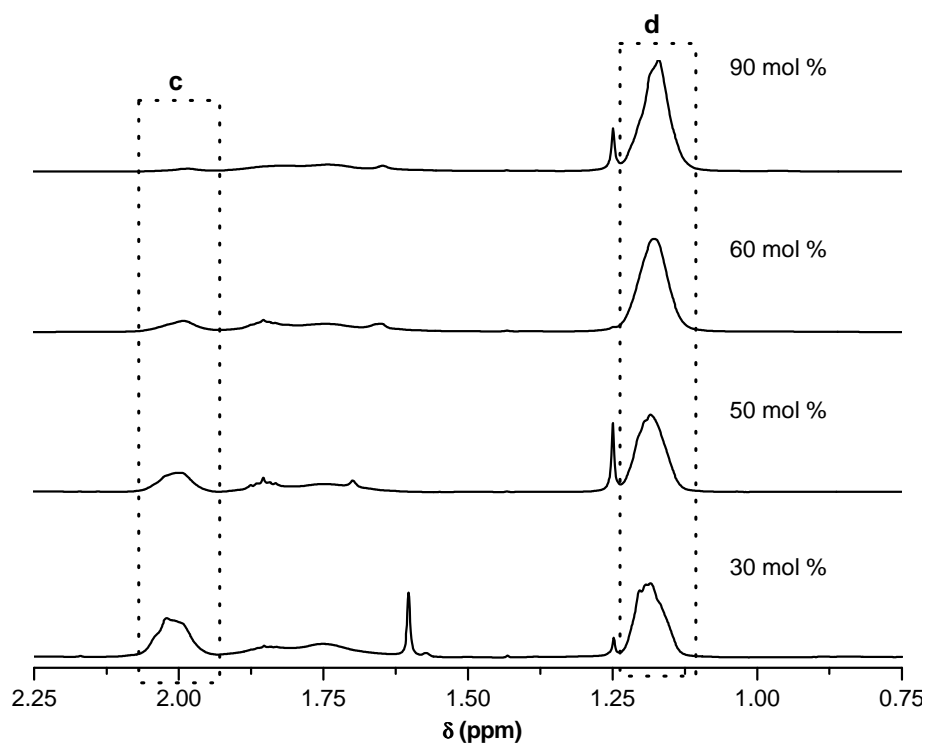


Fig. 3.3 ^1H NMR spectra of VPi/VAc copolymers of varying VPi feed ratios (mol %).

However deviations in the monomer feed ratio and copolymer contents were observed. The amount of VPi (mol %) in the copolymer was higher than the amount in the feed. This was because during copolymerization the conversion of VPi predominated that of VAc. This was confirmed by the reactivity ratios of VPi and VAc which are 3.1 and 1.6 respectively.² This

behavior was observed to be independent of polymerization temperature and initiator concentration^{2,17}

3.5 Conclusions

Photoinitiation proved to be superior to low temperature thermal initiation in obtaining high conversions of high molecular weight PVPi and VPi/VAc copolymers, over relatively short periods of time. This was attributed to the differences in activation energies of the two processes. Low temperature thermoinitiation leads to a low concentration of initiating radicals in the reaction medium whilst in a UV initiated system high quantities of initiating radicals are produced in the system regardless of what the temperature might be. By varying the comonomer feed ratios, VPi/VAc copolymers with varying comonomer contents were prepared. ^1H NMR was successfully used to determine the copolymer composition. The amount of VPi in the copolymer was higher than in the feed showing that the reactivity of VPi is higher than that of VAc. This is in agreement with the reactivity ratios for VPi (r_1) and VAc (r_2) which are 3.1 and 1.6 respectively.²

References

1. Finch, C. A., *Poly(vinyl alcohol) : Properties and Applications*. John Wiley and Sons: London, 1973.
2. Lyoo, W. S.; Blackwell, J. *Macromolecules* **1998**, 31, 4253–4259.
3. Lyoo, W. S.; Ha, W. S. *Polymer* **1999**, 40, 497–505.
4. Lyoo, W. S.; Han, S. S.; Kim, J. H.; Yoon, W. S.; Lee, C. J.; Kwon, I. C.; Lee, J.; Ji, B. C.; Han, M. H. *Angew. Makromol. Chem.* **1999**, 271, 46–52.
5. Nagara, Y.; Nakano, T.; Okamoto, Y.; Gotoh, Y.; Nagura, M. *Polymer* **2001**, 42, 9679–9686.
6. Lyoo, W. S.; Yeum, J. H.; Ji, B. C.; Ghim, H. D.; Kim, S. S.; Kim, J. H.; Lee, J. Y.; Lee, J. *J. Appl. Polym. Sci.* **2003**, 88, 1482–1487.
7. Lyoo, W. S.; Ha, W. S. *J. Polym. Sci., Part A: Polym. Chem.* **1997**, 35, 55–67.
8. Lyoo, W. S.; Ha, W. S. *Polymer* **1996**, 37(14), 3121–3129.
9. Bovey, F. A.; Bowden, M. J.; Kwei, T. W.; Loan, L. D.; Matsuoka, S.; Winslow, F. H., *Macromolecules : An Introduction to Polymer Science*. Academic Press Inc: New Jersey, 1979.
10. Lyoo, W. S.; Kim, S. S.; Ghim, H. D.; Kim, J. P.; Lee, S. S. *J. Appl. Polym. Sci.* **2002**, 85, 1992–2003.
11. Lyoo, W. S.; Han, S. S.; Yoon, W. S.; Ji, B. C.; Lee, J.; Cho, Y. W.; Choi, J. H.; Ha, W. S. *J. Appl. Polym. Sci.* **2000**, 77, 123–134.
12. Lyoo, W. S.; Han, S. S.; Choi, J. H.; Ghim, H. D.; Yoo, S. W.; Lee, J.; Hong, S. I.; Ha, W. S. *J. Appl. Polym. Sci.* **2001**, 80, 1003–1012.
13. Lyoo, W. S.; Ghim, H. D.; Kim, J. H. *Macromolecules* **2003**, 36, 5428–5431.
14. Ghim, H. D.; Kim, J. P.; Lyoo, W. S. *Polymer* **2003**, 44, 895–900.
15. Amiya, S.; Uetsuki, M. *Macromolecules* **1982**, 15, 166–170.
16. Wu, T. K.; Ovenall, D. W. *Macromolecules* **1974**, 7(6), 776–779.
17. Yeum, J. H.; Ji, B. C.; Noh, S. K.; Jeon, H. Y.; Kwak, J. W.; Lyoo, W. S. *Polymer* **2004**, 45, 4037–4043.

CHAPTER 4

Synthesis of syndiotacticity-rich poly(vinyl alcohol) microfibrils

4.1 Introduction

PVA fibers are prepared by electrospinning,¹ crystal mat drawing,² zone drawing,^{3,4} gel spinning⁵ and wet spinning.⁶ These techniques involve relatively complex multiple steps of dissolution of fiber forming material, extrusion, drawing and heat treatment.^{7,8} Recently Lyoo *et al.*⁹⁻¹³ developed a new technique for the preparation of syndiotacticity rich PVA microfibrils in a two step process. The first step involves the synthesis of highly syndiotactic PVPi precursor and the second its saponification to PVA using a chain orienting saponifying agent.¹² This process is termed *in situ* fibrillation^{10,14,15} as the fibers are formed while the polymer is being saponified.

The main factors affecting *in situ* fibrillation and their optimum conditions were investigated by Lyoo *et al.*¹¹ and are tabulated in Table 4.1. The most important parameters are the molecular weight of PVPi, syndiotacticity, saponifying agent composition and stirring speed. PVA microfibrils prepared via *in situ* fibrillation are well oriented and have dimensions of 1–50 μm in diameter and 0.5–200 mm in length. They have irregular cross-sections, needle point-like ends, crystal orientation indices of over 0.880, high crystallinity, and excellent thermal and mechanical properties.¹⁰

In this study high molecular weight PVPi was prepared by using low initiator concentrations and UV initiated FRP, as described in Section 3.2.3. The saponifying agent used consisted of KOH, methanol and water. KOH was used as a catalyst and water as a chain orienting agent. Chain orientation is a crucial step in fiber formation and water fulfils this role by reducing the hydrogen bond interactions between polymer chains.¹¹ Highly syndiotactic PVA microfibrils with s-diad contents of upto 61.8% were prepared and characterized using ¹H and ¹³C NMR, scanning electron microscopy (SEM), thermogravimetric analysis (TGA), differential scanning calorimetry (DSC) and X-ray powder diffraction (XRD). Syndiotacticity was varied by saponifying copolymers of VPi and VAc of varying comonomer contents. The effects of syndiotacticity on the morphology, crystallinity, thermal decomposition temperature, and crystalline melting temperature of PVA microfibrils were investigated.

Table 4.1 Parameters used for *in situ* fibrillation of PVA

Parameter	Description
PVPi solvent ¹¹	THF, acetone, MEK
Molecular weight of PVPi ¹⁵	$P_n > 1140$
Molecular weight of PVA ¹⁵	$P_n > 800$
Syndiotacticity ¹⁴	s-diad content: $> 57\%$
Degree of saponification ¹⁴	85.0–99.9%
Saponifying agent ^{16,17}	20% KOH or 15% NaOH in methanol/water (90/10)(v/v)
Saponification temperature ^{11,15}	50–60 °C
Atmosphere ^{11,15}	Nitrogen (oxygen free)
Stirring speed ¹⁴	Maximum: 10000 rev min ⁻¹

4.2 *In situ* fibrillation of PVA

4.2.1. Materials

PVPi/PVPi-co-VAc (samples 1–7, Section 3.2), tetrahydrofuran (THF, Saarchem), methanol (MeOH, Merck), magnesium sulphate (MgSO₄, Saarchem), potassium hydroxide (KOH, Merck), deionized water.

4.2.1.1 Purification of reagents

THF was partially dried by drying over MgSO₄. Methanol was also dried over MgSO₄ and distilled. KOH was used as received.

4.2.2 Saponification of PVPi

PVPi (3 g) was dissolved in THF (300 mL) and placed in a three neck round-bottom flask equipped with a reflux condenser, dropping funnel (containing 60 mL of a 6% alkali solution of KOH/methanol/water (90/10, v/v)), a nitrogen inlet and a magnetic stirrer. The PVPi solution was flushed with nitrogen for 20 min before the temperature of the flask and contents was raised to 65 °C. Degassing was continued for a further 20 min. The alkali solution was then added dropwise with stirring at 100 rev min⁻¹, and then the mixture left to react overnight under a nitrogen atmosphere. The fibers produced were treated with an ultrasonic generator, filtered, washed several times with MeOH, and dried in an oven under vacuum.

4.2.3 Saponification of PVPI-co-VAc

PVPI-co-VAc (2 g) was dissolved in THF (100 mL) and the solution placed in a three neck round bottom flask equipped with a reflux condenser, dropping funnel (containing 20 mL of a 5% alkali solution of KOH/methanol/water (90/10 v/v)), a nitrogen inlet and a magnetic stirrer. The PVPI-co-VAc solution was flushed with nitrogen for 20 min before the temperature of flask and contents was increased to 65 °C and degassing continued for a further 20 min. The alkali solution was added dropwise with stirring at 100 rev min⁻¹ and then the mixture stirred overnight under a nitrogen atmosphere. The product was filtered, washed several times with MeOH and dried in a vacuum oven.

4.3 Analyses

4.3.1 ¹H and ¹³C NMR

NMR spectra were acquired using a Varian 400 and a 600 MHz Varian ^{Unity} Inova instrument. DMSO-*d*₆ was used as the solvent and tetramethylsilane (TMS) as the reference.

4.3.2 Scanning electron microscopy (SEM)

Imaging was accomplished using a Leo® 1430VP and a Cambridge S200 scanning electron microscopes. The conditions applicable to the former were an accelerating voltage of 7 kV and a probe current of 150 pico amperes (pA) and the conditions applicable to the latter were an accelerating voltage of 10 kV and a probe current of 50 pA.

4.3.3 Thermal analysis

Differential scanning calorimetry (DSC). The crystalline melting temperatures (T_m) were determined using a TA Instruments Q100 Differential Scanning Calorimeter. Samples of between 8–10 mg were weighed and analyzed at a heating rate of 10 °C/min, under a nitrogen atmosphere.

Thermogravimetric analysis (TGA). Non isothermal thermogravimetry was carried out using a TA Instruments Q500 Thermogravimetric Analyzer. The samples were heated from 10 °C to 900 °C at a heating rate of 15 °C/min, under a nitrogen atmosphere.

4.3.4 X-ray diffraction (XRD)

X-ray diffraction studies were carried out using an X-ray Powder Diffractometer Bruker D8

ADVANCE with Bragg-Brentano geometry. The radiation source was Cu K α . A step size of 0.2° was used and 2 θ varied from 5–60°.

4.4 Results and discussion

4.4.1. Degree of polymerization of PVA

The degree of polymerization (DP), of a polymer is defined as the number of repeat units in a polymer chain. It is related to the number average molecular weight of the polymer (M_n), by equations 4.1 and 4.2, where M_{r1} and M_{r2} are the molecular weights of VPi and VAc monomers respectively. n_1 and n_2 are the comonomer compositions of VPi and VAc in the polymer respectively (determined in Section 3.4.3).

$$DP = \frac{M_n}{M_{r1}} \quad (4.1)$$

$$DP = \frac{M_n}{(M_{r1} \times n_1) + (M_{r2} \times n_2)} \quad (4.2)$$

Table 4.2 tabulates the DP values of polymer samples 1–7. It can be deduced from the results that the PVA samples were of sufficient high molecular weight (the required DP for fiber formation ought to be greater than 800). The samples would thus be expected to form fibers upon saponification, provided they are sufficiently syndiotactic.

Table 4.2 Degree of polymerization of PVA microfibrils

Sample	VPi (mol %) in polymer	DP
1	100	5887
2	100	1672
3	100	3592
4	98.8	3871
5	76.9	4541
6	58.8	2912
7	38.5	2139

4.4.2 Microstructural analysis

Chain microstructure in PVA microfibrils was analyzed and quantified using ^1H and ^{13}C NMR. The degrees of saponification and the stereoregularity were quantified as described in the following sections.

4.4.2.1 Degree of saponification

The degree of saponification (DS) gives an indication of the extent of conversion of poly(vinyl ester) to PVA. Typically for PVA, incomplete hydrolysis (illustrated in Fig. 4.1A) results in the subsequent PVA having a mixture of the properties of both the hydrolyzed and unhydrolyzed polymer. DS was determined using ^1H NMR, based on the pivaloyl protons signal (labeled f in Fig. 4.1A and shown at 1.0 ppm in Fig. 4.2A). In samples where the signal was absent (illustrated in Fig. 4.2B) saponification was assumed to be greater than 99% and where present, the ratios of the pivaloyl (f) and methylene (e) proton signals were compared and the DS calculated as shown in equation 4.3.

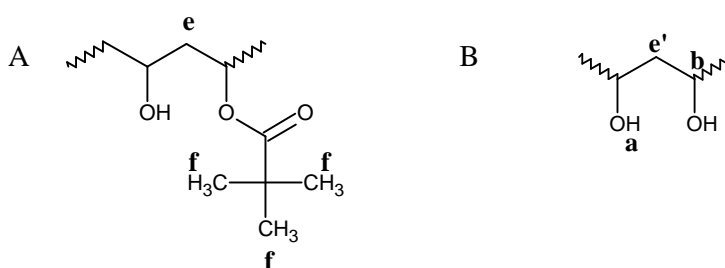


Fig. 4.1 Poly(vinyl alcohol): (A) partially hydrolyzed and (B) fully hydrolyzed.

$$D.S. (\%) = \left[1 - \frac{2 \text{Area}_f}{9 \text{Area}_{e+e'}} \right] \times 100 \quad (4.3)$$

Area_f is the area under signal f and $\text{Area}_{e+e'}$ is the area under signal e (e' accounts for the methylene protons labeled e' in Fig 4.1B). Signals f and e are shown in Fig. 4.2A, 2 and 9 are the factors accounting for the number of methylene and pivaloyl protons respectively.

Fig. 4.2B is a typical ^1H NMR spectrum for fully hydrolyzed PVA. The signals a–e were fully assigned as tabulated in Table 4.3. Water was present as a contaminant in all the samples analyzed by NMR when $\text{DMSO-}d_6$ was used as a solvent.

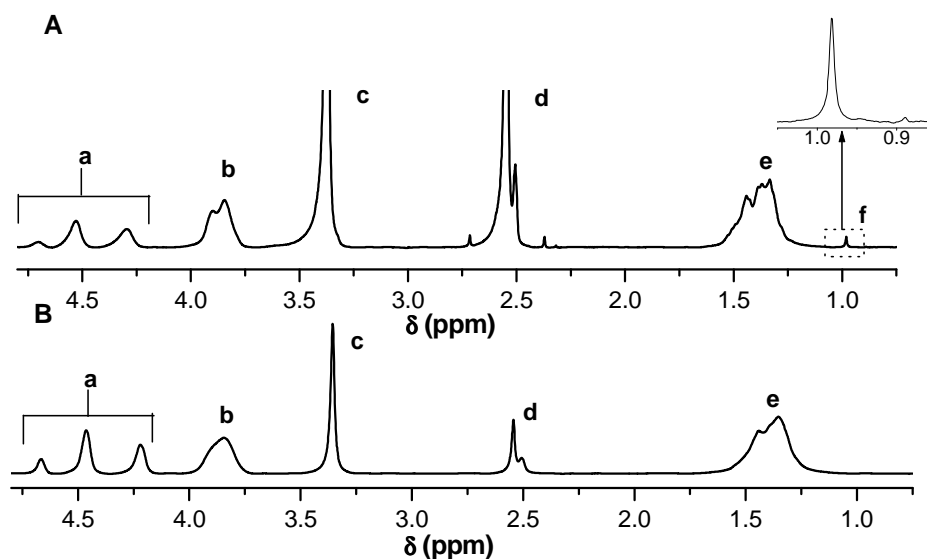


Fig. 4.2 ^1H NMR spectra of PVA with varying degrees of saponification: (A) 98 % and (B) > 99%.

Table 4.3 Assignment of signals in ^1H NMR spectrum of PVA (solvent used: $\text{DMSO-}d_6$)

Peak label	Chemical shift (ppm)	Assignment ^{12,18}
a	4.7	-OH (isotactic)
	4.5	-OH (heterotactic)
	4.3	-OH (syndiotactic)
b	3.8	-CH (methine)
c	3.4	water
d	2.6	DMSO
e	1.3	-CH ₂ (methylene)
f	1.0	-C(CH ₃) ₃ (pivaloyl)

4.4.2.2 Stereoregularity

The tacticity of the PVA samples 1–7 was determined using ^1H and ^{13}C NMR. Triad tacticity was quantified by ^1H NMR using the hydroxyl protons (labeled a in Fig. 4.2), and by ^{13}C NMR using the signals of the methine carbon atom. The methine carbon triad was observed at 62.5–68.0 ppm (shown in Fig. 4.3A). It was attributed to isotacticity (*mm*), heterotacticity (*mr*) and syndiotacticity (*rr*) from high to low frequency.¹⁹ The *mm* and *mr* regions were further split into heptads and the *rr* region split into pentads.²⁰ The assignments of these heptads and pentads are given in Appendix 1.

Tetrad tacticity was determined from ^{13}C NMR by following the methylene carbon signals at 43.5–46.0 ppm. The methylene carbon atom signal was split into a quartet, which was assigned to the following tetrads *rrr*, *rmr*, *mrr*, *mr*, *mrm*, *mmr*, and *mmm* from high to low frequency¹⁹ (as shown in Fig. 4.3B). The two central signals were composed of overlapping *rmr* + *mrr* and *mrm* + *mmr* signals.

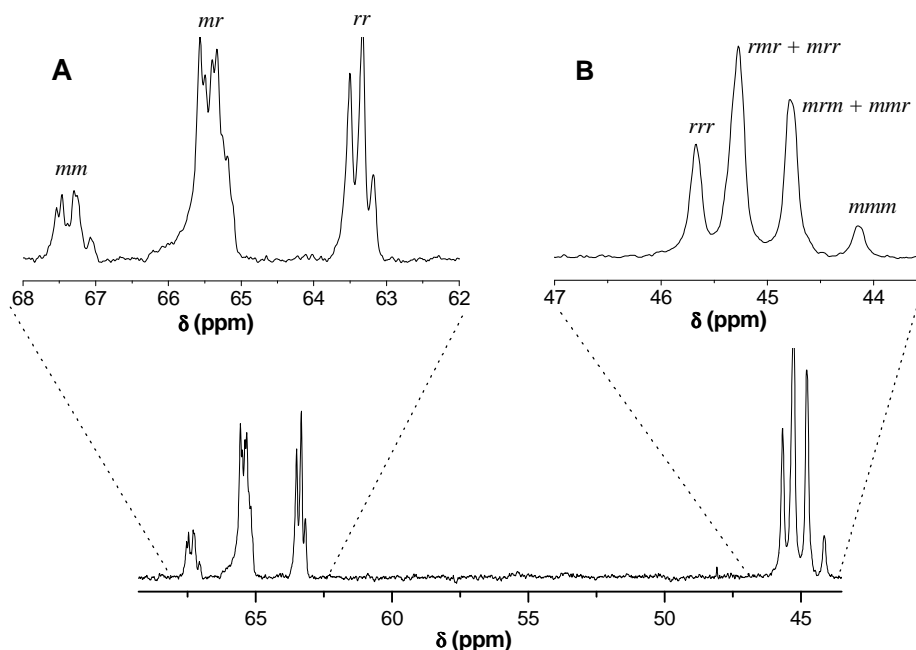


Fig. 4.3 ^{13}C NMR spectrum of PVA: (A) methine carbon region and (B) methylene carbon region.

The propagation mechanism for FRP obeys Bernoullian statistics,²⁰⁻²² meaning that the stereoregularity of the growing polymer chain is not affected by the ultimate or penultimate monomer added. The Bernoullian process can be described by the parameters P_m and P_r : P_m is the probability that a growing chain will form an isotactic sequence and P_r the probability that a syndiotactic sequence will form. These parameters are described by equations 4.4 and 4.5 and can be used to calculate *n*-ad tacticity.

$$P_m = (mm)^{1/2} = 1 - (rr)^{1/2} \quad (4.4)$$

$$P_r = (rr)^{1/2} = 1 - (mm)^{1/2} \quad (4.5)$$

The equations for calculating triad and tetrad tacticities using the Bernoullian model can be simplified as shown in equations 4.6–4.8 for the former and equations 4.9–4.14 for the latter.

For triad tacticities:

$$mm = (P_m)^2 \quad (4.6)$$

$$mr = 2P_m(1 - P_m) \quad (4.7)$$

$$rr = (1 - P_m)^2 \quad (4.8)$$

Tetrad tacticities

$$mmm = P_m^3 \quad (4.9)$$

$$mmr = 2P_m^2(1 - P_m) \quad (4.10)$$

$$rmr = P_m(1 - P_m)^2 \quad (4.11)$$

$$mrm = P_m^2(1 - P_m) \quad (4.12)$$

$$rrm = 2P_m(1 - P_m)^2 \quad (4.13)$$

$$rrr = (1 - P_m)^3 \quad (4.14)$$

Diad tacticity was obtained from the triad tacticity using the following equations.

$$m = mm + 0.5mr \quad (4.15)$$

$$r = rr + 0.5mr \quad (4.16)$$

Determination of syndiotacticity. The area intensities of the hydroxyl proton signals were quantified and the results are tabulated in Table 4.4. The samples prepared via thermoinitiation (samples 1 and 2) showed a decrease in syndiotacticity (rr) with an increase in the polymerization temperature. A similar result was observed by Lyoo *et al.*¹⁰ Generally, photoinitiated polymerization resulted in PVA microfibrils with higher syndiotacticities than thermoinitiated polymerization (samples 1 and 3). This justifies the use of photoinitiated FRP for the synthesis of a PVA precursor.

There was a decrease in syndiotacticity with a decrease in VPi content for the samples prepared by the saponification of VPi/VAc copolymers (samples 4–7). Syndiotacticity in PVA depends on the bulkiness of the side group of the parent polymer. VPi has the huge tertiary butyl group whilst VAc has the less bulky methyl group. The observed decrease in syndiotacticity thus occurred as a result of the decrease in the number of the tertiary butyl groups in the precursor polymer. This effect of VPi/VAc composition on the syndiotacticity of PVA indicates that copolymerization of VPi and VAc affords an easy route to stereochemical control in PVA.

Table 4.4 Triad tacticity from hydroxyl protons signals of PVA

Sample	Triad tacticity ^a			Diad tacticity ^b	
	<i>mm</i>	<i>mr</i>	<i>rr</i>	<i>m</i>	<i>r</i>
1	0.161	0.484	0.354	0.403	0.597
2	0.161	0.516	0.323	0.419	0.581
3	0.132	0.500	0.368	0.382	0.618
4	0.147	0.500	0.353	0.397	0.603
5	0.165	0.510	0.325	0.420	0.580
6	0.175	0.509	0.316	0.429	0.571
7	0.186	0.509	0.302	0.443	0.557

^a Observed from hydroxyl proton triad; *mm*-isotactic, *mr*-heterotactic, *rr*-syndiotactic, ^b Calculated from triad tacticity using equations 4.15 and 4.16

Isotacticity (*mm*) increased with an increase in VAc content and heterotacticity (*mr*) remained relatively constant. The increase in isotacticity indicates that PVAc favors the isotactic stereosequence in PVA. The diad tacticity results also show a similar trend of an increase in isotacticity accompanied by a decrease in syndiotacticity as the VPI content decreased.

Table 4.5 gives the quantitative data of the triad tacticities of samples 1–7 obtained from ¹³C NMR. The trends in stereosequences obtained were in agreement with those obtained from the hydroxyl proton resonances. The syndiotacticity of samples 3–7 decreased and the isotacticity increased with an increase in VAc content.

Table 4.5 Triad tacticity of PVA based on ¹³C NMR

Sample	Triad tacticity ^a			Parameter ^b		
	<i>mm</i>	<i>mr</i>	<i>rr</i>	P_m	P_r	$P_m + P_r$
1	0.145	0.507	0.348	0.381	0.590	0.971
2	0.105	0.610	0.284	0.324	0.533	0.857
3	0.164	0.478	0.358	0.405	0.598	1.003
4	0.057	0.586	0.356	0.239	0.597	0.836
5	0.153	0.492	0.354	0.391	0.595	0.986
6	0.179	0.518	0.304	0.423	0.551	0.974
7	0.192	0.519	0.288	0.463	0.537	1.000

^a Observed from methine carbon atom triad, ^b Calculated from *mm* and *rr* using equations 4.4 and 4.5

The Bernoullian parameters P_m and P_r were obtained from the results of triad tacticity using equations 4.4 and 4.5. For samples 3–7 the probability that a polymer with a syndiotactic

sequence would form (P_r) decreased with a decrease in VPi content. This confirms the dependence of syndiotacticity of PVA on the structure of the precursor polymer.

Table 4.6 tabulates the observed as well as calculated intensities of the methylene carbon atom signals. It is worth noting that a bulky substituent group (tert butyl group) does not affect the mechanism of FRP,²⁰ hence VPi polymerization can be described by the Bernoullian model.

Table 4.6 Tetrad tacticity of PVA based on ¹³C NMR data

Sample	1	2	3	4	5	6	7
Tetrad tacticity ^a							
<i>rrr</i>	0.120	0.161	0.167	0.130	0.125	0.122	0.070
<i>rmr + mrr</i>	0.455	0.452	0.450	0.435	0.425	0.439	0.426
<i>mrm + mmr</i>	0.361	0.339	0.333	0.348	0.375	0.354	0.426
<i>mmm</i>	0.072	0.048	0.050	0.087	0.075	0.085	0.078
Tetrad tacticity ^b							
<i>rrr</i>	0.205	0.151	0.214	0.212	0.211	0.168	0.155
<i>rmr + mrr</i>	0.428	0.398	0.432	0.338	0.338	0.409	0.400
<i>mrm + mmr</i>	0.297	0.348	0.290	0.291	0.293	0.333	0.345
<i>mmm</i>	0.069	0.102	0.065	0.066	0.066	0.090	0.099

^a Observed from ¹³C NMR spectra, ^b Calculated assuming Bernoullian statistics for P_r

There was reasonable agreement between the tacticities obtained from ¹³C NMR by calculating the area intensities and the tacticities calculated using the Bernoullian parameters. However a slight discrepancy was observed in the tetrad syndiotacticities (*rrr*) of samples 1 and 2. The differences in the observed and calculated tetrad syndiotacticity values were probably due to errors made while processing the NMR data.

Fig. 4.4 summarizes all the quantitative data obtained for the syndiotacticities of samples 4–7. For all the methods used there was a correlation between syndiotacticity and VPi content in the copolymer. Syndiotacticity increased with an increase in VPi content.

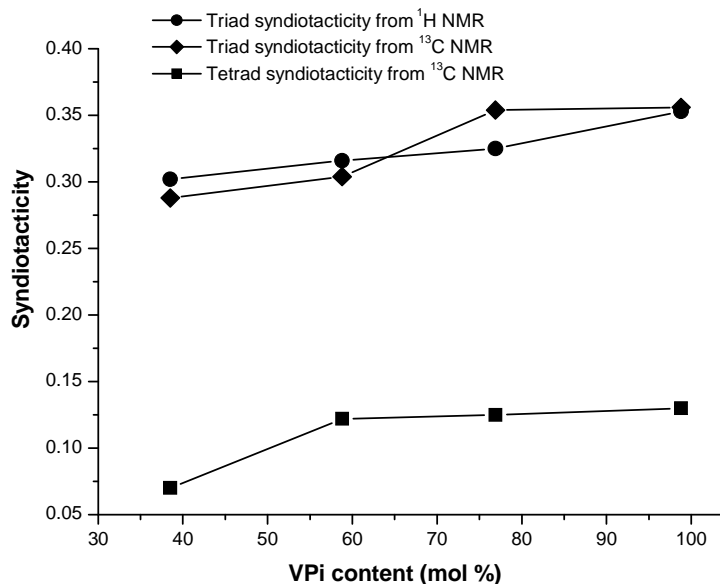


Fig. 4.4 Effect of VPi content on syndiotacticity of PVA.

4.4.3 Number average lengths

Making use of the triad tacticities of the samples as determined from the hydroxyl proton spectra, the number average lengths of the isotactic and syndiotactic regions were calculated. An estimation of these values can aid one in predicting the nature of the syndiotactic and isotactic regions (i.e. whether they are composed of short or long blocks).

The number average lengths of the isotactic (n_m) and syndiotactic (n_r) blocks were calculated using equations 4.17 and 4.18. From these values the number average lengths (n) for all blocks were determined using equation 4.19.¹³

$$n_m = 1 + 2 (mm) / (mr) \quad (4.17)$$

$$n_r = 1 + 2 (rr) / (mr) \quad (4.18)$$

$$n = 0.5 (n_m + n_r) \quad (4.19)$$

mm , mr and rr are the fractions of isotactic, heterotactic and syndiotactic triads (obtained from the hydroxyl proton signals) respectively. The number average lengths for samples 3–7 were calculated and plotted as a function of VPi content (mol %), as illustrated in Fig. 4.5. The number average lengths of the isotactic blocks increased from 1.528–1.731 whilst the number average lengths of the syndiotactic blocks decreased from 2.472–2.187 as the VPi content

(mol %) decreased. For samples 3–7 the values for n were 1.96–2.00 indicating the presence of short blocks in the copolymer.

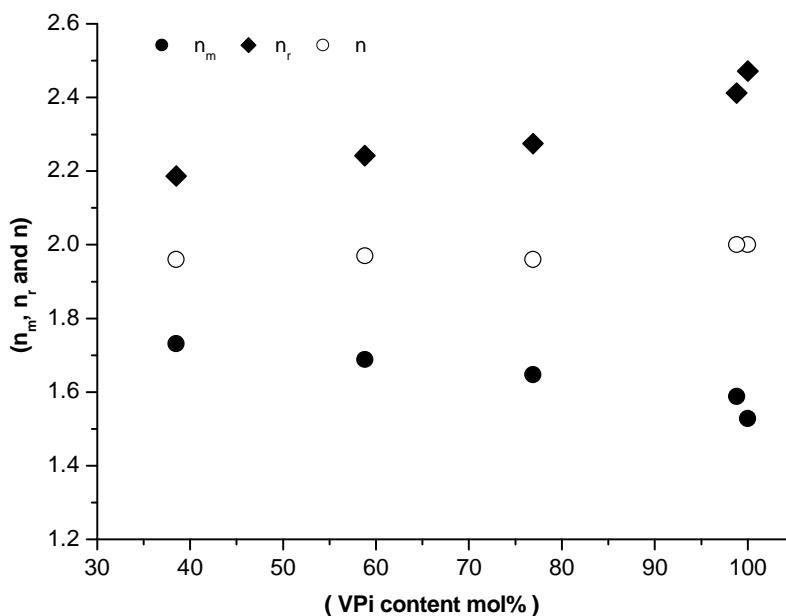


Fig. 4.5 Number average lengths of PVA.

4.4.4 Crystallinity of PVA

The conventional method for determining the crystallinity of polymers is by using DSC. However PVA starts to decompose close to its crystalline melting temperature which makes DSC unsuitable here. X-ray powder diffraction (XRD) was thus used to track changes in crystallinity with changes in syndiotacticity. The XRD profiles of the syndiotactic PVA samples (3–7) show sharp crystalline reflections with strong maxima at approximately $2\theta = 19.5^\circ$. The diffractogram shown in Fig. 4.6 illustrates a typical result obtained in this study. The diffractograms for the other samples are shown in Appendix 2.

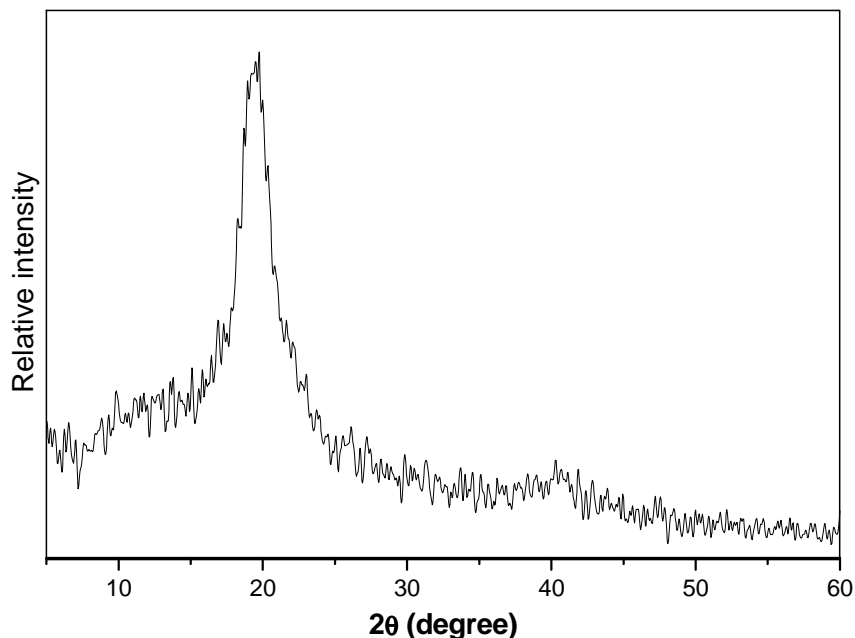


Fig. 4.6 X-ray powder diffraction profile of syndiotactic PVA microfibrils (s-diad content = 60.3%).

4.4.5 Effect of syndiotacticity on the morphology of PVA microfibrils

The morphology of the PVA microfibrils was studied and the effect of syndiotacticity and comonomer composition on the morphology established. The saponification of highly syndiotactic PVPi led to fine PVA fibers composed of well-aligned microfibrils, as shown in Fig. 4.8A. The ability of highly syndiotactic PVA to form fibrillar structures during saponification lies in its high crystallinity.

The accepted unit cell structure for atactic PVA (s-diad content < 53%) is monoclinic, with the following dimensions $a=7.81 \text{ \AA}$, $b=2.53 \text{ \AA}$ (chain axis), $c=5.51 \text{ \AA}$ and $\beta=91^\circ 42'$.^{23,24} It comprises two vinyl alcohol monomer units held together by strong hydrogen bond interactions as shown in Fig. 4.7. When the syndiotacticity is increased the crystallites become larger and less distorted, resulting in a lateral contraction of the crystal structure. The hydrogen bond interactions become stronger and the unit cell size smaller (dimensions: $a=7.63 \pm 0.02 \text{ \AA}$, $b=2.54 \pm 0.01 \text{ \AA}$, $c=2.54 \pm 0.01 \text{ \AA}$ and $\beta=91.2 \pm 0.1^\circ$).²³ This reduction in unit cell size leads to better chain packing and higher crystallinity.

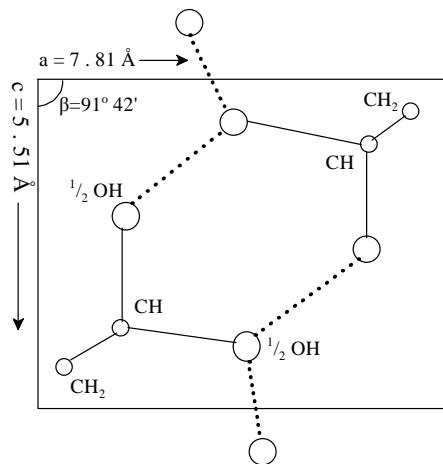


Fig. 4.7 Unit cell of PVA (monoclinic) (solid lines represent covalent bonds and dotted lines represent hydrogen bonds).

Despite there being a number of factors (given in Table 4.1) involved in the *in situ* fibrillation of PVA, syndiotacticity is by far the most important. The *in situ* fiber formation behavior of PVA is unique to PVA derived from VPi homopolymer and copolymers of VPi/PVAc of sufficient syndiotacticity (s-diad > 57%). The saponification of PVAc of high molecular weight and an s-diad content of less than 53% yielded shapeless, globular morphologies.^{7,13,15}

Fig. 4.8 compares the morphologies of PVA samples 3, 5, 6 and 7 with syndiotacticities of between 55.7 and 61.8% and VPi comonomer contents of between 38.5 and 100 mol %. Fig. 4.8A (i) is the optical micrograph of a PVA fiber with an s-diad content of 61.8% prepared via the saponification of VPi homopolymer. Fig. 4.8A (ii) is a zoom in of the PVA fiber in Fig. 4.8A (i), using SEM. The image shows that the PVA fibers were composed of well-aligned microfibrils with dimensions of 0.4–1.2 μm in diameter. When the syndiotacticity was reduced to 60.3% (VPi content in precursor polymer was 98.8 mol %), the fibers comprised fairly well aligned microfibrils. The image illustrating this is shown in Appendix 3.

Fig.s 4.8B (i and ii) are the SEM images of PVA sample 5 (s-diad content of 58.0 % and VPi content in precursor polymer of 76.9 mol %) taken at different magnifications. The PVA sample was not composed of bundles of microfibrils like samples 3 and 4 but instead was composed of individual microfibrils with spherical particles on their surfaces.

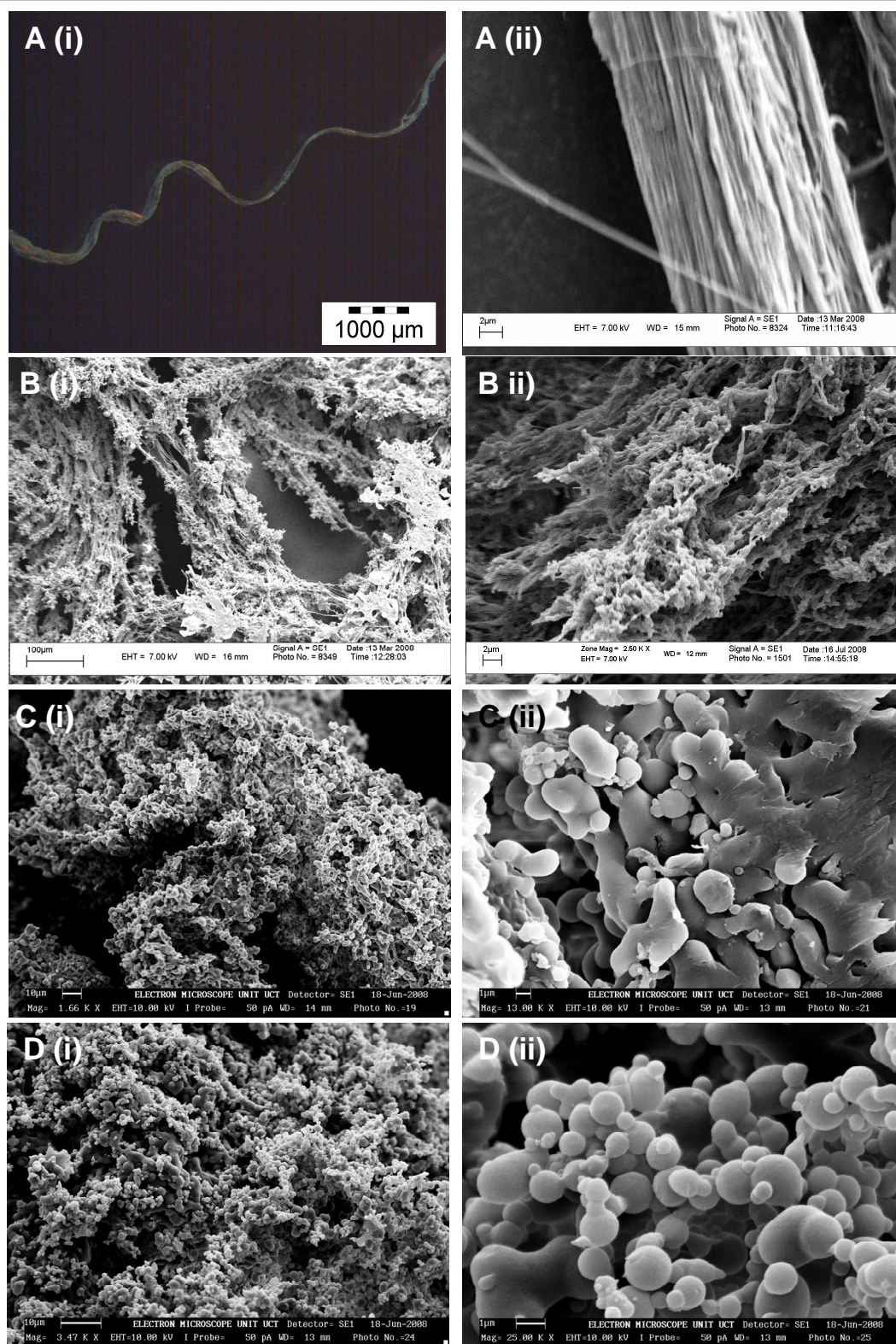


Fig. 4.8 Images of PVAs with different s-diad contents: (A) 61.8% (i) optical micrograph and (ii) SEM image; (B) 58.0% (i) x1000 and (ii) x2500; (C) 57.1% (i) x1660 and (ii) x3000; (D) 55.7% (i) x3470 and (ii) x25000.

Fig. 4.8C (i and ii) shows PVA sample 6 (s-diad content of 57.1% and VPi content in precursor polymer of 58.8 mol %). The sample consists of poorly formed spherical particles and very few fibrous regions. The fibers were short and had diameters of 3.8–6.3 μm whilst the particles were 2.5–3.8 μm in diameter. These results were in agreement with those predicted by Ghim *et al.*²⁵ When the comonomer composition of VPi:VAc is about 50:50 (mol %) the copolymer comprises very short blocks. Upon saponification it is thus expected that poorly formed fibrous material will result.

This loss of fibrous morphology with a decline in syndiotacticity was attributed to a decrease in crystallinity. A certain level of crystallinity is required to stabilize the fibers.⁷ The SEM images for sample 7 (s-diad content of 55.7% and VPi content in precursor polymer 38.5 mol %) are shown in Fig. 4.8D (i and ii). The fibrous morphology of syndiotactic PVA was completely lost and the sample was composed entirely of spherical particles which had diameters of 3–12.1 μm . These results were also in agreement with those of Ghim *et al.*²⁵ When the VPi content is less than 40 mol % the VPi/VAc copolymer comprised VAc blocks subdivided by an almost single VPi unit. This is insufficient to bring about chain orientation that is necessary for fibrillation, hence no fibers were observed. However, the formation of PVA particles in this manner was unprecedented.

4.4.6 Effect of syndiotacticity on thermal properties

The effects of syndiotacticity on the thermal properties of PVA were then investigated using TGA and DSC.

Thermogravimetric analysis. The thermal degradation behavior of the PVA samples (3–7) was studied at a heating rate of 10 $^{\circ}\text{C min}^{-1}$, under a nitrogen atmosphere. The accepted mechanism for thermal decomposition of PVA involves two steps (illustrated in Fig. 4.9). The first involves the elimination of water and the second involves pyrolysis via main chain scission.^{26,27} In atactic PVA, the first degradation step occurs at 220–275 $^{\circ}\text{C}$ and the second step at 300–350 $^{\circ}\text{C}$.²⁸ Table 4.7 tabulates the T_{onset} and mass loss data (DTGA) for syndiotactic PVA (s-diad content of 55.7–61.8 %). The slight weight loss below 100 $^{\circ}\text{C}$ occurring in all the samples was attributed to water loss. Water elimination occurs at 268–306 $^{\circ}\text{C}$ and pyrolysis at 454–466 $^{\circ}\text{C}$. These results clearly show an enhancement in thermal stability with an increase in syndiotacticity. This increase in thermal stability is attributed to higher chain compactness owing to the tight intermolecular hydrogen bonding and higher stereoregularity.¹²

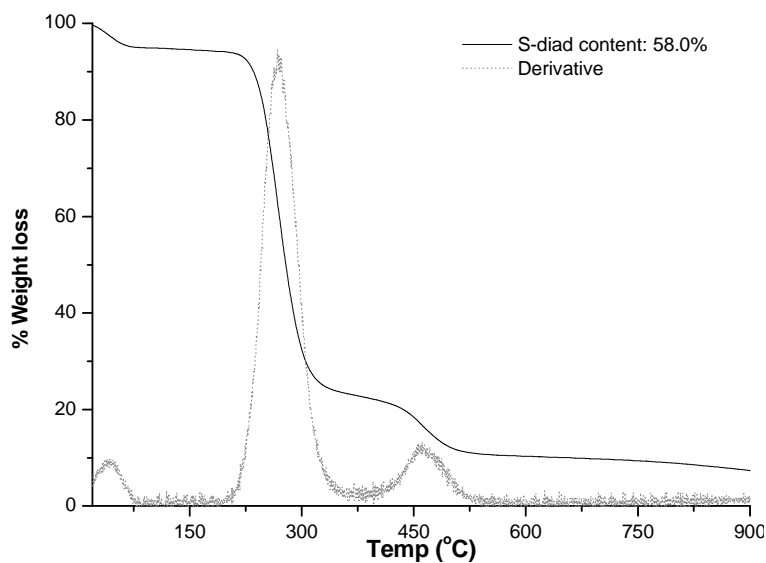


Fig. 4.9 TG and DTGA thermograms of PVA microfibrils.

Table 4.7 TGA analysis of PVA with varying syndiotacticity

Sample	^a s-diad (%)	^b D.S (%)	^c T _{onset} (°C)	^d DTGA peak (°C)	^e Weight loss (%)	^f Residue at 900 °C
3	61.8	>99	275	50	5.9	5.9
				306	73.9	
4	60.3	>99	255	465	12.4	4.1
				43	5.4	
5	58.0	98	236	303	79.1	7.3
				462	7.4	
6	57.1	>99	249	41	5.5	5.6
				268	71.1	
7	55.7	>99	264	466	12.3	3.1
				60	4.3	
				283	77.1	
				464	11.1	
				53	3.7	
				285	83.3	
				454	6.8	

^a Diad syndiotacticity obtained from ¹H NMR, ^b Degree of saponification obtained as given in Section 4.4.3.1, ^c Onset temperature for thermal decomposition, ^d Differential mass loss peak maxima, ^e Weight loss at DTGA peak maximum, ^f Carbon residue at 900 °C

Thermal decomposition of PVA is affected by the degree of saponification, method of preparation of polymer and, to some extent, tacticity.¹² Thermogravimetric studies carried out on highly isotactic (HI, $mm=0.762-0.791$), lowly isotactic (LI, $mm=0.400-0.630$), syndiotactic (S) and atactic (A) PVA showed that thermal stability decreased in the following order: HI-PVA>S-PVA>A-PVA>LI-PVA.²⁸

Differential scanning calorimetry. The glass transition temperature (T_g) could not be observed in all the samples analyzed in this work. The crystalline melting temperature, T_m was observed at temperatures greater than 210 °C. The main factors affecting T_m are the degree of saponification, degree of branching, tacticity and 1,2 glycol content.¹²

Table 4.8 tabulates the dependence of T_m on the syndiotacticity and degree of saponification. Generally there was an increase in T_m with an increase in syndiotacticity. This was because with an increase in syndiotacticity the intermolecular hydrogen bonding also increases and the polymer becomes highly crystalline. Consequently higher temperatures will be required to effect crystalline melting.

Table 4.8 Effects of syndiotacticity and DS of PVA on T_m

Sample	S-diad (%)	DS (%)	T_m (°C)
3	61.8	>99	249
4	60.3	>99	242
5	58.0	98	216
6	57.1	>99	231
7	55.7	>99	228

The lower T_m of sample 5 is due to the low degree of saponification. The presence of the carbonyl groups not only disrupts crystallinity but also reduces hydrogen bonding between polymer chains. Less energy is thus required to overcome the interactions between polymer chains to effect polymer melting.

4.5 Conclusions

Highly syndiotactic PVA microfibrils were prepared via *in situ* fibrillation by saponification of high molecular weight PVPI. The ability of PVA to form fibres during saponification was attributed to the high crystallinity of syndiotactic PVA, which was brought about by the enhanced chain packing and strong hydrogen bond interactions. When the syndiotacticity was reduced by saponification of VPI/VAc copolymers of varying comonomer compositions the morphology of the fibers also changed. When the comonomer feed composition of 30/70 (VPI/VAc mol %) was used only spherical particles were obtained. The formation of spherical PVA particles following the saponification of VPI/VAc copolymers prepared by FRP in bulk was novel. This was novel as spherical PVA particles are obtained only by emulsion or suspension polymerizations. These particles have potential use in biomedical applications^{29,30} and as fillers in the paper industry.

Syndiotactic PVA has better thermal and mechanical properties compared to atactic PVA owing to its high level of molecular orientation. This makes it potentially a better material for application.

References

1. Wang, Y.; Hsieh, Y.-L. *J. Membr. Sci.* **2008**, 309, 73–81.
2. Kanamoto, T.; Kiyooma, S.; Tovmasyan, Y.; Sano, H.; Narukawa, H. *Polymer* **1990**, 31, 2039–2046.
3. Kunugi, T.; Kawasumi, T.; Ito, T. *J. Appl. Polym. Sci.* **1990**, 40, 2101.
4. Garrett, P. D.; Grubb, D. T. *Polym. Commun.* **1988**, 29, 60.
5. Grubb, D. T.; Kearney, F. R. *J. Appl. Polym. Sci.* **1990**, 39, 695–705.
6. Liu, S.; Sun, G. *Carbohydr. Polym.* **2008**, 71, 614–625.
7. Lyoo, W. S.; Chvalun, S.; Ghim, H. D.; Kim, J. P.; Blackwell, J. *Macromolecules* **2001**, 34, 2615–2623.
8. Nagara, Y.; Nakano, T.; Okamoto, Y.; Gotoh, Y.; Nagura, M. *Polymer* **2001**, 42, 9679–9686.
9. Lyoo, W. S.; Kim, J. H.; Ghim, H. D. *Polymer* **2001**, 42, 6317–6321.
10. Lyoo, W. S.; Han, S. S.; Kim, J. H.; Yoon, W. S.; Lee, C. J.; Kwon, I. C.; Lee, J.; Ji, B. C.; Han, M. H. *Angew. Makromol. Chem.* **1999**, 271, 46–52.
11. Lyoo, W. S.; Ha, W. S. *Polymer* **1999**, 40, 497–505.
12. Lyoo, W. S.; Ha, W. S. *J. Polym. Sci., Part A: Polym. Chem.* **1997**, 35, 55–67.
13. Lyoo, W. S.; Blackwell, J. *Macromolecules* **1998**, 31, 4253–4259.
14. Lyoo, W. S.; Ha, W. S. *Polymer* **1996**, 37(14), 3121–3129.
15. Lyoo, W. S.; Ghim, H. D.; Kim, J. H. *Macromolecules* **2003**, 36, 5428–5431.
16. Yeum, J. H.; Ji, B. C.; Noh, S. K.; Jeon, H. Y.; Kwak, J. W.; Lyoo, W. S. *Polymer* **2004**, 45, 4037–4043.
17. Lyoo, W. S.; Kim, S. S.; Ghim, H. D.; Kim, J. P.; Lee, S. S. *J. Appl. Polym. Sci.* **2002**, 85, 1992–2003.
18. Moritani, T.; Kuruma, I.; Shibatani, K.; Fujiwara, Y. *Macromolecules* **1972**, 5(5), 577–580.
19. Ovenall, D. W. *Macromolecules* **1984**, 17, 1458–1464.
20. Katsuraya, K.; Hatanaka, K.; Matsuzaki, K.; Amiya, S. *Polymer* **2001**, 42, 9855–9858.
21. Bovey, F. A.; Mirau, P. A., *NMR of Polymers*. Academic Press: New Jersey, 1996.
22. Tonelli, A. E. *Macromolecules* **1985**, 18, 1086–1090.
23. Cho, J. D.; Lyoo, W. S.; Chvalun, S. N.; Blackwell, J. *Macromolecules* **1999**, 32, 6236–6241.

24. Bhat, N. V.; Nate, M. M.; Kurup, M. B.; Bambole, V. A.; Sabharwal, S. *Nucl. Instrum. Meth B* **2005**, 237, 585–592.
25. Ghim, H. D.; Kim, J. P.; Lyoo, W. S. *Polymer* **2003**, 44, 895–900.
26. Thomas, P. S.; Guerbois, J. P.; Russell, G. F.; Briscoe, B. J. *J. Therm. Anal.* **2001**, 64, 501–508.
27. Holland, B. J.; Hay, J. N. *Polymer* **2001**, 42, 6775–6783.
28. Ohgi, H.; Sato, T.; Hu, S.; Horii, F. *Polymer* **2006**, 47, 1324–1332.
29. Lyoo, W. S.; Park, C. S.; Yeum, J. H.; Ji, B. C.; Lee, C. J.; Lee, S. S.; Lee, J. Y. *Colloid Polym. Sci.* **2002**, 280, 1075–1083.
30. Lyoo, W. S.; Kwak, J. W.; Yeum, J. H.; Ji, B. C.; Lee, C. J.; Noh, S. K. *J. Polym. Sci. AI* **2005**, 43, 780–800.

CHAPTER 5

Heterogeneous modification of PVA microfibrils

5.1 Introduction

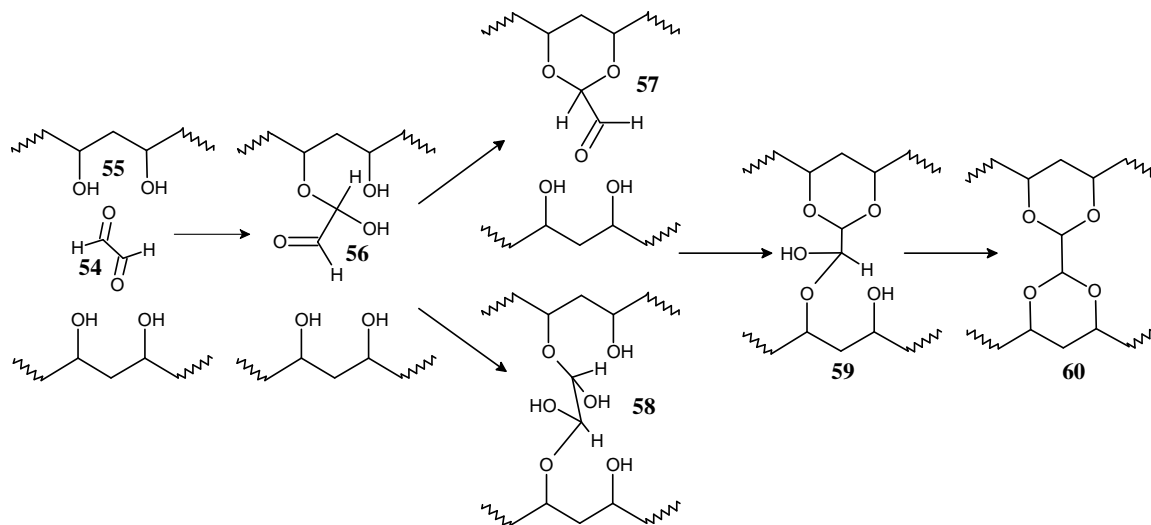
The need to modify PVA microfibrils was pointed out in Section 2.6.3 (Chapter 2). PVA microfibrils have potential application as filler retention aids in the paper industry. Cationic modification of PVA enhances fiber-filler interactions while anionic modification enables PVA microfibrils to also act as flocculants/dispersants of calcium carbonate. PVA is a linear polymer with side chains of secondary alcohol groups. This means that it is capable of undergoing all the reactions typical of secondary alcohols i.e. esterification, etherification and acetalization. The latter two reactions were of particular interest in this study.

This chapter will be presented in two main sections. The first covers the crosslinking of PVA microfibrils with glyoxal and the second the anionic and cationic modification of the resultant crosslinked PVA.

5.1.1 Crosslinking of PVA fibers. Crosslinking with glyoxal, a dialdehyde was carried out prior to cationic and anionic modification in order to insolubilize the amorphous regions of the PVA microfibrils. During the reaction of PVA with dialdehydes, acetalization takes place. This renders the fibers insoluble in water and also significantly preserves fiber structure and properties.¹ The general mechanism for crosslinking of PVA with dialdehydes involves hemiacetal and acetal formation, as illustrated in Scheme 5.1.^{1,2}

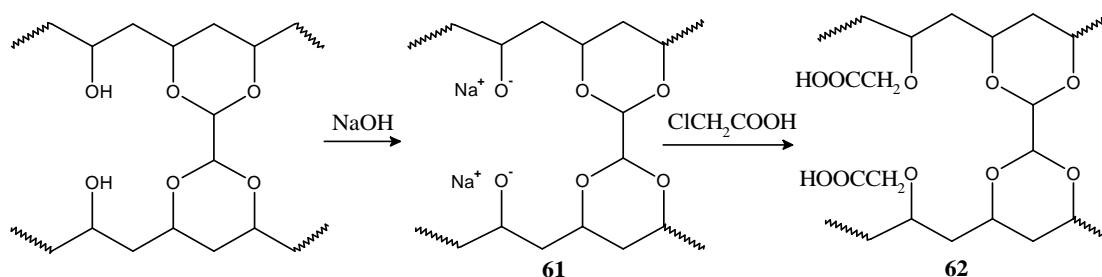
In the presence of a Brønsted acid catalyst the carbonyl oxygen of the glyoxal (structure **54**) is first protonated. This is then followed by nucleophilic attack of the electron deficient carbonyl carbon atom by the PVA hydroxyl group, resulting in a hemiacetal as shown in structure **56**. In the presence of excess acid the hemiacetal undergoes an intramolecular nucleophilic addition reaction with a second hydroxyl group resulting in an acetal **57**. The unreacted carbonyl group in **56** can also undergo an intermolecular nucleophilic addition reaction with an hydroxyl group of PVA resulting in a dihemiacetal as shown in structure **58**. The unreacted carbonyl group in **57** and the hemiacetal groups in **58** can then undergo a series of protonations, followed by nucleophilic addition reactions with PVA hydroxyl groups, resulting in a diacetal **60** as the final product. Acetalization was important as it minimized the

solubility of the PVA fibers in the aqueous media in which they were modified. Acetals are stable in basic media.^{2,3}



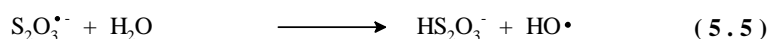
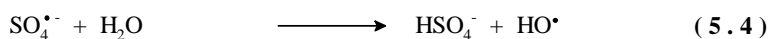
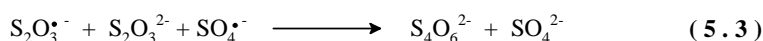
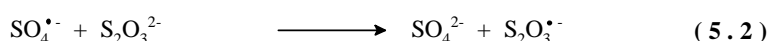
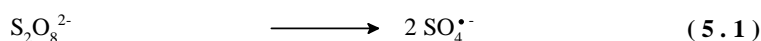
Scheme 5.1 Crosslinking of PVA with glyoxal

5.1.2 Heterogeneous cationic and anionic modification of PVA fibers. Following acetalization, the PVA fibers were swollen in aqueous media so as to expose the majority of the functional groups.⁴ Modification was carried out by carboxymethylation (using Williamson's ether synthesis) and grafting (using the "grafting from" technique). Carboxymethylation of PVA by Williamson's etherification is a two step process. The first step involves the formation of an alkoxide via the reaction of PVA with a strong base and the second step the reaction of that alkoxide with an alkyl halide containing the carboxylic acid functionality. These steps are illustrated in Scheme 5.2. To the author's knowledge the heterogeneous carboxymethylation PVA fiber has not been reported.



Scheme 5.2 Carboxymethylation of crosslinked PVA

The heterogeneous (surface) modification of PVA fibers was also carried out by grafting. Grafting is a most useful method for imparting new and desirable properties to polymers. Acrylic acid (anionic monomer) and 2-methacryloyloxyethyl trimethyl ammonium chloride (cationic monomer) were grafted from PVA using a potassium persulfate/sodium thiosulfate (KPS/Na₂S₂O₃) redox initiating system. The mechanism of grafting involves the generation of a radical on the carbon atom adjacent to the hydroxyl group of the PVA and then growth of a polymeric chain from it. Grafting is commonly carried out in solution; there is very little information in literature on grafting in heterogeneous media for the modification of PVA fibers. When KPS is used concurrently with Na₂S₂O₃ the initiating radical flux is increased (as shown in Equations 5.1–5.5) and more macroradicals are formed. This results in higher grafting yields.



Modified PVA microfibrils were characterized using PAS FT-IR, ¹H NMR and ¹³C NMR. An investigation into the thermal properties of the modified fibers was also carried out using TGA and DSC. The thermal properties of PVA are particularly important as they have a significant effect on its processing and applications.

5.2 Crosslinking PVA microfibrils with glyoxal

5.2.1 Materials

PVA microfibrils from sample 3 (Section 4.2.2) glyoxal (Merck, 40% aqueous solution), 37% HCl (Saarchem), deionized water. All reagents were used as received.

5.2.2 Procedure

The following typical procedure was used for the crosslinking reaction. PVA microfibrils (0.5 g) were treated with an aqueous solution of 1% glyoxal (50 mL) at pH ~2.5 (0.4 N HCl was used to adjust the pH). The mixture was stirred vigorously for a set time, filtered, washed once with water and then dried in air overnight. The microfibrils were then purified by

Soxhlet extraction, using methanol as the solvent, for 8 h and then dried in a vacuum oven overnight. The glyoxal concentration and the reaction time were varied, as shown in Tables 5.2 and 5.3 respectively.

5.2.3 Analyses

5.2.3.1 NMR

^1H and ^{13}C NMR spectra were recorded using a 600 MHz Varian *Unity* Inova instrument.

Preparation of samples. All samples were dissolved in DMSO-*d*₆. Solution NMR analysis of the crosslinked PVA fibers was possible as the fibers were crosslinked only on the surface. Water (the usual solvent for PVA) could not be used here because the crosslinked PVA samples were insoluble in water. The lack of solubility of the PVA microfibrils in water was attributed to their high level of syndiotacticity.

5.2.3.2 Thermal analysis

TGA and DSC analyses were carried out as described in Section 4.3.3

The degree of crystallinity was determined by comparing the observed heat of fusion (melting) ($\Delta H'_m$) of the PVA samples with that of a 100% crystalline PVA polymer sample (ΔH_m) as shown in equation 5.6. The value of ΔH_m used was 156.2 J/g as obtained from literature.⁵

$$\text{Degree of crystallinity (\%)} = \frac{\Delta H'_m}{\Delta H_m} \times 100 \quad (5.6)$$

5.2.4 Results and discussion

5.2.4.1 Evidence of crosslinking

Fig. 5.1 shows the ^1H NMR spectra of uncrosslinked and crosslinked PVA fibers. The spectrum for uncrosslinked PVA was assigned fully in Section 4.4.2.1. Intermolecular acetalization (crosslinking) was confirmed by the signals at 4.15 and 3.22 ppm. These were attributed to the glyoxal protons (labeled g) and the methine protons adjacent to the acetal ring (labeled h) respectively. In all the spectra obtained the ratio of the glyoxal protons (g) to the methine protons (h) was 2:4. This confirmed the proposed crosslinking of acetalization.

The degree of crosslinking was determined by comparing the areas of the PVA methylene protons (labeled e in Fig. 5.1) and the glyoxal protons (labeled g),⁶ as shown in Equation 5.7.

$$\text{Degree of crosslinking} = \frac{\text{Area}_g}{\text{Area}_e} \times 100 \quad (5.7)$$

where area_g and area_e are the area intensities of the signals labeled g and e respectively (there are two protons per signal which cancel out in the above simplified equation).

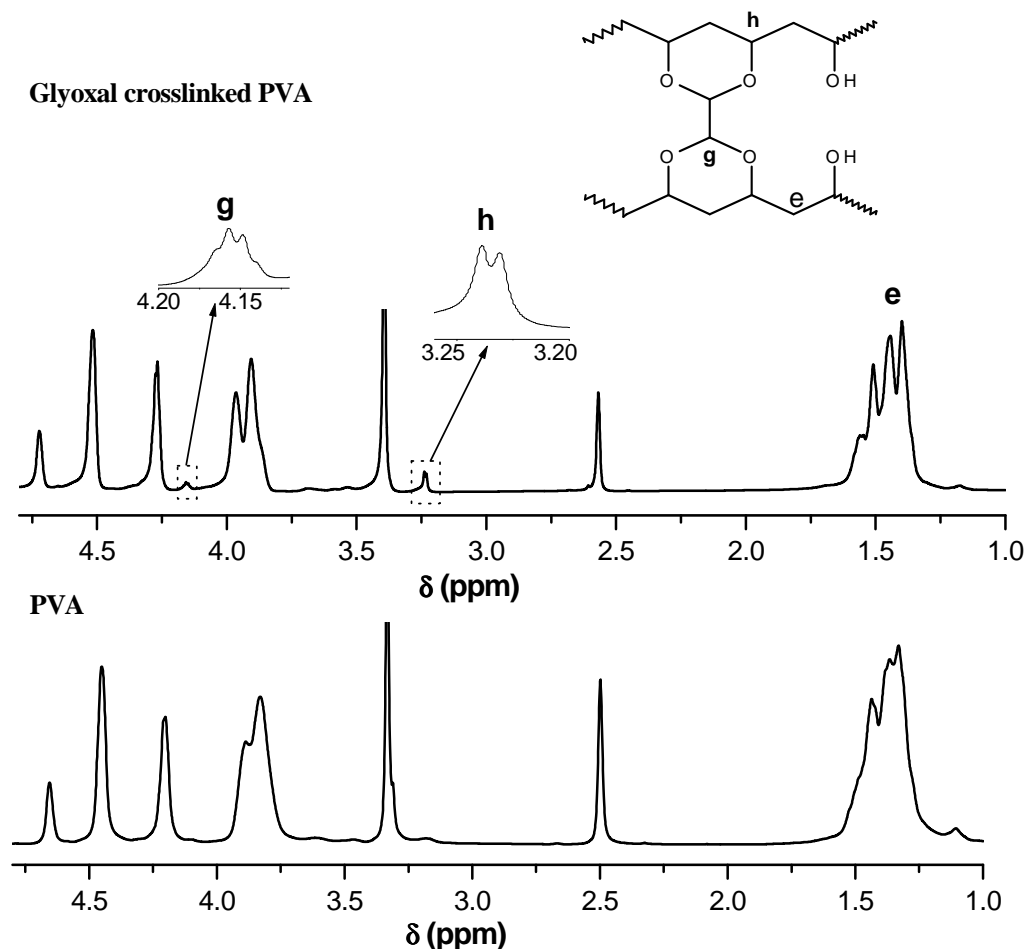


Fig. 5.1 ¹H NMR spectra of crosslinked and unmodified PVA microfibrils.

5.2.4.2 Factors affecting the degree of crosslinking

The degree of crosslinking is affected by a number of factors. These include the concentration and amount of crosslinking agent and the crosslinking time and temperature. In this study, a brief investigation into the effects of crosslinking time and glyoxal concentration on the degree of crosslinking was carried out.

Effect of glyoxal concentration. The glyoxal concentration was varied as shown in Table 5.2 and a constant crosslinking time of 180 seconds was used. It was observed that the degree of crosslinking increased with an increase in the glyoxal concentration. This was primarily because of the increased availability of glyoxal molecules in the vicinity of the PVA chains.

Table 5.2 Effect of glyoxal concentration on the degree of crosslinking of PVA

Sample	[glyoxal] ^a %	Degree of ^b crosslinking
3e	1	0.313
3d	5	0.461
3c	10	0.637

^a Glyoxal concentration (v/v) in water, ^b degree of crosslinking determined from ¹H NMR data using equation 5.7

Effect of crosslinking time. In order to investigate the effect of crosslinking time on the degree of crosslinking, a constant glyoxal concentration of 10% (v/v) was used and the crosslinking time was varied as shown in Table 5.3.

Table 5.3 Effect of crosslinking time on the degree of crosslinking of PVA microfibrils

Sample	Crosslinking time (sec)	^a Degree of crosslinking
3a	30	0.218
3b	90	0.371
3c	180	0.637

^a Determined from ¹H NMR data using equation 5.7

The degree of crosslinking increased with an increase in crosslinking time. This was expected as an increase in reaction time gives the reagents more time to react.

5.2.5 Thermal properties

Thermal stability. The differences in the thermal behavior between uncrosslinked and crosslinked PVA microfibrils (sample 3d) are evident from the TGA and DTGA curves shown in Fig. 5.2. In uncrosslinked PVA the mechanism of thermal degradation involves two well separated mechanisms of water elimination and depolymerization, which are characterized by the two steps in the TGA thermogram. In crosslinked PVA two mechanisms are also involved but there is partial overlapping of these two, owing to the enhancement of the thermal stability of the PVA fibers brought about by crosslinking.⁷

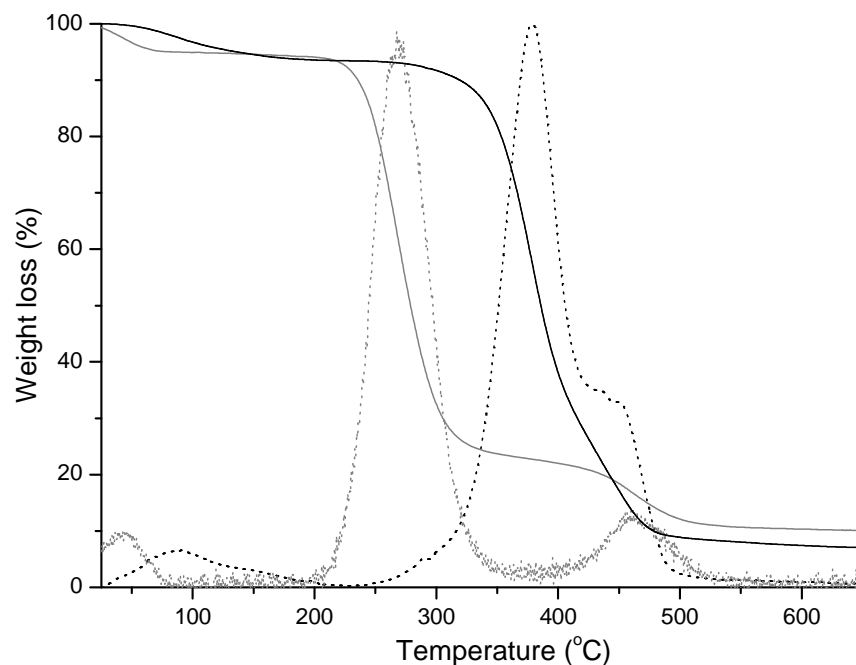


Fig. 5.2 TGA (solid line) and DTGA (dotted line) thermograms of uncrosslinked (grey) and crosslinked (black) PVA microfibrils.

Table 5.4 tabulates the thermal analysis data of uncrosslinked and crosslinked PVA. Crosslinking resulted in a massive shift in the T_{onset} of the PVA fibers from 275 °C to over 340 °C. There was also a huge shift in the DTGA maximum temperature (temperature at which there was maximum weight loss) from 306 to about 388 °C. These results show that crosslinking enhances the thermal stability of the fibers. However, no relationship was observed between the degree of crosslinking and the thermal stability of the fibers.

Table 5.4 Thermal analysis data on crosslinked PVA microfibrils

Sample	Degree of Crosslinking	^a T_{onset} (°C)	^b DTGA max (°C)
Uncrosslinked PVA	0	275	306
3a	0.218	349	385
3b	0.371	341	380
3c	0.637	350	384
3d	0.461	361	388
3e	0.313	341	382

^a Onset temperature of thermal degradation, ^b peak max for differential mass loss temperature

Crystalline melting temperature and crystallinity. Polymer degradation did not overlap with crystalline melting due to the increase in the thermal stability of the microfibrils. As a result of this the percentage crystallinity of each of the crosslinked samples was determined using DSC.

Table 5.5 Crystalline melting temperature and crystallinity of crosslinked PVA microfibrils determined by DSC

Sample	T_m^a	Degree of crosslinking	Crystallinity (%) ^b
Uncrosslinked PVA	249	0	-
3a	233	0.218	60.48
3b	234	0.371	59.11
3c	233	0.637	58.67
3d	240	0.461	56.60
3e	229	0.313	63.25

^a Crystalline melting temperature observed from DSC data, ^b Crystallinity determined from the enthalpy of fusion for PVA crystals

The glass transition temperature (T_g) of all the samples could not be observed at the heating rate used (10 °C/min). Table 5.5 tabulates data for the crystalline melting temperature (T_m) as well as the crystallinity of uncrosslinked and crosslinked PVA fibers. The crystallinity of the unmodified PVA fibers could not be determined owing to the thermal decomposition of the fibers, which commenced close to the crystalline melting temperature.

The T_m of the PVA fibers decreased as a result of the crosslinking. This occurred because during acetalization with glyoxal, hydrogen bond interactions between hydroxyl groups are disrupted and stronger covalent bonds are formed. The formation of these covalent bonds (acetal rings) enhances the thermal stability of the fibers but in the process disrupts the crystallinity.⁸ Hence there was a decrease in crystallinity with an increase in the degree of crosslinking as evident in samples 3a–c.

5.3 Cationic and anionic modification

5.3.1 Materials

Acetalized PVA microfibrils (sample 3c); monochloroacetic acid (MCAA, J.T. Baker Chemical Co.); acrylic acid (AA, Acros); 2 methacryloyloxy ethyl trimethyl ammonium

chloride (DMC, Sigma–Aldrich); sodium hydroxide (NaOH, Merck); potassium persulfate (KPS, Sigma-Aldrich); sodium thiosulfate ($\text{Na}_2\text{S}_2\text{O}_3$, Merck); glacial acetic acid (Merck), methanol (MeOH, Merck), isopropanol (IPA, Sigma-Aldrich), pH indicator paper (0–14). Acrylic acid was purified by distillation under reduced pressure at 30 °C. The other reagents were used as received.

5.3.2 Anionic modification

Prior to modification the acetalized (crosslinked) PVA microfibrils were treated by drying under vacuum at 60 °C to a constant mass. The fibers were weighed immediately before use.

5.3.2.1 Carboxymethylation of PVA microfibrils

The following typical procedure was used for carboxymethylation of PVA microfibrils (e.g. for the preparation of CMPVA 2; Table 5.6). MCAA (2.148 g, 0.023 moles) was dissolved in IPA and neutralized with aqueous NaOH (45% (w/v)). The mixture was stirred vigorously and then PVA microfibrils (1.070 g in 15 mL water, preswollen in water and cooled) and NaOH (0.909 g, 0.023 moles) were added. The temperature of the mixture was held at 60 °C for 3 h. At the end of the reaction the mixture was neutralized with glacial acetic acid (or 0.1 N HCl) and washed several times with MeOH and water until no more chloride ions could be detected. The MCAA and NaOH concentrations were varied, as shown in Table 5.6.

Table 5.6 Reagents used for the synthesis of CMPVA

Sample	PVA (g)	MCAA (g)	NaOH (g)
CMPVA 1	1.072	1.071	0.456
CMPVA 2	1.070	2.148	0.909
CMPVA 3	1.071	4.289	1.822

5.3.2.2 Grafting PAA from PVA microfibrils

The acetalized PVA microfibrils (0.520 g in 20 mL) were swollen for 1 h in water at 80 °C in a four neck round bottom flask equipped with a reflux condenser, mechanical stirrer and a nitrogen inlet. The temperature was then reduced to room temperature (with continuous stirring) and the acrylic acid (0.272 g, 0.0038 moles) added. The mixture was thoroughly degassed by bubbling nitrogen and the initiator components, KPS/ $\text{Na}_2\text{S}_2\text{O}_3$ ($1.1 \times 10^{-5}/5.0 \times 10^{-5}$ (mol/mol)) added. The temperature was raised to 70 °C and the reaction allowed to run for 24 h. Afterwards, the mixture was poured into an excess of methanol, filtered and washed with methanol and water to remove unreacted monomer. The product was further cleaned by

Soxhlet extraction using methanol and the homopolymer was obtained from the extracts. The quantity of monomers used was varied, as shown in Table 5.7.

Table 5.7 Reagents used for grafting PAA from PVA microfibrils

Sample	PVA (g)	Acrylic acid (g)	Moles Na ₂ S ₂ O ₃ per mol KPS
PVA-g-PAA 1	0.52	0.272	4.540
PVA-g-PAA 2	0.52	0.581	4.541

5.3.3 Cationic modification

5.3.3.1 Grafting PDMC from PVA microfibrils

The graft copolymerization of poly(methacryloyloxy ethyl trimethyl ammonium chloride) (PDMC) from PVA was carried out in a similar manner to that for PAA. PVA microfibrils (~1 g in 40 mL) were swollen for 1 h in water at 80 °C in a four neck round bottom flask equipped with a reflux condenser, mechanical stirrer and a nitrogen inlet. The temperature was reduced to room temperature (with continuous stirring) and DMC (2.363 g, 0.012 moles) added. The mixture was thoroughly degassed by bubbling nitrogen and the initiator components, KPS/Na₂S₂O₃ ($1.1 \times 10^{-5}/5.0 \times 10^{-5}$ (mol/mol)) added. The polymerization was then carried out at 70 °C for 24 h. Afterwards, the mixture was poured into an excess of methanol, filtered and washed with methanol. The homopolymer was then separated from the graft copolymer by Soxhlet extraction using methanol as the solvent. The extracts were treated in a similar way as described in Section 5.3.2. Table 5.8 tabulates the details on how the monomer concentration was varied.

Table 5.8 Reagents used for grafting PDMC from PVA microfibrils

Sample	PVA (g)	DMC (g)	Moles Na ₂ S ₂ O ₃ per mol KPS
PVA-g-PDMC 1	1.020	1.448	4.540
PVA-g-PDMC 2	1.021	2.363	4.540

5.3.4 Analyses

5.3.4.1 Grafting parameters

The grafting efficiency (GE %) and grafting yield (G %) are the parameters used to quantify grafting gravimetrically. GE % and G % of PAA and PDMC from PVA were calculated as follows:

$$\% \text{ GE} = \frac{(W_g - W_o)}{m} \times 100 \quad (5.8)$$

$$\% \text{ G} = \frac{(W_g - W_o)}{W_o} \times 100 \quad (5.9)$$

where W_g , W_o and m denote the masses of grafted PVA, ungrafted PVA and monomer respectively.

5.3.4.2 PAS-FTIR spectroscopy

The FTIR scans of modified PVA microfibrils were conducted using a Perkin Elmer Paragon 1000 PC FTIR Spectrometer equipped with a Photoacoustic MTEC 300 cell. The samples to be analyzed were placed into the sample holder, which was then placed inside a sealed chamber. The chamber was flushed with helium in order to promote the acoustic waves. The instrument resolution was 8 cm^{-1} and the number of scans 128, with a mirror speed of 0.15 cm/s .

^1H NMR, ^{13}C NMR, TGA and DSC analyses were carried out as described in Section 4.3.3, and SEM as described in Section 4.3.2.

5.4 Results and discussion

5.4.1 Carboxymethylation of PVA microfibrils

5.4.1.1 Evidence of carboxymethylation

Evidence of carboxymethylation was provided by PAS-FTIR spectroscopy. The spectrum of CMPVA (Fig. 5.3) not only shows the characteristic absorption bands for PVA, i.e. CH_2 bending at 1416 cm^{-1} , C–O stretching and O–H bending at 1079 cm^{-1} , but also additional absorption bands at 1714 and 1620 cm^{-1} , which are characteristic of the carboxymethyl group.

At 1620 cm^{-1} the absorption band is due to the presence of the carboxylate ion (COO^-) while that at 1714 cm^{-1} can be attributed to the stretching vibration of the carbonyl (C=O) bond.⁹ The fully assigned infrared spectrum of unmodified PVA microfibrils is given in Appendix 4.

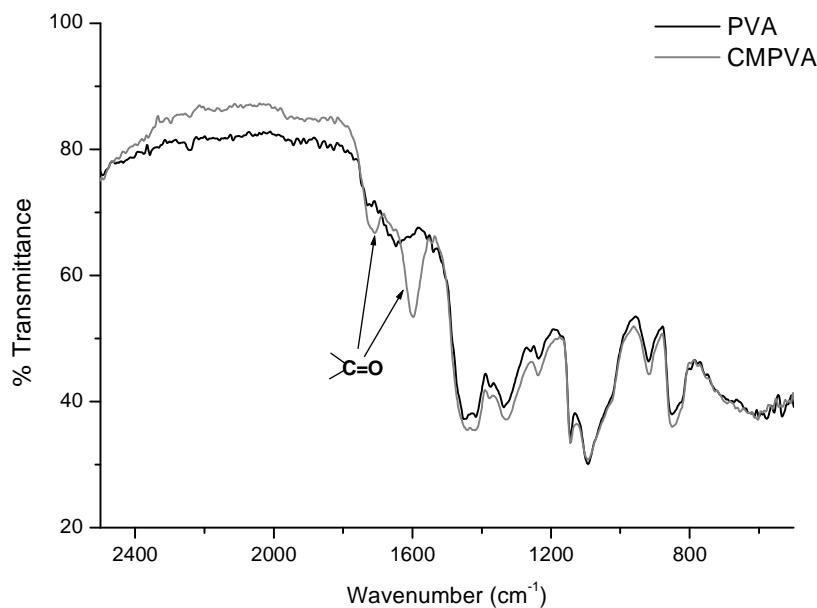


Fig. 5.3 PAS-FTIR spectra of PVA and carboxymethylated PVA (CMPVA).

Further evidence of carboxymethylation was provided by ^1H NMR (see Appendix 5). This could however not be used to confirm carboxymethylation as there was no relevant data in literature that could be used to verify this.

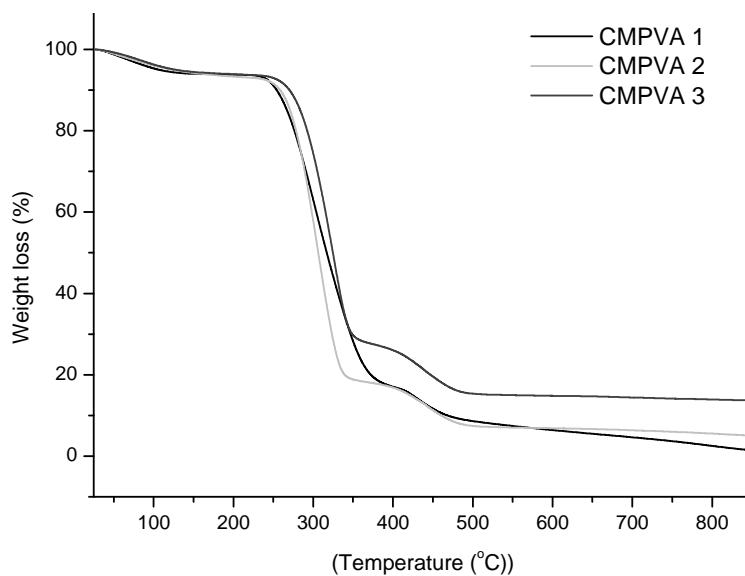
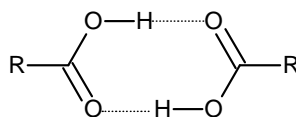
5.4.1.2 Thermal analysis

TGA analysis. The thermal decomposition of CMPVA occurs via two steps, as shown in Fig. 5.4 (the mass loss occurring at about $100\text{ }^\circ\text{C}$ was attributed to moisture loss). The three thermograms of the CMPVA samples show that the same mechanism was involved in the thermal degradation of all the samples. Table 5.9 shows that there was a decrease in thermal stability as a result of the carboxymethylation. The decrease in T_{onset} was a result of the presence of the carbonyl groups, which are known to enhance thermal degradation in polymers. Also, carboxymethylation interferes significantly with the crystallinity of PVA, thus reducing the thermal stability of the crystals.¹⁰⁻¹²

Table 5.9 Thermogravimetric analysis of CMPVA

Sample	T _{onset} (°C)	DTGA (°C)
Unmodified (sample 3c)	350	384
CMPVA 1	259	299
CMPVA 2	269	305
CMPVA 3	277	328

It was however expected that an increase in the carbonyl group content would result in a decrease in thermal stability but this was not the case. As the degree of modification increased, the T_{onset} also increased. The most probable reason for this was that with an increase in the carboxylic acid group content, the hydrogen bond interactions between the carboxylic acid groups (illustrated in Scheme 5.3) also increased, resulting in a slight increase in the thermal stability of the PVA microfibrils.¹³

**Fig. 5.4** Thermogravimetric analysis of CMPVA.**Scheme 5.3** Hydrogen bonding between carboxylic acid groups of CMPVA

DSC analysis. The typical DSC thermogram for CMPVA is given in Appendix 6. Table 5.10 tabulates the data on the crystalline melting temperature (T_m) as well as the crystallinity of CMPVA samples 1–3. There was a decrease in T_m with an increase in the degree of carboxymethylation. This shows that carboxymethylation has an effect on the crystalline structure of the PVA microfibrils. Despite there being hydrogen bond interactions between carboxylic acid groups, the large size of the carboxylic acid group (compared to the hydroxyl group) disrupts the crystallization of PVA,¹⁴ thus leading to a decrease in T_m and crystallinity.

Table 5.10 Crystalline melting temperature and crystallinity of CMPVA

Sample	T_m (°C)	^a Crystallinity (%)
Unmodified PVA	233	58.7
CMPVA 1	238	45.5
CMPVA 2	232	36.7
CMPVA 3	227	34.5

^a Determined using equation 5.7

5.4.1.3 SEM analysis

The morphologies of the carboxymethylated PVA microfibrils were analyzed using SEM. The typical SEM micrograph for CMPVA microfibrils obtained in this work is given in Appendix 7. The SEM image shows that the heterogeneous carboxymethylation techniques employed resulted in a loss in the “well-aligned” morphology of the PVA microfibrils. However, the overall fibrous morphology of the fibers was preserved.

5.4.2 Grafting PAA from PVA microfibrils

5.4.2.1 Evidence of grafting

Following grafting, the purified and dried polymer grafts were weighed. Although the observed increases in mass indicated that grafting had taken place PAS-FTIR was used to obtain reliable evidence of grafting. Fig. 5.5 shows the spectra for PVA and PVA-g-PAA. Both spectra show the same absorption bands typical of PVA (see Appendix 4). In addition to these, there is an intense carbonyl stretching vibration at 1714 cm^{-1} (in the spectrum of grafted PVA), which can be attributed to the PAA carboxylic acid functionality.

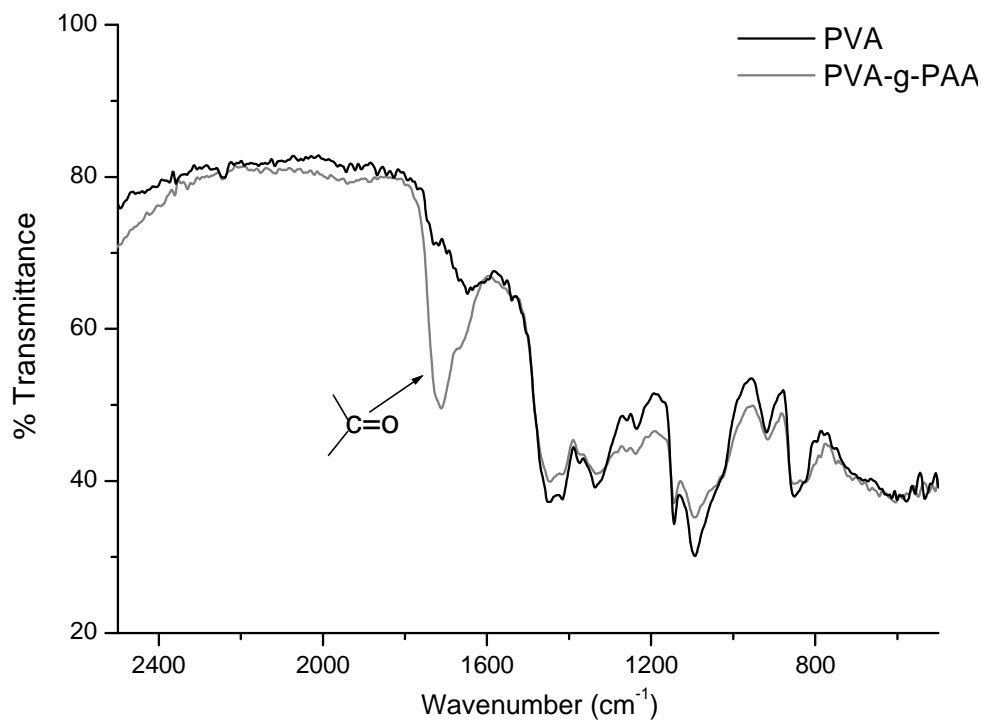


Fig. 5.5 PAS-FTIR spectra of PVA and PVA-g-AA.

Further evidence of grafting was provided by ^1H and ^{13}C NMR spectroscopy. The spectra of unmodified PVA were assigned fully in Section 4.4.2. Fig. 5.6 shows the typical ^1H NMR spectrum for PVA-g-PAA obtained in this study. There was significant overlapping of the hydroxyl triad signals (at 4.2 ppm) and partial overlap of these signals with the methine proton signal (at 3.8 ppm). The signal at 3.25 ppm was attributed to the glyoxal protons (labeled h). The presence of the glyoxal proton signals showed that the acetal linkages were stable and unaffected by the method of modification employed.³ The new signal at 2.2 ppm (labeled j) was attributed to the methine proton of the PAA.¹⁵ The methylene proton signal (labeled i at 1.8 ppm) was partially obscured by the signal of the methylene protons of the PVA polymer backbone.

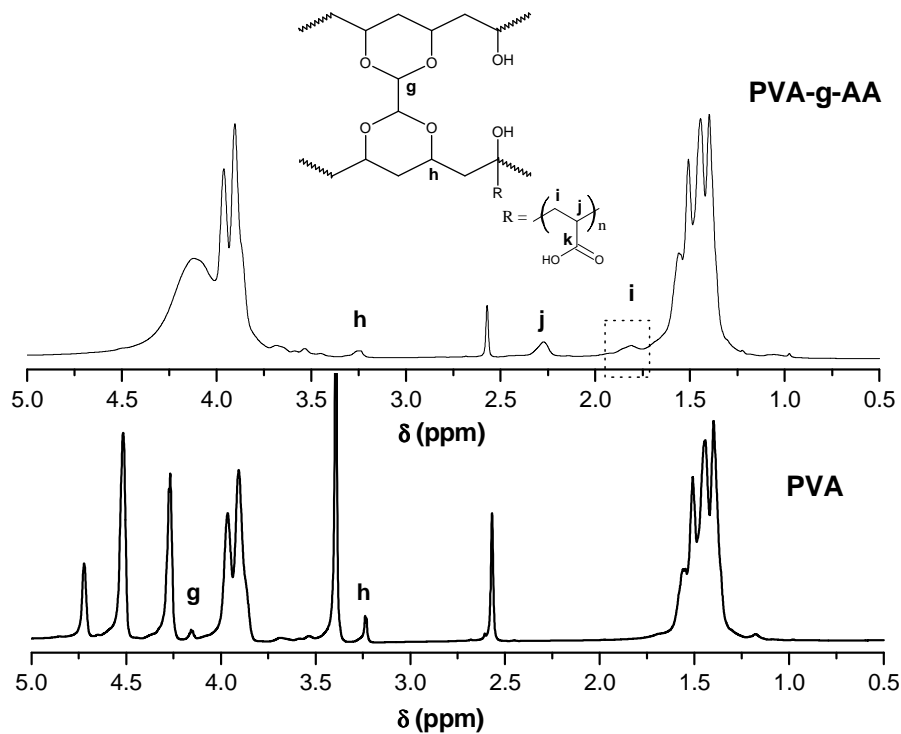


Fig. 5.6 ^1H NMR spectra of PVA and PVA-g-PAA.

The typical ^{13}C NMR spectrum of PVA-g-PAA is illustrated in Fig. 5.7. The presence of the carbonyl carbon atom at 176 ppm confirms the presence of polymer grafts.

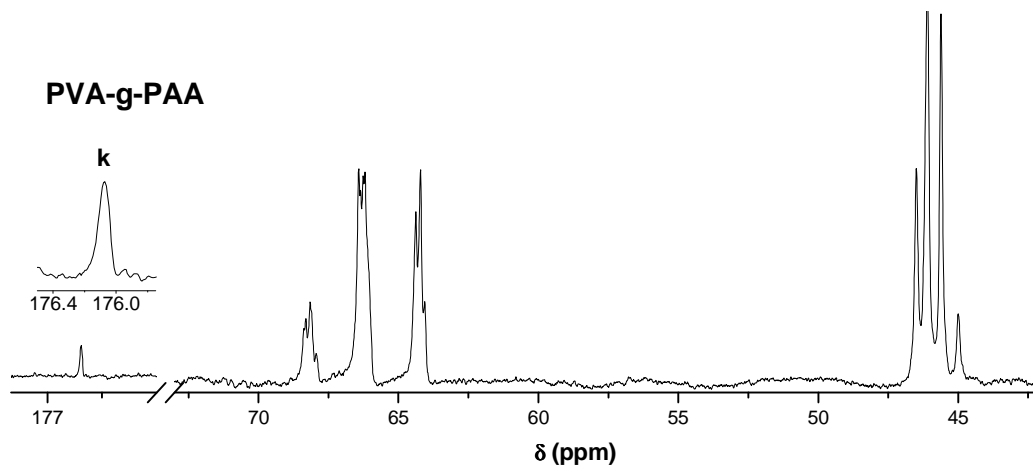


Fig. 5.7 ^{13}C NMR spectrum of PVA-g-AA.

The methylene and methine carbon atom signals of the polymer grafts could not be observed probably due to their overlap with the PVA signals.

5.4.2.2 Grafting parameters

The G % and GE % increased with an increase in the monomer feed, as indicated in the Table 5.11. The G % was low, as expected owing to the conditions under which the modifications were carried out (heterogeneous conditions). Under heterogeneous conditions not all hydroxyl groups of the PVA microfibrils were accessible for modification.¹⁶ Accordingly this results in high homopolymer content, as homopolymer formation would be favored over grafting.

Table 5.11 Parameters used for grafting PAA from PVA

Sample	GE (%)	G (%)	Homopolymer (%) ^{a†}
PVA-g-PAA 1	3.38	5.13	72.1
PVA-g-PAA 2	7.19	11.26	77.0

^a Homopolymer content was obtained as follows: $[m_{\text{homopolymer}} (\text{after extraction}) \div \text{mass}_{\text{monomer}}] \times 100$, [†] no PVA was found in PAA extracted (see Appendix 7 for ¹H NMR spectrum of the extract (see Section 5.3.2.2)).

The observed increase in GE % with an increase in monomer concentration is associated with an increase in the concentration of monomer molecules in the neighborhood of the macroradicals.¹⁷

5.4.2.3 Thermal analysis

TGA analysis. TGA analysis showed that modification of the microfibrils was successful. The DTGA thermograms for ungrafted and PAA grafted PVA microfibrils are compared in Fig 5.8. Both curves show two main decomposition steps. The minor peak occurring at < 150 °C was attributed to moisture loss.^{10,11,18} It is evident from the two thermograms of the modified and unmodified PVA that grafting PAA from the surface of PVA microfibrils had very little effect on the mechanism of the thermal decomposition of the PVA. However there was an overall decrease in the T_{onset} and DTGA maximum temperature, as shown in Table 5.12. This decrease in thermal stability was attributed to the acrylic acid polymer grafts.¹⁹ The thermal stability of the grafted PVA also decreases with an increase in G %, which was expected as the number of carbonyl groups had increased.

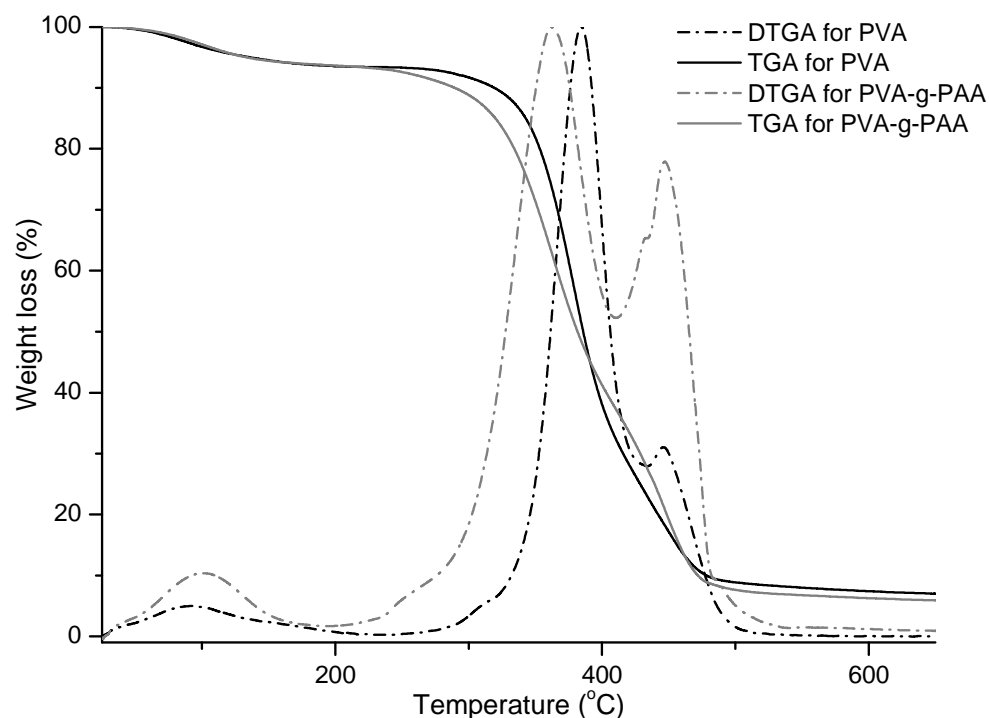


Fig. 5.8 TGA and DTGA thermograms of PVA (black) and PVA-g-AA (grey).

Table 5.12 Thermogravimetric analysis of PVA-g-PAA

Sample	T_{onset} (°C)	DTGA peak maximum (°C)
Unmodified PVA	350	384
PVA-g-PAA 1	307	362
PVA-g-PAA 2	294	360

DSC analysis. Grafting PAA from PVA resulted in decreases in the crystalline melting temperature and crystallinity, as shown in Table 5.13. The decline in crystallinity was attributed to the grafted polymer chains which reduce hydrogen bond interactions between polymer chains thus disrupting the crystalline structure of the fibers. Consequently this resulted in a decrease in the melting temperature of the PVA crystals.

Table 5.13 Crystalline melting temperature and crystallinity of PVA-g-PAA

Sample	T_m (°C)	Crystallinity (%)
Unmodified PVA	233	58.7
PVA-g-PAA 1	237	40.0
PVA-g-PAA 2	234	36.3

5.4.2.4 SEM analysis

The typical SEM micrograph of PVA-g-PAA microfibrils is given in Appendix 9. The SEM image shows that the surface of the fibers was indeed modified. However the overall fibrous morphology was preserved.

5.4.3 Grafting PDMC from PVA microfibrils

5.4.3.1 Evidence of grafting

Evidence of grafting PDMC from the surface of PVA microfibrils was provided by gravimetric analysis. Homopolymer was removed as given in Section 5.3.2.2. The purified grafted PVA microfibrils were dried and weighed to a constant mass. Further evidence of grafting was provided by PAS-FTIR. Two new absorption bands were observed at 1705 and 1250 cm^{-1} . These were attributed to the ester carbonyl stretching vibrations and amine (C–N) stretching respectively^{20,21}.

Grafting was confirmed by ^1H and ^{13}C NMR. Fig. 5.10 shows a typical ^1H NMR spectrum of PVA-g-PDMC. Two new resonance signals compared to the spectrum for unmodified PVA were observed at 1.98 and 0.98 ppm. These were attributed to the methylene protons (labeled g) and the methyl protons (labeled n) of the polymer grafts.²¹ The signals at 3.2 and 4.1 ppm were assigned to the glyoxal protons (labeled h and g respectively). The presence of these two signals indicated that the surface modification technique that was used had very little effect on the acetal structures formed during crosslinking.

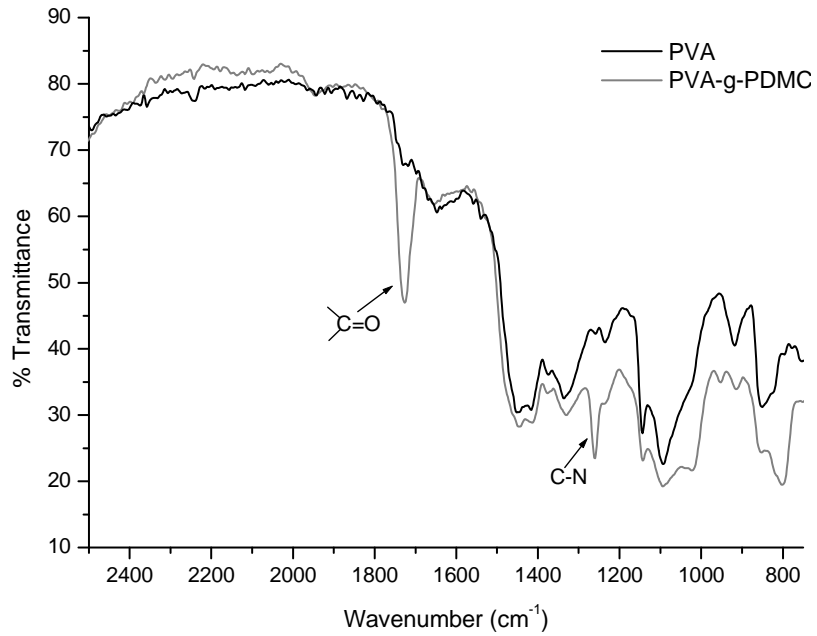


Fig. 5.9 PAS-FTIR spectra of PVA and PVA-g-PDMC.

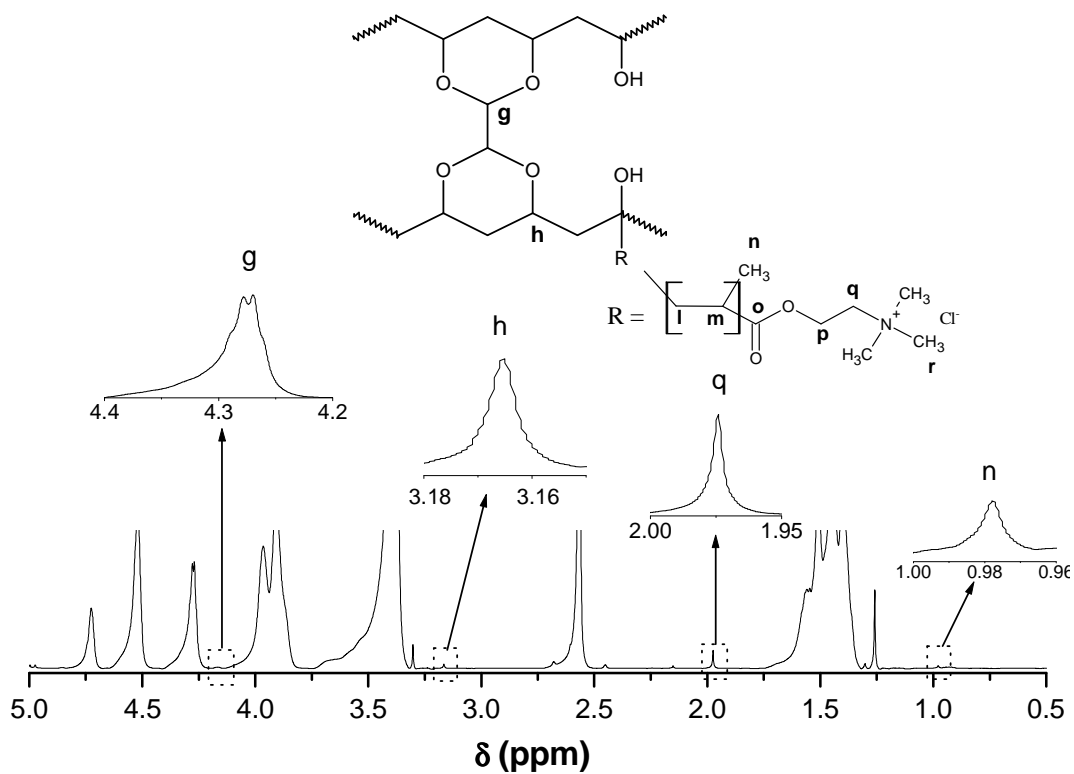


Fig. 5.10 ¹H NMR spectrum of PVA-g-PDMC.

In the ^{13}C NMR spectrum of PVA-g-PDMC (Fig. 5.11) new signals were observed at 52.8 and 26.4 ppm and these were assigned as follows: The signals at 52.8 ppm and 27.6 ppm were attributed to the trimethyl carbon r and the methylene carbon q atoms respectively. The carbon atoms labeled l, m could not be detected probably due to signal overlap of the polymeric grafts with the signals of the PVA backbone.

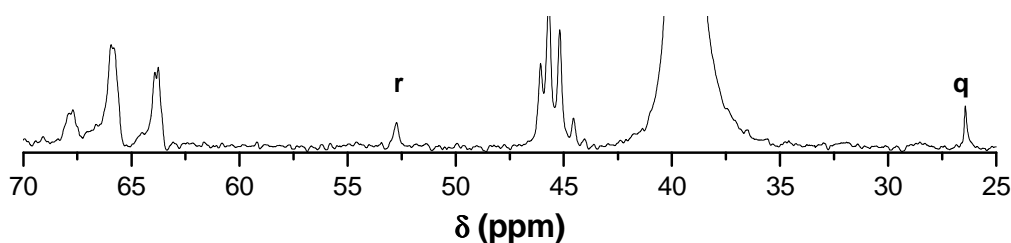


Fig. 5.11 ^{13}C NMR spectrum of PVA-g-PDMC.

5.4.3.2 Grafting parameters

The (G %) increased with an increase in the monomer feed. This was expected because of the increase in monomer molecules in the vicinity of the macroradical. This increase in G % was also accompanied by an increase in homopolymer content.

Table 5.14 Grafting parameters used for PVA-g-PDMC

Sample	GE (%)	G (%)	Homopolymer ^{a†} (%)
PVA-g-PDMC 1	6.01	2.80	65
PVA-g-PDMC 2	9.50	6.21	68

^a Homopolymer content was obtained as follows: $[m_{\text{homopolymer}}(\text{after extraction}) / \text{mass}_{\text{monomer}}] \times 100$, [†] no PVA was found in PDMC extracted (see Appendix 8 for the ^1H NMR spectrum of the extract (see Section 5.3.2.2)).

5.4.3.3 Thermal analysis

TGA analysis. Fig. 5.12 shows a typical TGA thermogram for PVA-g-PDMC. The decomposition profile shows three main peaks at 330, 371 and 447 °C, and two minor peaks at 240 and 284 °C indicating the different mechanisms involved in the thermal decomposition of PVA-g-PDMC. This deviation of the mechanism of thermal decomposition behavior of grafted PVA microfibrils from the unmodified PVA microfibrils was attributed to the PDMC polymer grafts. Further investigation into these mechanisms was not carried out.

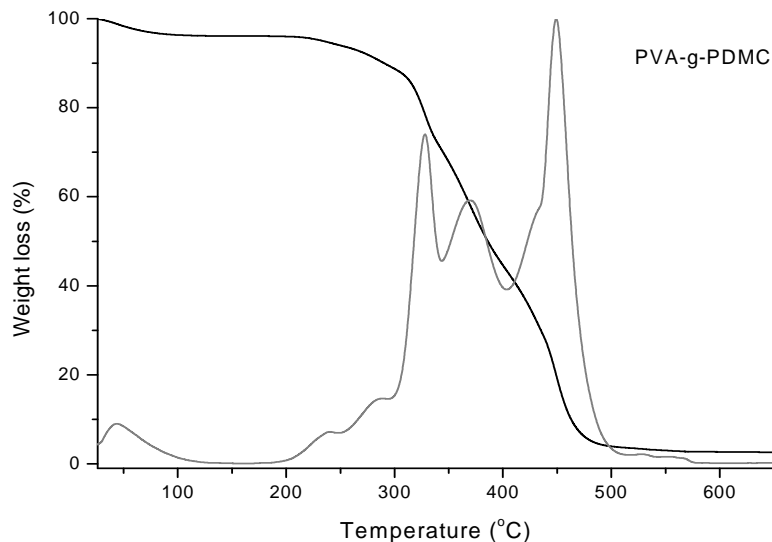


Fig. 5.12 TGA thermogram (black) and DTGA curve (grey) of PVA-g-PDMC.

Table 5.15 tabulates the thermogravimetric analysis data for unmodified PVA and PVA-g-PDMC. Grafting generally resulted in a decline in the T_{onset} for the fibers. However the differences in T_{onset} between the PVA-g-PDMC 1 and 2 were insignificant, the differences were within experimental error of the extrapolation method employed to obtain it.

Table 5.15 Thermogravimetric analysis of PVA-g-DMC

Sample	T_{onset} (°C)	DTGA peak maximum (°C)
Unmodified PVA	350	384
PVA-g-DMC 1	291	329
PVA-g-DMC 2	290	334

DSC analysis. Table 5.16 gives the T_m and the crystallinity data for unmodified PVA and PVA-g-PDMC. Grafting PDMC from PVA microfibrils resulted in the disruption of the hydrogen bond interactions necessary for crystallite formation and as a result, the crystallinity decreased. This decrease in crystallinity meant that less energy was required to effect crystalline melting and consequently, the crystalline melting temperature also decreased.

Table 5.16 Crystalline melting temperature and crystallinity of PVA-g-DMC

Sample	T_m (°C)	Crystallinity (%)
Unmodified PVA	233	58.7
PVA-g-DMC 1	238	35.6
PVA-g-DMC 2	236	34.7

5.4.3.4 SEM analysis

The PVA-g-PDMC microfibrils were analyzed using SEM. From the SEM micrograph illustrated in Appendix 11, it was evident that the “well-aligned” morphology of the PVA fibers was slightly disrupted. However, the overall fibrous morphology of the PVA fibers was preserved.

5.5 Conclusions

The heterogeneous cationic and anionic modification of PVA microfibrils was successfully carried out using the technique developed in this work. The developed technique involved crosslinking and swelling of the PVA microfibrils prior to modification. The fibers were crosslinked with glyoxal; so as to minimize the solubility of the amorphous regions during surface modification, whilst swelling was carried out in order to expose the majority of the functional groups.

The carboxymethylation of PVA microfibrils, could not be quantified gravimetrically because instead of there being an increase in mass of the polymer samples after modification, the mass of the modified PVA decreased. This mass loss was due to the increased solubility of the carboxymethylated microfibrils in aqueous media. Nonetheless, carboxymethylation was confirmed by PAS-FTIR. Two new absorption bands were observed at 1714 and 1620 cm^{-1} , and were attributed to the carboxylic acid group. TGA and DSC analysis also confirmed the occurrence of carboxymethylation. There was a decline in the thermal stability of the carboxymethylated PVA microfibrils, which was attributed to the carboxylic acid groups introduced. The carboxylic acid group had the effect of disrupting crystallinity and there was a decrease in T_m and % crystallinity, as observed by DSC.

PAA and PDMC were successfully grafted from PVA under heterogeneous conditions but the grafting yields and grafting efficiencies were low. This was expected as despite swelling the fibers prior to modification, not all the potential grafting sites were available for grafting. This also contributed to the formation of large amounts of homopolymer. The homopolymer was separated from the polymer grafts by soxhlet extraction and quantified. The extracted homopolymers were analyzed using ^1H NMR for dissolved PVA (see Appendixes 7 and 8). No signals that were attributed to PVA were observed in all the spectra showing that the acetalized PVA samples were stable and unaffected by the modification methods employed. Grafting was confirmed by PAS-FTIR, ^1H and ^{13}C NMR spectroscopy. The thermal properties were investigated using DSC and TGA.

References

1. Shtyagina, L. M.; Vainburg, V. M.; Vinogradova, L. E. *Russ. J. Appl. Chem* **2001**, 74(8), 1408–1409.
2. Xu, G. G.; Yang, C. Q.; Deng, Y. *J. Appl. Polym. Sci.* **2004**, 93, 1673–1680.
3. Smith, M. B.; March, J., *March's Advanced Organic Chemistry*. 5 ed.; John Wiley and Sons: Canada, 2001.
4. Hebeish, A.; Beliakova, M. K.; Bayazeed, A. *J. Appl. Polym. Sci.* **1998**, 68, 1709–1715.
5. Grubb, D. T.; Kearney, F. R. *J. Appl. Polym. Sci.* **1990**, 39, 695–705.
6. Gauthier, M. A.; Luo, J.; Calvet, D.; Ni, C.; Zhu, X. X.; Garon, M.; Buschmann, M. *D. Polymer* **2004**, 45, 8201–8210.
7. Vázquez-Torres, H.; Cauich-Rodríguez, J. V.; Cruz-Ramos, C. A. *J. Appl. Polym. Sci.* **1993**, 50, 777–792.
8. Yeom, C.; Lee, K. *J. Membrane. Sci.* **1996**, 109, 257–265.
9. Gohil, J. M.; Bhattacharya, A.; Ray, P. *J. Polym. Res* **2004**, 13, 161–169.
10. Gilman, J. W.; VanderHart, D. L.; Kashiwagi, T., Thermal Decomposition Chemistry of Poly(vinyl alcohol). In *Fire and Polymers II*, American Chemical Society: Washington DC, 1994.
11. Holland, B. J.; Hay, J. N. *Polymer* **2001**, 42, 6775–6783.
12. Shie, J.; Chen, Y.; Chang, C.; Lin, J.; Lee, D.; Wu, C. *Energy and Fuels* **2002**, 16, 109–118.
13. Mukherjee, G. S.; Shukla, N.; Singh, R. K.; Mathur, G. N. *J. Sci. Ind. Res.* **2004**, 63, 596–602.
14. Finch, C. A., *Poly(vinyl alcohol : Properties and Applications*. John Wiley and Sons: London, 1973.
15. Liu, Y.; Du, Z.; Li, Y.; Zhang, C.; Li, H. *Chinese J. Chem.* **2006**, 24, 563–568.
16. Freire, C. S. R.; Silvestre, A. J. D.; Neto, C. P.; Belgacem, M. N.; Gandini, A. *J. Appl. Polym. Sci.* **2006**, 100, 1093–1102.
17. Chowdhury, P.; Pal, C. M. *Eur. Polym. J.* **1999**, 35, 2207–2213.
18. Thomas, P. S.; Guerbois, J. P.; Russell, G. F.; Briscoe, B. J. *J. Therm. Anal.* **2001**, 64, 501–508.
19. Shukla, S.; Bajpai, A. K. *J. Appl. Polym. Sci.* **2006**, 102, 84–95.

20. Pavia, D. L.; Lampman, G. M.; Kriz, G. S., *Introduction to Spectroscopy*. Brooks/Cole: Washington, 2001.
21. Zheng, S.; Chen, Z.; Lu, D.; Lin, X. *J. Appl. Polym. Sci.* **2005**, 97, 2186–2191.

Chapter 6

Summary, conclusions and suggestions for future work

6.1 Summary

A PVA precursor (PVPi) was prepared by low temperature thermoinitiated and photoinitiated free radical polymerization of vinyl pivalate as described in Chapter 3. Photoinitiation was superior to low temperature thermoinitiation in providing high yields of high molecular weight PVPi over relatively short periods of time. VPi/VAc copolymers of varying copolymer contents were prepared by varying the VPi and VAc monomer feed ratios. The copolymer compositions were determined by ^1H NMR. The results obtained showed that the conversion of VPi was greater than that of VAc as the VPi content was higher in the copolymer than in the monomer feed. This was confirmed by the reactivity ratios of VPi and VAc, which were reported to be 3.1 and 1.6 respectively.

Chapter 4 was an extension of Chapter 3. The PVPi and VPi/VAc copolymers were saponified using a chain-orienting saponifying agent. Highly syndiotactic PVA microfibrils with an s-diad content of up to 61.8% were obtained from the PVPi homopolymer. The VPi/VAc copolymers were saponified in a similar way, and PVA with varying syndiotacticities were obtained. The stereoregularities of all PVA samples were quantified using ^1H and ^{13}C NMR. The results obtained showed a decrease in syndiotacticity with an increase in the VAc content in the precursor polymer. The decrease in syndiotacticity was accompanied by a decrease in the thermal stability and crystalline melting temperature, however no direct link between the s-diad content and T_{onset} was observed. T_m on the other hand decreased with a decrease in syndiotacticity owing to a decrease in crystallinity, ascribed to the grafted polymer chains.

The heterogeneous modification of PVA microfibrils was carried out with the aim of preserving the PVA fiber structure and properties as described in Chapter 5. Prior to surface modification, the PVA microfibrils were crosslinked with glyoxal. Crosslinking was carried out in order to minimize the solubility of the PVA amorphous regions in water during modification. Crosslinking by acetalization was confirmed by ^1H NMR. The crosslinked PVA fibers were analyzed using TGA and DSC. The TGA results showed an enhancement in T_{onset} (thermal stability) whilst DSC data showed a decrease in T_m .

The crosslinked PVA microfibrils were modified by carboxymethylation and grafting. In the carboxymethylation, Williamson's ether synthesis was employed and three levels of modification were obtained by varying the monomer concentration. In grafting, poly(acrylic acid) (PAA) and poly(methacryloyloxyethyl trimethyl ammonium chloride) (PDMC) were grafted from the PVA microfibrils. Two levels of grafting were obtained in both cases by varying the concentration of AA and DMC monomers. TGA data showed a decrease in thermal stability whilst DSC data showed a decrease in T_m and crystallinity, which was attributed to the grafted polymer chains.

6.2 Conclusions

Highly syndiotactic PVA fibers with an s-diad content of up to 61.8% were successfully prepared via *in situ* fibrillation during the saponification of high molecular weight VPi. The fibers were analyzed using TGA and DSC. The results obtained showed an increase in thermal stability and T_m compared to atactic PVA. This was attributed to the improved stereoregularity of the syndiotactic PVA.

VPi/VAc copolymers of varying comonomer contents were prepared by photoinitiated FRP in bulk. Upon saponification, PVA fibers of varying s-diad contents were obtained. A decrease in VPi content led to a decrease in syndiotacticity, confirming the dependence of syndiotacticity on the bulkiness of the side group of the poly(vinyl ester) precursor. The effect of syndiotacticity on the morphology of PVA microfibrils was also investigated. As the syndiotacticity decreased the fibrous morphology of the PVA was gradually lost, indicating that stereoregularity plays a significant role in *in situ* fibrillation. When the copolymer composition was 38.5/61.5 (VPi/VAc mol %), spherical particles were obtained. This finding is significant as the only method currently used for preparing syndiotactic PVA particles are emulsion/suspension polymerization followed by saponification.

The PVA microfibrils were modified using monochloroacetic acid by Williamson's etherification reaction. PAA and PDMC were successfully grafted from the crosslinked PVA microfibrils using the KPS/Na₂S₂O₃ redox initiation system. Grafting was confirmed by IR and NMR analyses and quantified using gravimetry. The fibers were characterized using TGA and DSC. A decrease in T_{onset} and % crystallinity following modification was attributed to the polymer grafts that disrupted the hydrogen bond interactions between adjacent polymer chains.

6.3 Recommendation for future research

Suggested future work includes optimizing the conditions for the formation of syndiotactic PVA particles via the saponification of VPi/VAc copolymers prepared by FRP in bulk. This facile synthesis of syndiotactic PVA particles opens doors for further research on the full characterization of these particles and their modification for advanced applications using anionic or cationic monomers.

The optimum conditions for the heterogeneous modification of PVA microfibrils by grafting should be investigated more fully. It would be interesting to determine the optimum pretreatment crosslinking reaction time and temperature, as well as initiator component system, that would result in high grafting yields accompanied by minimum homopolymer formation.

References

1. Lee, S. G.; Kim, J. P.; Lyoo, W. S.; Kwak, J. W.; Noh, S. K.; Park, C. S. *J. Appl. Polym. Sci.* **2005**, 95, 1539–1548.
2. Beliakova, M. K.; Aly, A. A.; Abdel-Mohdy, F. A. *Starch/Stärke* **2004**, 56, 407–412.
3. Mukherjee, G. S.; Shukla, N.; Singh, R. K.; Mathur, G. N. *Journal of Scientific & Industrial Research* **2004**, 63, 596–602.

Appendix 1

^{13}C NMR analysis of syndiotactic PVA

Fig. A1.1 is the ^{13}C NMR spectrum of PVA with an s-diad content 59.1% illustrating how the isotactic and heterotactic regions are split into heptads as well as how the syndiotactic region is split into pentads.

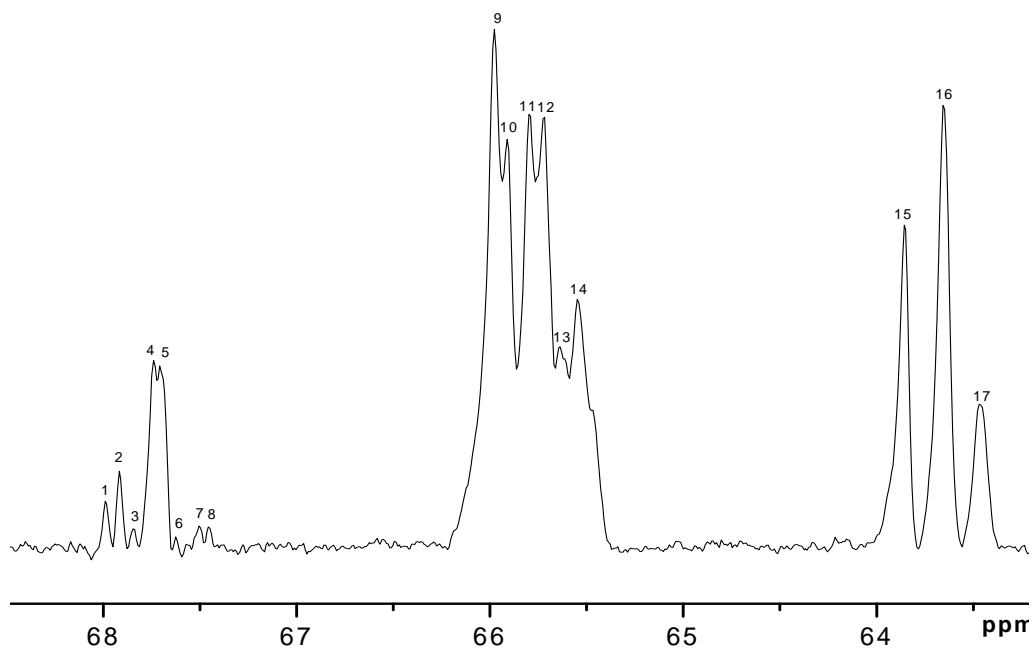


Fig. A1.1 ^{13}C NMR spectrum of methine carbon atom of PVA measured in $\text{DMSO-}d_6$.

Table A1.1 gives the quantitative heptad and pentad probabilities obtained from the area intensities of the heptad and pentad signals.

Table A1.1: Heptad assignment for methine carbon atom spectrum of PVA measured in DMSO- d_6

Peak no	Chemical shift (ppm)	Assignment	S-PVA ^a (r = 0.610)		^c S-PVA fiber (r = 0.591)
			Observed	Calculated ^b	Observed ^d
1	67.99	<i>rrmmrr</i>	0.021	0.020	0.018
2	67.92	<i>mrmmrr</i>	0.029	0.028	0.034
3	67.84	<i>mrmmrm+mmmmrr</i>	0.013	0.010	0.014
4	67.74	<i>rmmmr</i>	0.037	0.041	0.022
5	67.70	<i>rmmmr</i>	0.016	0.018	0.038
6	67.62	<i>mmmmrm</i>	0.013	0.011	0.014
7	67.50	<i>rmmmmr</i>	0.007	0.008	0.008
8	67.46	<i>mmmmmr+mmmmmm</i>	0.011	0.013	0.008
9	65.98	<i>rrmrrr+rrmrrm</i>	0.105	0.108	0.106
10	65.91	<i>mrmmrr+mrmmrm</i>	0.080	0.074	0.090
11	65.79	<i>rrmrrr+rrmrrm</i>	0.068	0.074	0.114
12	65.72	<i>mrmmrr+mrmmrm+</i> <i>rmmrrr+mmmmrr</i>	0.108	0.116	0.090
13	65.64	<i>rmmrrr+mmmmrr</i>	0.056	0.045	0.04
14	65.55	<i>mmrm</i>	0.078	0.075	0.078
15	63.86	<i>rrrr</i>	0.123	0.126	0.116
16	63.66	<i>mrrr</i>	0.170	0.173	0.154
17	63.47	<i>mrrm</i>	0.065	0.060	0.056

^a Obtained from literature for S-PVA prepared from PVPi (r = 0.61), ^b Assuming Bernoullian statistics for P_m = 0.39, ^c Obtained from S-PVA fiber prepared from PVPi (r = 0.59)

Appendix 2

XRD analysis of PVA samples of varying syndiotacticities

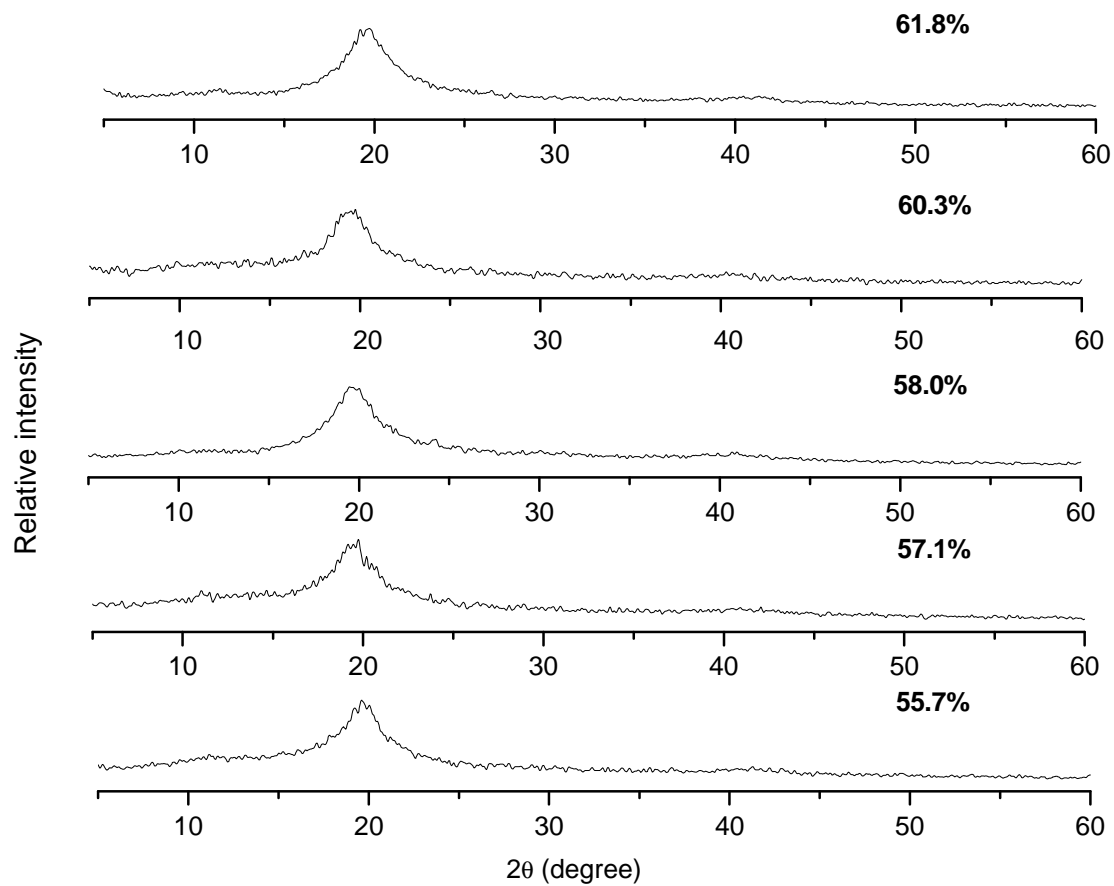


Fig. A2.1 X-ray powder diffraction profiles for PVA samples of varying s-diad contents.

Appendix 3

SEM image of PVA with an s-diad content of 60.3%

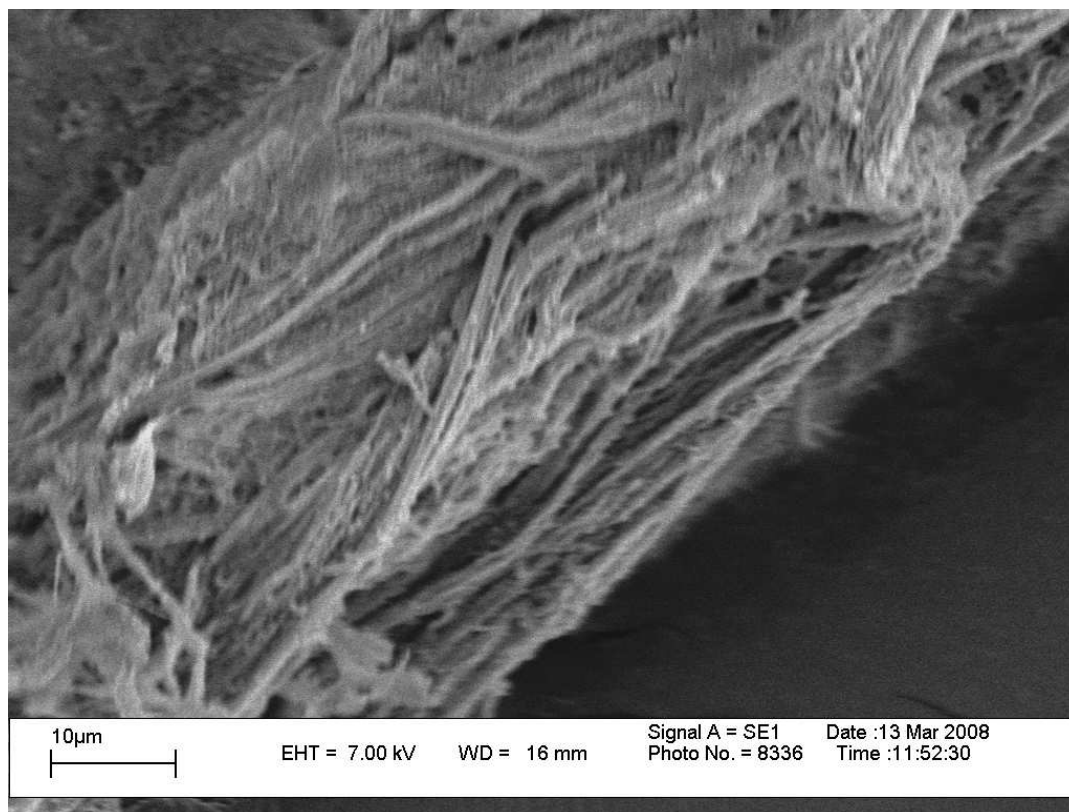


Fig. A3.1 SEM image of PVA (s-diad content of 60.3%, VPi content in precursor: 98.8 mol %).

Appendix 4

Infrared spectrum of unmodified PVA microfibrils

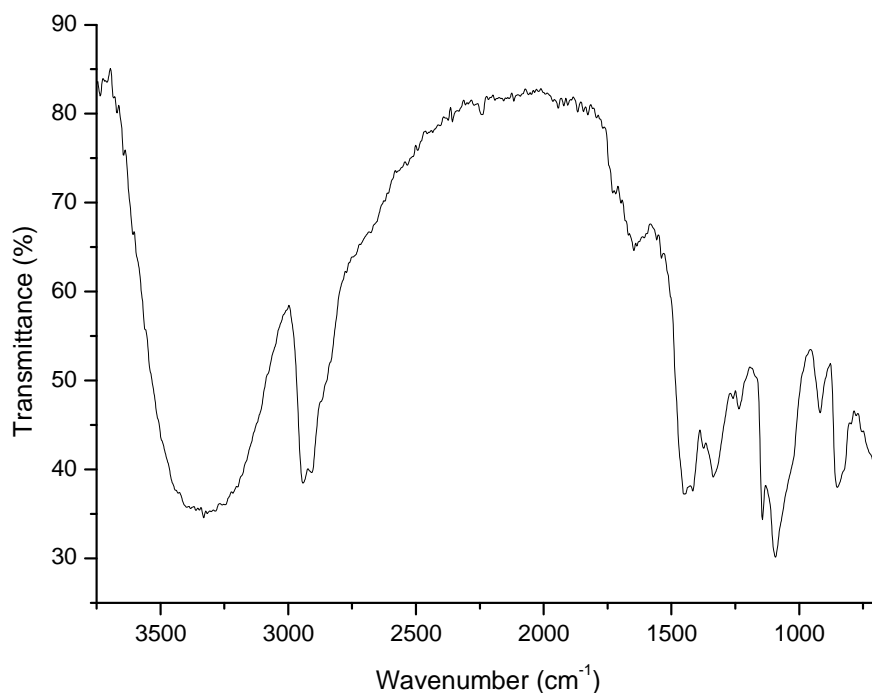


Fig. A4.1 FT-IR spectrum of unmodified poly(vinyl alcohol).

Table A4.1 Assignments of IR spectrum of unmodified PVA

Wavenumber (cm ⁻¹)	Intensity	Assignment
3327	Very strong	O-H stretching
2945	Strong	C-H stretching
2919	Strong	C-H stretching
1441	Strong	O-H and C-H bending
1416	Strong	CH ₂ bending
1370	Weak	CH ₂ wagging
1338	Medium	C-H and O-H bending
1227	Weak	C-H wagging
1137	Medium	C-C and C-O stretching
1079	Strong	C-O stretch and O-H bending
917	Medium	Syndiotactic (skeletal)
845	Medium	CH ₂

Appendix 5

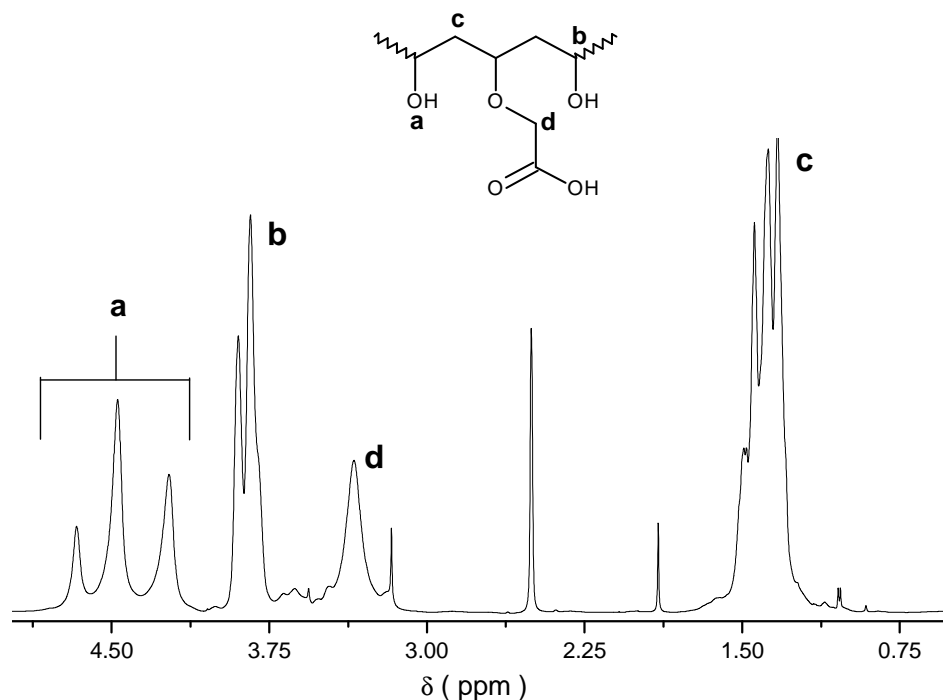
 ^1H NMR spectrum of CMPVA

Fig. A5.1 ^1H NMR spectrum of carboxymethylated PVA fibers.

Fig. A5.1 above is an example of the spectrum obtained following ^1H NMR analysis of CMPVA. The signals at 4.50 ppm (labeled a) were attributed to the hydroxyl proton triads of *mm*, *mr* and *rr* from high to low frequency, whilst the signals labeled b and c were ascribed to the PVA polymer backbone (methine and methylene protons respectively). The signal at 3.50 ppm was attributed to the carboxymethyl methylene protons. Unfortunately there was no relevant data in literature to confirm this.

The signals at 3.16, 2.48 and 1.89 ppm were attributable to the following solvent contaminants methanol, DMSO and acetic acid respectively.

Appendix 6

DSC analysis of CMPVA

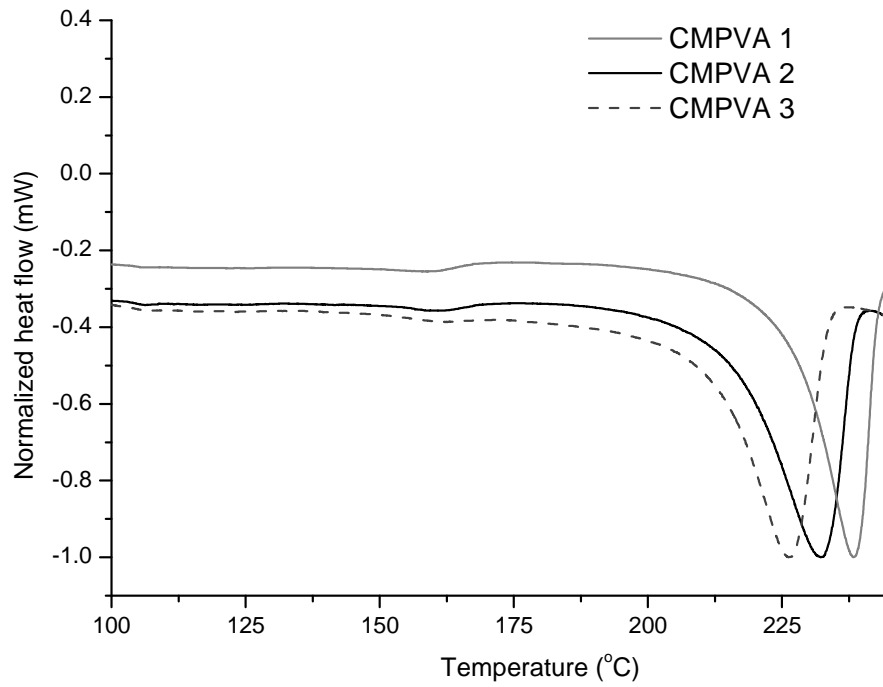


Fig. A6.1 DSC thermograms of carboxymethylated PVA microfibrils (CMPVA).

Appendix 7

SEM image of carboxymethylated PVA fibres

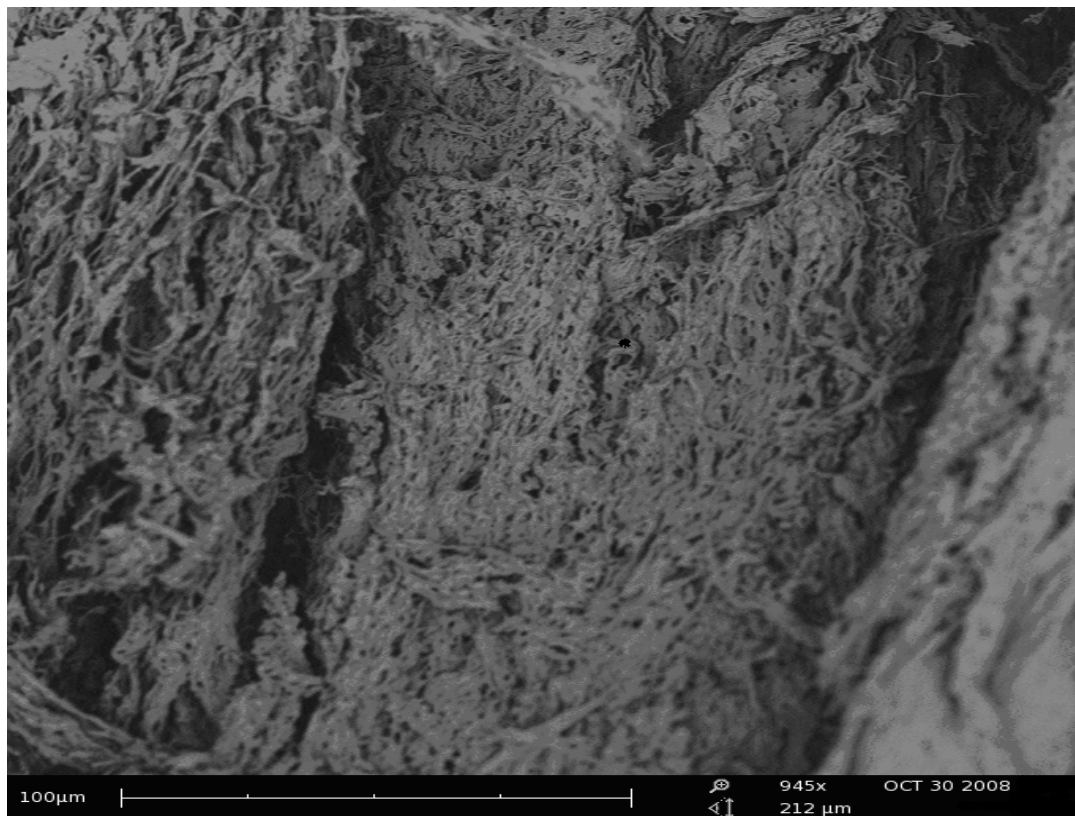


Fig. A7.1 SEM image of carboxymethylated PVA microfibrils.

Appendix 8

^1H NMR analysis of PAA homopolymer extracts

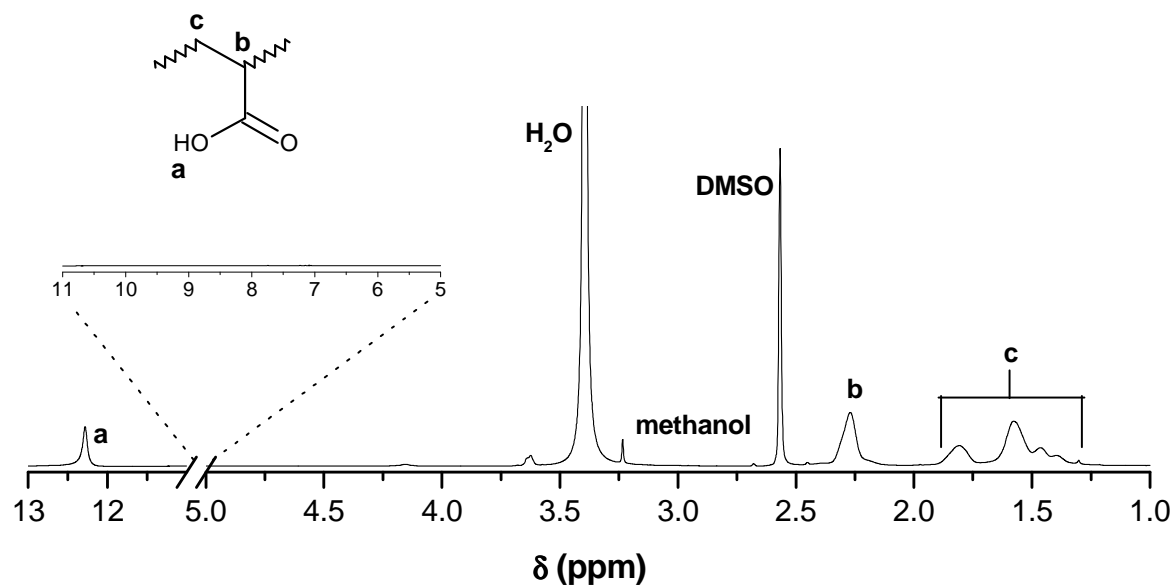


Fig. A8.1 ^1H NMR spectrum of extracted PAA homopolymer in $\text{DMSO-}d_6$.

Fig A8.1 is the ^1H NMR spectrum of the extracted PAA homopolymer. The absence of the PVA methine and hydroxyl proton signals at 3.9 and 4.5 ppm respectively,¹ confirms the absence of PVA in the homopolymer extracts.

¹ Spěvácěk, J.; Suchopárek, M. *Polymer* **1995**, 36(21), 4125–4130.

Appendix 9

SEM image of PVA-g-PAA microfibrils

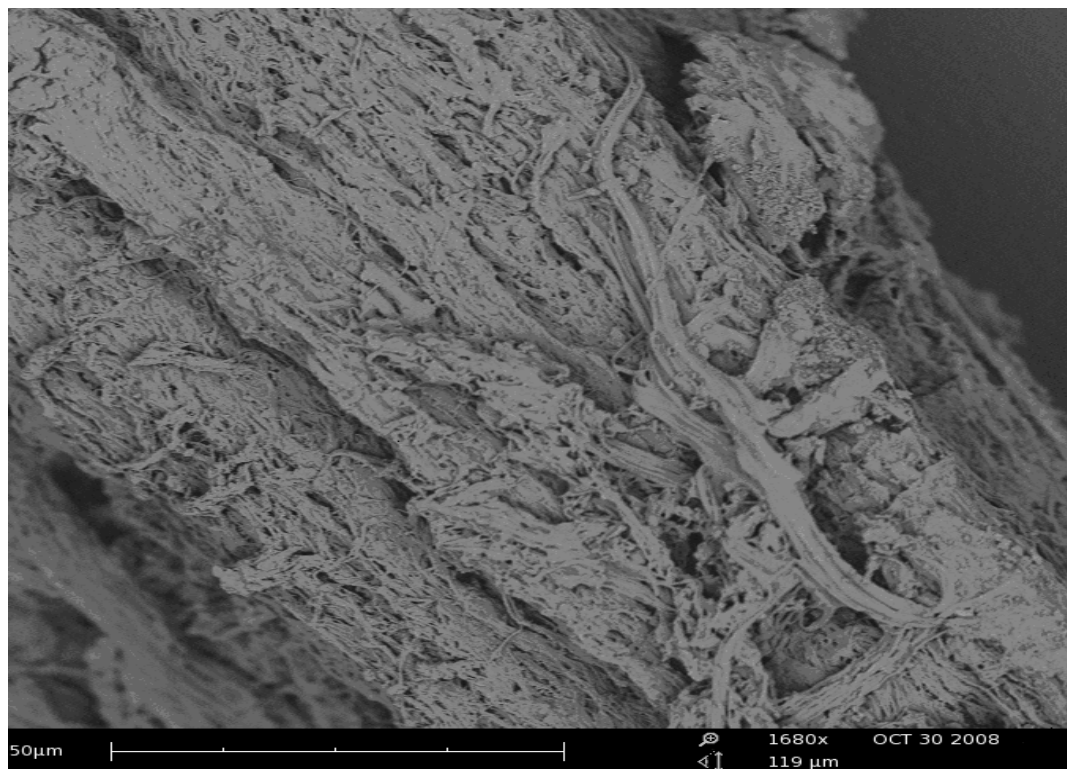


Fig. A9.1 SEM image of PVA-g-PAA microfibrils.

Appendix 10

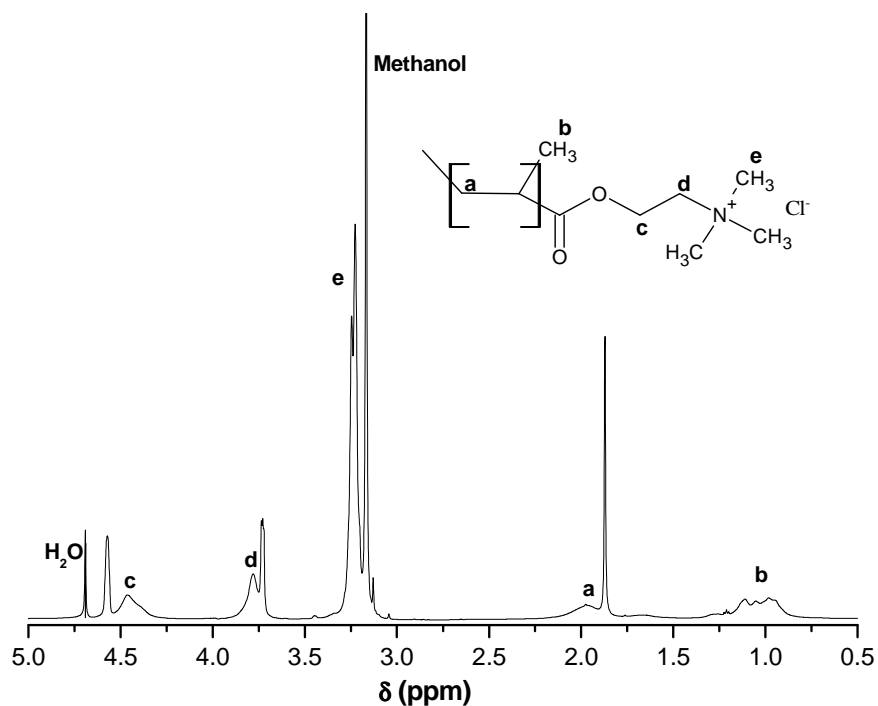
 ^1H NMR analysis of PDMC homopolymer extracts

Fig. A10.1 ^1H NMR spectrum of extracted PDMC homopolymer in D_2O .

Fig A10.1 is the ^1H NMR of the extracted PDMC homopolymer. The absence of the PVA methylene and methine proton signals at 1.5 and 4.0 ppm respectively,² confirms the absence of PVA polymer in the homopolymer extracts.

² Zheng, S.; Chen, Z.; Lu, D.; Lin, X. *J. Appl. Polym. Sci.* **2005**, 97, 2186–2191.

Appendix 11

SEM image of PVA-g-PDMC microfibrils

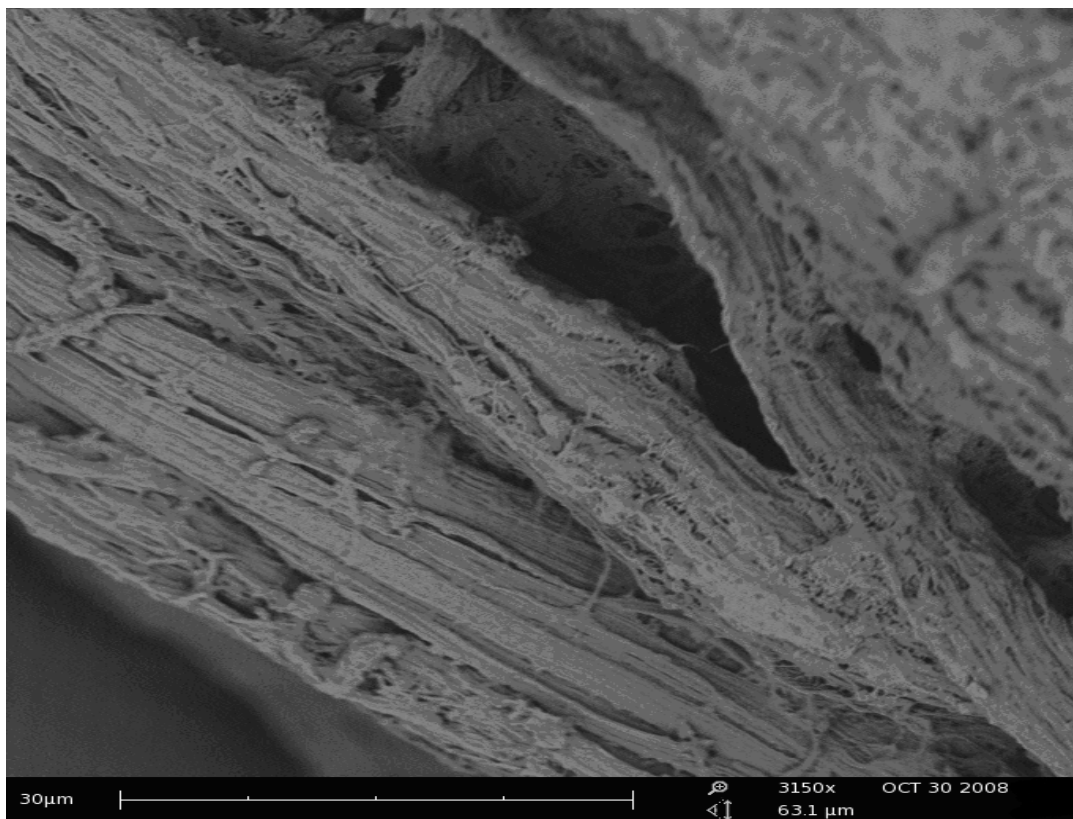


Fig. A11.1 SEM image of PVA-g-PDMC microfibrils.